TÉCNICO LISBOA

Techno-economic assessment of interconnection of offshore wind farms using Hydrogen-based solutions

Gonçalo Duarte Calado

Thesis to obtain the Master of Science Degree in

Electrical and Computer Engineering

Supervisors: Prof. Rui Manuel Gameiro de Castro
Eng. Miguel Jorge Marques

Examination Committee

Chairperson: Prof. Célia Maria Santos Cardoso de Jesus
Supervisor: Prof. Rui Manuel Gameiro de Castro
Members of the Committee: Prof. Armando José Pinheiro Marques Pires
Eng. João Gonçalo Maciel

September 2021

Declaration

I declare that this document is an original work of my own authorship and that it fulfills all the requirements of the Code of Conduct and Good Practices of the Universidade de Lisboa.

Abstract

Hydrogen can fulfil the role of energy storage and even act as an energy carrier, since it has a much higher energetic density than batteries and can be easily stored. Considering that the offshore wind sector is facing significant growth and technical advances, hydrogen has the potential to be combined with offshore wind energy to aid in overcoming disadvantages such as the high installation cost of electrical transmission systems and transmission losses.

In this thesis, two hydrogen producing systems were modelled, one with the electrolyzer offshore, the other with the electrolyzer onshore, along with a conventional wind farm. To do so, each component was individually modelled and combined to construct the systems. Furthermore, an hourly optimisation algorithm was developed to control the operation of the systems and a neural network was implemented to forecast day ahead power production and electricity price, so that the regulation costs could be modelled. Using cost projections for 2030 and 2050, the simulations were also performed for those years.

Results show that the onshore electrolyzer system is always more economically interesting than the offshore electrolyzer system, mainly due to its ability of purchasing electricity from the grid. This system is profitable in 2020 for a hydrogen price of 6€/kg, in 2030 for 4€/kg and in 2050 for 3€/kg, while the offshore electrolyzer system is only profitable for a hydrogen price of 9€/kg, 5€/kg and 3€/kg in 2020, 2030 and 2050, respectively. The conventional wind farm is never economically viable in any of the simulated years.

Keywords

Resumo

O hidrogénio pode servir como meio de armazenamento de energia, ou até como meio de transporte visto que possui uma densidade energética superior à encontrada em baterias e pode ser facilmente armazenado. Considerando que o setor eólico offshore tem evoluído rapidamente, o hidrogénio tem potencial de ser combinado com energia eólica offshore para ajudar a superar certas desvantagens como o custo elevado de sistemas de transmissão elétricos e perdas de transmissão.

Nesta dissertação, dois sistemas produtores de hidrogénio foram modelados, um com o eletrolisador offshore e outro onshore, juntamente com um parque eólico convencional. Para tal, cada componente foi modelado individualmente, posteriormente combinando todos os componentes para construir os sistemas. Um algoritmo de otimização foi desenvolvido para controlar a operação dos sistemas a cada hora e uma rede neuronal foi treinada para gerar previsões horárias do preço da eletricidade e produção eólica para o dia seguinte para que os custos de regulação pudessem ser modelados. Através de projeções de custo para 2030 e 2050, as simulações também foram efetuadas para estes anos.

Os resultados mostram que o sistema com eletrolisador onshore é economicamente mais interessante que o outro sistema, o que se deve à sua capacidade de comprar eletricidade à rede. Este sistema é lucrativo em 2020 para um preço de hidrogénio de 6€/kg, em 2030 para 4€/kg e em 2050 para 3€/kg, enquanto que o sistema offshore é lucrativo para preços de 9€/kg, 5€/kg e 3€/kg em 2020, 2030 e 2050. O parque eólico convencional nunca é economicamente viável.

Palavras Chave

hidrogénio verde; vento offshore; análise tecno-económica; eletrólise da água; integração na rede; previsão horária do dia seguinte;

Contents

List of Figures

List of Tables

Acronyms

AEL	Alkaline Electrolyzer
AFC	Alkaline Fuel Cell
CHP	Combined Heat and Power
CNN	Convolutional Neural Network
CSP	Concentrated Solar Power
DPB	Discounted Payback Period
FCR	Frequency Containment Reserve
HVAC	High Voltage Alternating Current
HVDC	High Voltage Direct Current
IRR	Internal Rate of Return
LCOE	Levelized Cost Of Energy
LCOH	Levelized Cost Of Hydrogen
LNG	Liquified Natural Gas
LSTM	Long Short-Term Memory
MAE	Mean Average Error
MAPE	Mean Average Percent Error
MCFC	Molten Carbonate Fuel Cell
MFNN	Multilayer Feedfoward Neural Network
MIBEL	Iberian Electricity Market
MILP	Mixed-Integer Linear Program
MLP	Multilayer Perceptron
NPV	Net Present Value
P2P	Power to Power

P2M   Power to Mobility

P2G   Power to Gas

PAFC   Phosphoric Acid Fuel Cell

PEMEL   Proton Exchange Membrane Electrolyzer

PEMFC   Proton Exchange Membrane Fuel Cell

PV   Photovoltaic

RMSE   Root Mean Square Error

SMR   Steam Methane Reform

SOE   Solid Oxide Electrolyzer

SOFC   Solid Oxide Fuel Cell

VMD   Variational Mode Decomposition

List of Symbols

a	Project's rate of return
a_{loan}	Loan's rate of return
bid_h	Day ahead market electricity bid at hour h
$c_{sp,cp}$	Compressor's specific energy consumption
$c_{sp,el}$	Electrolyzer's specific energy consumption
$c_{wa,el}$	Electrolyzer's specific water consumption
ee_h	Energy fed into the electrolyzer at hour h
efc_h	Electricity produced by the fuel cell at hour h
ep_h	Electricity produced at hour h
ep_h^{for}	Forecasted electricity production at hour h
es_h	Electricity sold at hour h
hc_h	Hydrogen consumed by the fuel cell at hour h
hp_h	Hydrogen produced at hour h
h_{LHV}	Hydrogen's lower heating value
hs_h	Hydrogen sold at hour h
H_{max-p}	Electrolyzer's maximum hydrogen production rate
imb_h	Electricity imbalance at hour h
I_i	Initial investment in %
I_s	Cost of replacing the electrolyzer's stack
I_t	Total investment
ph	Price of hydrogen

P_{cp}	Compressor's nominal power
P_{el}	Electrolyzer's nominal power
$P_{el_{max}}$	Electrolyzer's maximum operating power
$P_{el_{min}}$	Electrolyzer's minimum operating power
P_{fc}	Fuel cell's nominal power
P_{Park}	Wind farm's nominal power
RC_h	Regulation costs at hour h
RC_n	Regulation costs at year n
R_{max}	Upper bond of the electrolyzer's operating range
R_{min}	Lower bond of the electrolyzer's operating range
R_n	Revenue at year n
R_n^E	Revenue from selling electricity at year n
$R_n^{H_2}$	Revenue from selling hydrogen at year n
R_t	Total revenue
sp_h	Day ahead electricity price at hour h
sp_h^{for}	Forecasted day ahead electricity price at hour h
sp_h^+	Positive imbalance price at hour h
sp_h^-	Negative imbalance price at hour h
ss_h	Current amount of hydrogen stored at hour h
ss_{h-1}	Previous amount of hydrogen stored at hour h-1
ss_{max}	Maximum hydrogen storage
ss_{res}	Hydrogen storage reserve
y_{ee}	Electrolyzer's binary variable
y_{fc}	Fuel cell's binary variable
y_{imb}	Imbalance's binary variable
y_{ss}	Storage's binary variable

1

Introduction

1.1 Motivation

Hydrogen is a gas that can be easily produced using electrolysis and has several potential applications, ranging from energy source for transportation to being mixed into the natural gas grid, along with current applications in fuel refining and fertilizer production. Historically, hydrogen production is based on fossil fuels and emits a large amount of CO2, however, in the last decades, significant advances have been made in electrolysis and renewable energy production, making the production of green hydrogen at a reasonable price point possible.

Furthermore, with governments pushing the reduction of carbon emissions and lowering the dependence on fossil fuels, the demand for green hydrogen has quickly risen and is expected to rise substantially in the coming years. With the help from incentives and policies, green hydrogen is being heavily investigated around the world with the objective of producing hydrogen without carbon emissions that with a small incentive can compete with traditional hydrogen production methods.

One of the potential uses for hydrogen is electricity generation in a fuel cell, which is a device that uses hydrogen to produce electricity, with the only by-products being water and heat. In recent years fuel cells have also experienced significant advancements and are starting to be used in commercial applications, like passenger cars, trucks, buses, and grid-connected dispatchable power plants. Since one of the reasons electrical grids are dependent on fossil fuels is the need to control power generation, considering that renewable sources are intermittent (hydroelectric dams with reservoir provide some flexibility, but ultimately are dependent on rainfall upstream), the use of fuel cells can aid in reducing the use of fossil fuels in electricity generation.

In the electricity markets, purchase and selling bids are placed either in the day ahead market or in the intraday market, where the bids are then organized based on their price. In the case of selling electricity in the day ahead market (where most of the electricity transactions happen), the bids specify for each hour of the following day the amount of energy to be sold and the price. Then, the bids are organized from less expensive to more expensive and the power plants with the lowest price are selected to generate electricity until the supply of electricity meets the demand. Ultimately, the power plants all sell their electricity at the same price, which is the price of the most expensive energy bid that is still required to meet the electricity demand at that specific hour.

Whenever a power plant's electricity generation doesn't match the previously placed bids, an imbalance occurs and a regulation cost must be payed since the power plant wasn't able to deliver the amount of energy it had committed. These imbalances can be either positive, where the amount of energy injected into the grid is greater than the electricity bid, or negative, where the amount of energy injected into the grid is lower than the electricity bid. Taking into consideration that day ahead forecasts for wind power generation are challenging to do accurately, the integration of hydrogen in offshore wind farms can provide additional flexibility and reduce the electricity imbalances, saving on regulation costs.

Wind power produces roughly 5% of the world's electricity [1], with most installations onshore. However, higher wind speeds and more consistent wind can be found offshore which leads to higher energy production per turbine installed, with the disadvantages being higher cost and technical challenges due to the rough sea conditions the equipment is subjected to.

One of the challenges is transporting the electricity back to shore since traditional AC power cables have higher capacitance, thus higher losses than overhead lines, and more recent High Voltage Direct Current (HVDC) systems are expensive due to the converter stations necessary at each end of the transmission line. Considering that underwater pipeline installation is cheaper than electrical cables and that transport of a gas in a pipeline suffers much smaller losses ($< 0.1\%$) [2, 3], a case can be made for the production of hydrogen offshore with pipelines to transport it to shore.

Two system configurations can be found, the first consists of an offshore wind farm, offshore electrolyzer, and onshore hydrogen storage, while in the second system the electrolyzer is located onshore. A fuel cell can be added in both systems to provide electricity in high-demand periods and act as frequency control for the grid. For the first system, the electricity generated by the wind turbines travels a short distance to the electrolyzer platform, where hydrogen is produced, compressed, and transported to shore on a pipeline.

On the other hand, for the second system, the electricity is transmitted to shore by a traditional cable, where a choice can be made: sell the electricity directly to the grid or produce hydrogen. This is known as a hybrid system, where the operator can control the amount of power being sold to the grid or fed into the electrolyzer, even being able to buy electricity from the grid to produce hydrogen during periods of low electricity prices, which provides load flexibility to the grid operator as well.

1.2 Overview

This thesis is concerned with hydrogen production using electricity coming from offshore wind farms, i.e., green hydrogen production. The thesis offers an overview of the current situation on the subject by highlighting the main features of the technologies used by the different components of the hydrogen production system, as well as an outline of the system configuration options (offshore vs onshore electrolyzer location) and potential uses of hydrogen. Moreover, the thesis reviews the main recent research topics related to the subject by performing a thorough literature review, including state-of-the-art reports and journal papers.

The aim is to develop and compare two green hydrogen producing systems with a conventional floating offshore wind farm without hydrogen production, analysing both the technical point of view, such as the main challenges to overcome, as well as an economical point of view, assessing the cost competitiveness against commonly used solutions. Since the thesis focuses on the potential application

3

of these systems in the Iberian Peninsula, the wind farms being used in the hydrogen producing systems as well as the conventional wind farm must be floating wind farms, on account of the deep waters that surround the peninsula.

In order to properly simulate the complex hydrogen production, transmission and storage system, a model is developed to simulate each main component of the system as a whole, resulting in a simulation capable of representing the operation of the system and allowing the techno-economic analysis to be performed.

A neural network is also trained to forecast the day ahead wind power production and electricity prices, since one of the advantages of implementing hydrogen in an offshore wind farm is the added system flexibility. This neural network is a one dimensional Convolutional Neural Network (CNN) that receives the previous 64 hours of data to forecast the 24 hours of the following day. To further enhance the neural network's accuracy, the initial signal containing the 64 hours of data is divided into several signals of different frequencies using a technique known as Variational Mode Decomposition (VMD). Through the use of multiple signals, the neural network can detect patterns more easily.

Furthermore, the historic Iberian Electricity Market (MIBEL) prices and wind speeds off the coast of Galicia, Spain are modelled to simulate how each system would perform in past conditions, which can provide an idea of how it would perform in case one of the hydrogen producing systems was implemented in that location.

The simulations are conducted for two locations at different distances to shore so that the effect of placing the wind turbines further out to sea can be analysed. Additionally, using cost projections for the technologies that compose each system, simulations for 2030 and 2050 are also performed to assess how the field of green hydrogen production using offshore wind energy might develop in the coming years.

Since the operation of these systems isn't linear, an optimisation algorithm for each system is developed to guarantee maximum revenue. This algorithm takes into account, among others, the generated electricity, the electricity price and previously placed bid to ensure that at each hour, the production of hydrogen and/or electricity is properly managed in order to maximize the revenue from both sources of income.

A sensitivity analysis is included, where parameters such as total system CAPEX, project's rate of return and capacity factor of the offshore wind farm (present in all systems) are varied to assess their impact on the systems. Through this analysis, the effect that any possible deviations from the cost projections will impact the systems can be estimated.

1.3 Objectives

This thesis aims to determine the economic viability of two hydrogen producing systems, while also establishing a baseline comparison with a conventional wind farm that only generates electricity. Consequently, this thesis might be of use to enterprises looking to invest in offshore green hydrogen production, providing a foundation that can be adapted to suit the investors' needs. In addition, when considering the governmental push towards green technologies, this thesis can also shed some light on the technical or economical downsides of offshore green hydrogen production so that fair policies can be implemented. To do so, the main objectives of this work are:

- Perform a comprehensive literature review regarding the current situation of green hydrogen production and floating wind technologies, along with the future projections on how these fields might progress.

- Provide an hourly day ahead forecasting model for wind power production and electricity prices, based on a CNN with VMD pre-processing, generating forecasts with the same accuracy as the ones present in literature.

- Develop a detailed model capable of representing the behavior of a conventional wind farm as well as the hydrogen producing systems (with the electrolyzer located either offshore or onshore), operating in the MIBEL and a parallel hydrogen market.

- Implement an hourly optimisation model to set the conditions that maximize the economic performance of each system in a market environment.

- Analyse the performance of the modelled systems and evaluate their techno-economic viability in a base configuration for the years of 2020, 2030 and 2050.

- Compare the hydrogen producing systems to ascertain their strengths and weaknesses, in addition to the favourable conditions for their implementation.

- Analyse the distribution of the investment among the systems' components, to understand what components carry an economic burden.

- Conduct an economic analysis that provides economic conclusions if any deviations from the base scenario conditions occur.

1.4 Innovative Contributions

A paper based on this thesis has been published in Applied Sciences, Q2 (JCR), Q2 (WoS), 5-year Impact Factor: 2.736 (2020), DOI: https://doi.org/10.3390/app11125561. The article can also be seen

5

in appendix F.

This thesis extends the reviewed literature by implementing an optimisation algorithm that takes into account not only electricity price and hydrogen price, but also regulation costs based on the previous bids placed in the day ahead market. By considering the regulation costs, the added flexibility of integrating hydrogen can be valued in the economic analysis.

Furthermore, the present work focuses on implementing green hydrogen production systems in the Iberian Peninsula, unlike the articles presented in the literature that consider locations more typically associated with offshore wind energy, such as the North Sea.

1.5 Structure

The remainder of the paper is organized as follows. In Chapter 2, the state-of-the-art review is presented, containing a discussion of the system components used for hydrogen production from offshore wind power and the systems' configurations, i.e., the option between the offshore and onshore location of the electrolyzer are discussed. It also provides a summary of the main hydrogen uses, a brief introduction to day ahead forecasting using deep learning and the literature review of the main subject areas being investigated.

In chapter 3 the proposed models that were used in the simulations are presented, starting with an overview on how the simulations were performed and moving to the individual modelling of each component. Moreover, the hourly optimisation algorithms for each hydrogen producing system are detailed, from their implementation to an explanation on how the maximum possible revenue is determined. The economic model is also contemplated, where the CAPEX and OPEX values for 2020, 2030 and 2050 are presented, along with the investment distribution among the systems' components. The chosen economic performance metrics are also detailed.

Chapter 4 focuses on the day ahead forecasting models, starting with the theoretical background, discussing the implemented neural network and analysing its performance in forecasting wind power production and electricity price.

Chapter 5 presents the results from the simulations, from the technical aspects to the economic performance metrics. Additionally, the operation of the fuel cell is analysed and the conditions in which the fuel cell's operation is beneficial are highlighted. The sensitivity analysis is presented for the conventional wind farm without hydrogen production and also for the hydrogen producing systems.

In Chapter 6 the main conclusions from the work are drawn, from the optimal way to operate the systems to the economic results. The conditions where a certain system is more economically viable are presented, along with the projections for the coming years.

Moving on to the appendixes, Appendix A details how binary variables were implemented in the

hourly optimisation algorithm and Appendix B contains a short explanation on how the layers of the neural network operate. Appendixes C through E present additional results from the economic analysis, more specifically, Appendix C details the optimal sizing ratios for the electrolyzer, Appendix D provides additional results from the economic analysis, Appendix E provides the sensitivity analysis for 2020, 2030 and 2050 for both considered locations and appendix F contains the published article regarding the state-of-the-art review.

2

State-of-the-art review

2.1 System Components

2.1.1 Offshore Wind

When analysing fixed bottom wind turbines or floating turbines the main differences are cost and locations where each technology can be implemented. The fixed bottom is the most used technology by a significant margin, with only 62 MW of floating wind installed at the end of 2020 [4], so it has had more time to mature, and prices have come down significantly. However, floating wind prices are expected to lower rapidly in the next few years and allow access to much deeper waters, useful in countries that do not have shallow water far from shore. Figure 2.1 portrays the water depth around Europe, where only the North Sea, Irish Sea, and a couple of other areas have a somewhat shallow depth that allows for fixed bottom foundations to be installed. On the other hand, the water around the Iberian Peninsula and southern Europe can get much deeper without getting too distant from the shore.
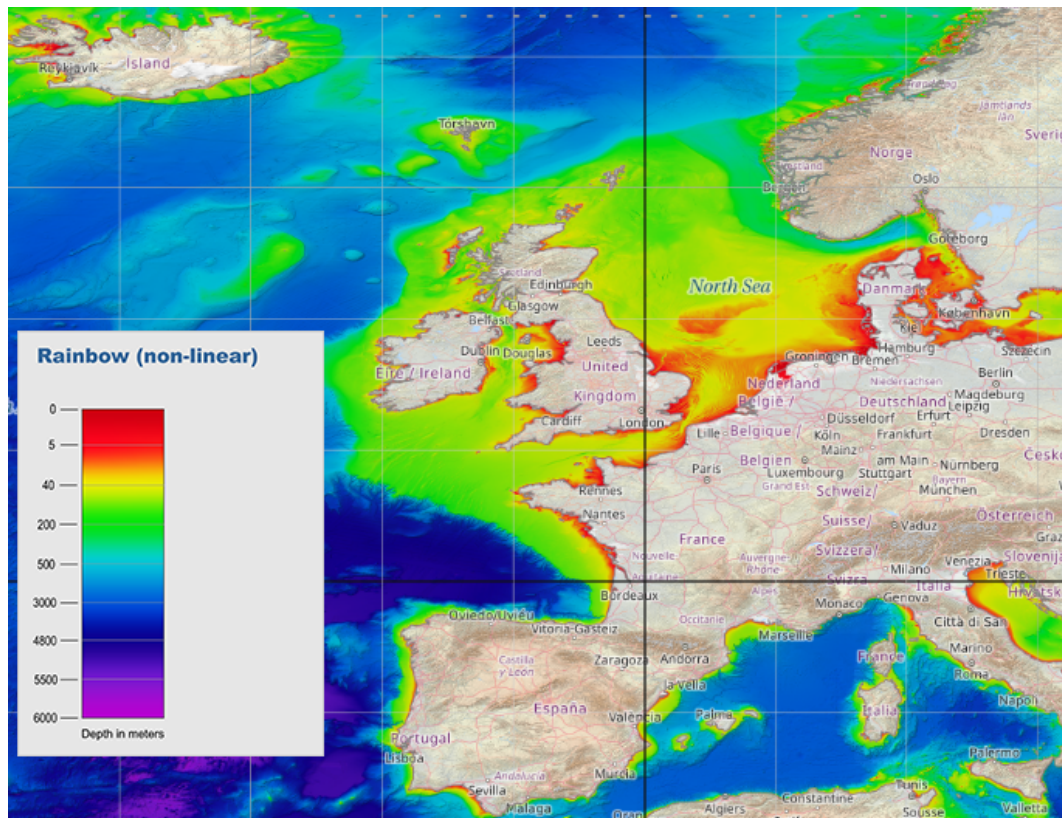
Figure 2.1: Water depth in the sea around Europe. Source: EMOD [5]

Figure 2.2 shows a projection of the Levelized Cost Of Energy (LCOE) of both bottom fixed and floating wind as well as the strike price for the Dogger Bank wind farm. Dogger Bank is a large sandbank between England and Denmark with high wind speeds and shallow depth, which makes it a perfect candidate for fixed bottom wind turbines. The wind farm will be built in 3 phases each with 1.2 GW and

will be located between 130 km to 190 km off the coast from England.
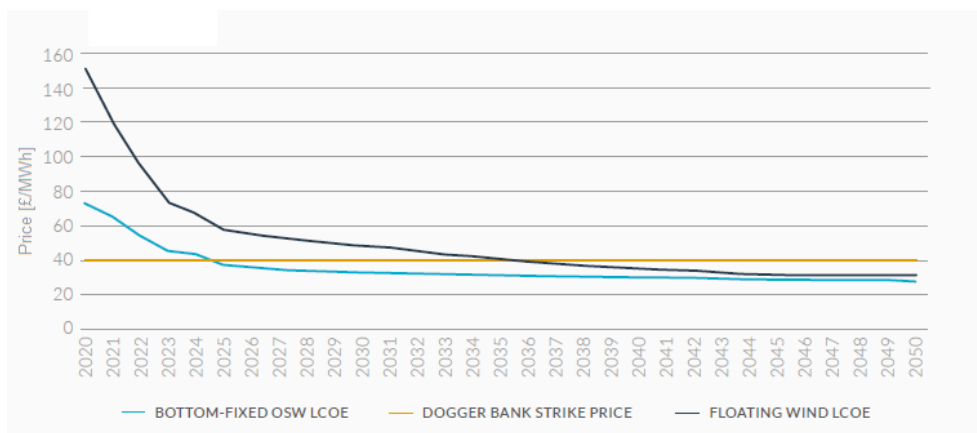
Figure 2.2: LCOE projections for offshore wind until 2050. Source: ORE Catapult [6]

The installation of fixed bottom wind turbines involves the use of a specialized boat capable of burying the foundations deep in the seabed, along with being equipped with a crane to assemble the tower, nacelle, and individual blades. Comparing with floating wind, this newer approach can be fully assembled on land or dry dock and afterward be towed by a regular tugboat to the project's location, a much simpler installation which can be another factor in lowering the costs when more floating substructures are built, and economies of scale have their effect. Europe is the leader in offshore wind power and most of the installed power is in the North Sea (79% according to WindEurope [4]), a location with high wind speed (figure 2.3) and relatively shallow water, a good candidate for fixed bottom installations.
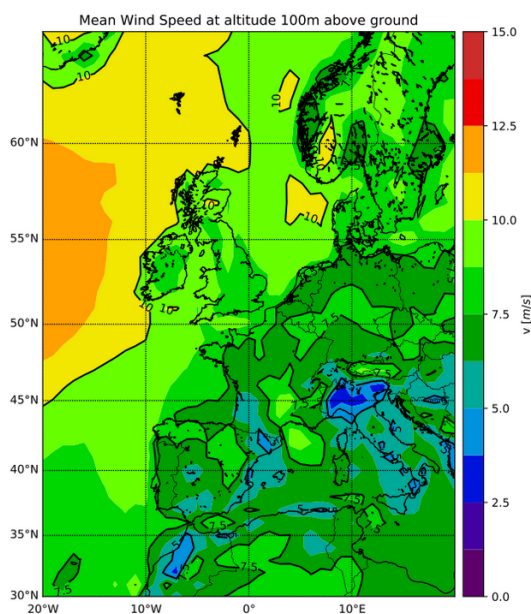
Figure 2.3: Mean wind speed in Europe. Source: Airborne Wind Europe [7]

Around 80% of offshore wind resources are located in waters deeper than 60 m (where fixed bottom installations are not feasible) and average wind speeds increase further from shore as can be concluded by analysing figure 2.3. To access all of this potential, floating wind currently represents the best approach and with the number of installations planned in the coming years the future of floating wind is looking bright [4].

The first floating wind farm ever built on a commercial level is Hywind Scotland [8,9], it has been producing energy since 2017 and is composed of 5 turbines of 6 MW each, supported by a spar buoy. The buoys are 78 m in length, attached to the seabed by 3 mooring lines. Although this is a simple design, added installation problems can arise from the dimensions of the buoy, unlike other designs, such as the inability to be assembled on a simple port. More specifically, for hydrogen production, the individual electrolyzer approach is not as straightforward due to the cylindrical shape of a spar buoy, which limits the amount of space available to install an electrolyzer and the remaining infrastructure. Consequently, this structure requires more substantial modifications when compared to a semi-submersible platform, making the latter the most cost-competitive floating platform for an individual electrolyzer project [10].

One of the first wind farms deployed on a commercial level using a semi-submersible platform is WindFloat Atlantic in Viana do Castelo, Portugal (figure 2.4). It was commissioned in 2020 [4] and is composed of 3 turbines of 8.4 MW each, supported by a semi-submersible structure made of 3 cylindrical buoys 30 m high and 50 m apart. Some advantages of this design are the simple assembly of the wind turbine on the structure in port and, in the case of hydrogen production by individual electrolyzer, can provide an unobstructed area of 1082 m^2 with some modifications. Several other projects using similar platform designs are planned in the coming years [4].

Figure 2.4: WindFloat Atlantic off the coast of Viana do Castelo, Portugal. Source: Dock90

2.1.2 Electrolyzer Technologies

An electrolyzer is a device that receives DC electricity and demineralized water and separates the hydrogen and oxygen atoms from the water molecule through a chemical reaction, generating high purity oxygen and hydrogen. While different technologies for electrolyzers operate in slightly different ways, all have an anode and cathode that are separated by an electrolyte.

Currently, there are two technologies used in commercial applications for the production of hydrogen, Alkaline Electrolyzer (AEL) and Proton Exchange Membrane Electrolyzer (PEMEL). Another technology undergoing intense research and development is Solid Oxide Electrolyzer (SOE), which promise high efficiencies and flexibility, at the cost of high operating temperatures (500 to 1000 °C, varies according to the chemistry) and durability.

2.1.2.A Alkaline electrolyzers

AEL are currently the cheapest technology and have the longest lifetime, due in part to being the oldest of the technologies mentioned above [11, 12]. This type of electrolyzer has been used in the industry for roughly 100 years, so while further progress is expected, both PEMEL and SOE development will surely be faster. However, they cannot react as fast to changes in production, maintenance of the alkaline fluid is complex, cannot operate below a certain threshold for safety reasons, take longer to start, and present a rather low current density when compared to PEMEL, around 5 times lower [13]. In addition, the output pressure of the hydrogen produced is lower, which requires higher compression for transport and storage, reducing the advantage the lower CAPEX provided initially.

Historically, this type of electrolyzer has been operated at almost constant power while connected to the grid and recently has seen improvements in the ability to change hydrogen production rate without relevant efficiency losses. One of the highest-powered electrolyzers is a 4 MW module [14], which is claimed to have a dynamic response fast enough to follow the production of a renewable power plant. Furthermore, it is also said that the current density is double compared to the previous generation, the energy efficiency is equivalent to a PEMEL, the output pressure is 30 bar, and has increased longevity compared to newer technologies.

2.1.2.B Proton Exchange Membrane Electrolyzers

PEMEL are more recent than AEL and come with several advantages, such as much faster start-up times, higher current densities which lead to smaller electrolyzer footprint, higher hydrogen purity ($\geq$ 99.8%), can operate beyond nominal power, and higher output pressure [11–13]. Figures 2.5 and 2.6 provide additional numbers comparing both technologies.

Technology		ALK		PEM	
	Unit	2017	2025	2017	2025
Efficiency	kWh of electricity/ kg of H_2	51	49	58	52
Efficiency (LHV)	%	65	68	57	64
Lifetime stack	Operating hours	80 000 h	90 000 h	40 000 h	50 000 h
CAPEX – total system cost (incl. power supply and installation costs)	EUR/kW	750	480	1 200	700
OPEX	% of initial CAPEX/year	2 %	2 %	2 %	2 %
CAPEX – stack replacement	EUR/kW	340	215	420	210
Typical output pressure*	Bar	Atmospheric	15	30	60
System lifetime	Years	20		20	

Figure 2.5: Comparison of PEMEL and AEL in 2017 and 2025. Source:IRENA [11]

	ALKALINE	PEM
Load range	15–100 % nominal load	0–160 % nominal load
Start-up (warm – cold)	1–10 minutes	1 second–5 minutes
Ramp-up / ramp-down	0.2–20 %/second	100 %/second
Shutdown	1–10 minutes	Seconds

Figure 2.6: Comparison of the reaction times between PEMEL and AEL. Source:IRENA [11]

When combined with a renewable power source, the ability to easily adjust the power to suit the conditions, including a quick start-up time, are two great features that allow this technology to extract the most out of intermittent power sources. During periods of shutdown low amounts of energy are required to maintain the system operational [11, 12], this is an important fact to consider if the electrolyzer is to be kept offshore or if it won't be grid-connected. Furthermore, a backup power source must be provided if coupled with a renewable power source, since the intermittent nature of this type of power does not guarantee the necessary energy during shutdown periods.

Despite in recent years PEMEL having made significant progress in higher efficiency, output pressure, ramp up and ramp down times, and CAPEX, they are still considerably more expensive than AEL [12, 15]. The main reason for the high price is the significant amount of platinum needed to build the stack of the electrolyzer. The efficiency for a PEMEL according to the power can be observed in figure 2.7.

13
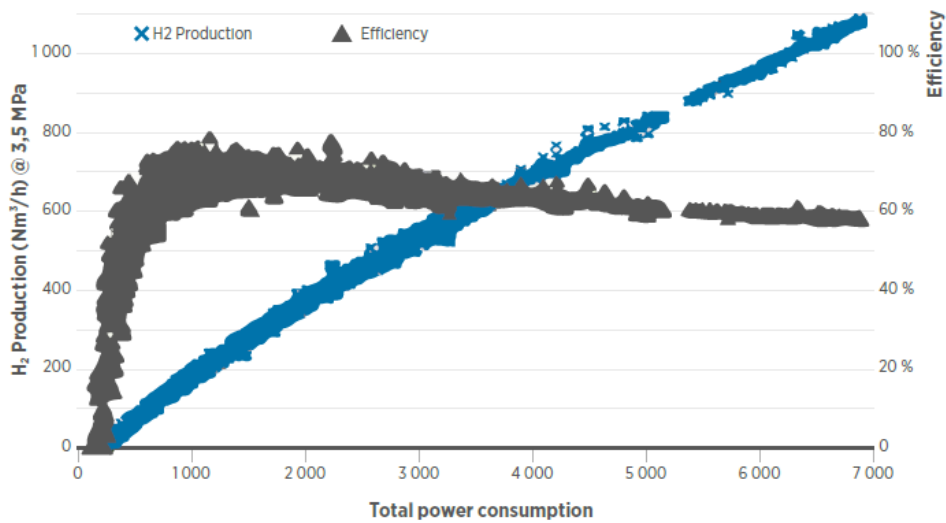
Figure 2.7: Efficiency curve of a PEMEL. Source: IRENA [11]

2.1.2.C   Solid Oxide Electrolyzer

The SOE is the newest of the three technologies, currently rarely used in commercial applications due to the high operating temperatures (usually in the range of 650-850 °C) and lower longevity. This type of electrolyzer promises better efficiency than all other technologies and unlike PEMEL does not require any precious metals, which makes it possible to reach a lower CAPEX once the technology matures [12]. While the high operating temperature is a disadvantage, especially for intermittent power sources, it does not present as big an obstacle when coupled with nuclear or combined cycle power plants. In the case of renewable energy, Concentrated Solar Power (CSP) accompanied with an SOE is an option under study, since the waste heat from CSP can be used in heating the SOE.

2.1.3   Hydrogen Storage

Storage of hydrogen is similar to natural gas, with a few key differences, mainly when some metals come in contact with hydrogen can suffer hydrogen embrittlement, which leads to increased degradation and chance of material failure. Another difference to consider is increased leakage, especially in underground natural structures such as aquifers, but also in links between pipeline sections or links in valves, due to the small size of the hydrogen molecule [16]. The bacterial reaction also constitutes a problem, since some bacteria decompose hydrogen, leading to what can be considered losses as the purity of stored hydrogen goes down [2]. The main approaches in storing hydrogen are gaseous storage and liquid storage, other approaches like chemical storage exist but only on a much smaller scale so they won't be considered.

Gaseous storage can be divided into two methods, fabricated tanks (usually metal) and storage in natural underground structures, like aquifers and salt caverns. Hydrogen density has a nearly linear relation with pressure, as shown in figure 2.8, so a greater storage pressure leads to a smaller volume needed to store a certain amount of hydrogen gas. However, due to material properties and operational costs, hydrogen is not stored at pressures higher than 100 bar [16], which corresponds to a density of roughly 7.8 kg/m³ [16].
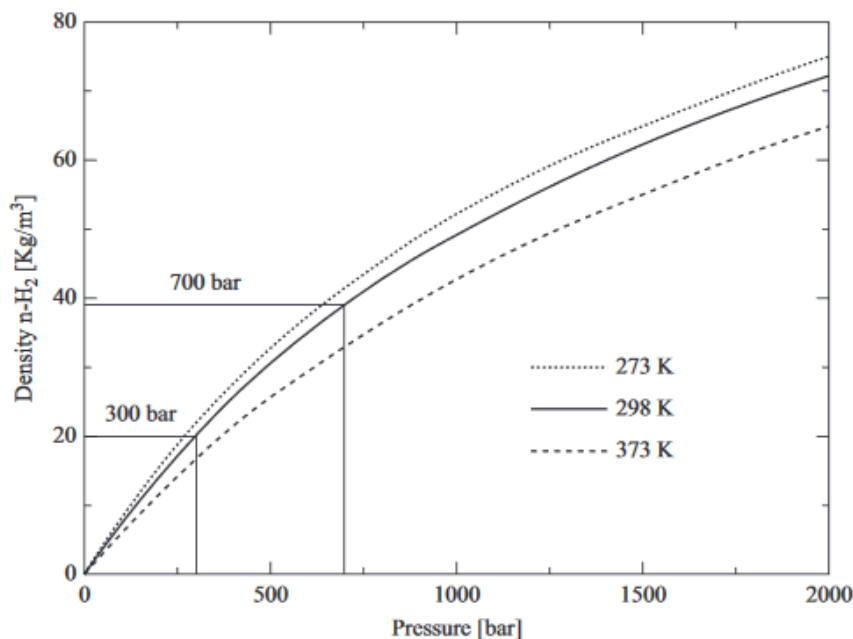
Figure 2.8: Hydrogen's density at different temperatures according to the pressure. Source: [17]

Considering a few examples of power plants ranging from 10 to 1000 MW, and knowing that 1 kg of hydrogen equals 11.1 Nm³ of hydrogen [11], the dimensions for the storage facilities needed for each example can be calculated. Table 2.1 contains the weight and volume of hydrogen produced per day if the electrolyzers are run at full power and table 2.2 contains a possible radius and height for cylindrical tanks to be able to store all the hydrogen produced during 24 hours with the electrolyzers at full power.

Calculations were done based on a typical electrolyzer, more specifically a hydrogen production of 5000 Nm³/h for a 25 MW electrolyzer. A similar commercial 17.5 MW PEM electrolyzer produces 340 kg/h, when linearly scaled to 25 MW a production rate of 11.6 tons/day is achieved, a similar value to the one presented in Table 1. To convert the hydrogen flow rate (Q_n) from Nm³/h to mass (M) in ton/day, equation 2.1 is used, and to obtain the volume required to store the hydrogen produced per day, a density of 7.8 kg/m³ is considered.

$$M = \frac{0.024 \cdot Q_n}{11.1} \ \text{[ton/day]} \tag{2.1}$$

To estimate the dimensions of the cylindrical storage tanks, the equation for a cylinder's volume (equation 2.2) was used, where V is the storage tanks' volume, h is the height and r is the radius.

$$V = h \cdot \pi \cdot r^2 \ \ [\text{m}^3/\text{day}] \tag{2.2}$$

Table 2.1: Mass and volume of hydrogen produced

Power [MW]	Hydrogen Mass [ton/day]	Hydrogen volume at 100 bar [m³/day]
25	10.8	1.400
100	43.2	5.500
500	216	27.700
1000	432	55.400

Table 2.2: Dimensions for gaseous storage facilities

Power [MW]	Cylinder radius [m]	Cylinder height [m]
25	9	6
100	13	11
500	25	15
1000	30	20

The most cost-effective and practical way of storing large quantities of hydrogen as a gas is using underground natural structures. Aquifers are not as well sealed as salt caverns, which leads to increased leakage [16, 18]. While some leakage might be reasonable when storing natural gas, due to the small size of the hydrogen molecule the leakage rate increases significantly, for this reason, aquifers are not as adequate to store hydrogen. The best underground storage structures are salt caverns for several reasons, including low construction costs, low leakage rates, fast withdrawal, and injection rates, and a harsh environment for bacteria, which decreases unwanted bacterial activity [2, 16, 18]. Initial research shows no significant difference between storing hydrogen compared to natural gas in these structures and pure hydrogen is already stored using this approach in Teeside, UK, and Texas, USA [2, 18].

The second approach consists of storing liquid hydrogen in metal tanks, a process similar to what is widely used for Liquified Natural Gas (LNG). The main advantage is the high density in liquid state of 70 kg/m³, almost 10 times the density of hydrogen in a gas state at a pressure of 100 bar. However, the liquefaction of hydrogen is a very energy-intensive process, with anywhere from 6 to 10 kWh of electricity needed to liquefy 1 kg of hydrogen [16, 19]. The current installed liquefaction capacity is around 355 tons per day, below the necessary capacity needed for the example of a 1 GW plant. The main reasons for the low liquefaction capacity are the high initial investment associated with liquefaction plants and the high energy consumption to liquefy the hydrogen. Furthermore, since highly pressurized hydrogen can provide an adequate range for vehicles and reasonable dimensions for static storage, there has not been a big incentive to invest in liquified hydrogen solutions.

2.2 System Configuration

There are two possible options for the system configuration related to the location of the electrolyzer. It can be placed offshore, near the wind farm, or onshore, near the existing grid coupling point.

2.2.1 Offshore Electrolyzer Scenario

One of the significant costs in an offshore wind farm is the equipment to bring the electricity to shore, namely the cables, transformers, and power electronics. Considering a High Voltage Alternating Current (HVAC) transmission system losses are around 1% to 5% for wind farms with nominal power from 500 to 1000 MW, located 50-100 km from shore [20, 21]. For a HVDC system, losses range from 2% to 4% depending on nominal power and distance [20, 21]. However, hydrogen travelling through a pipeline has considerably lower losses, under 0.1% [2, 3], along with reduced initial costs for an underwater pipeline compared to underwater electrical cables and the power electronics needed. Figure 2.9 contains an overview of the centralized offshore electrolyzer system.
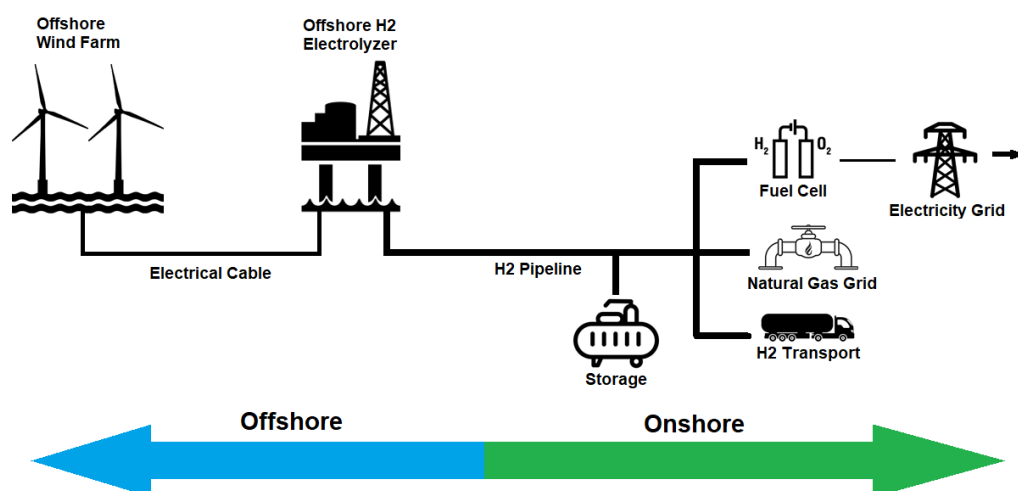
Figure 2.9: Offshore electrolyzer system

PEMEL represent the best choice for this system due to the smaller footprint and easier maintenance [11], which in an offshore scenario means the platform can be smaller and the maintenance trips can be done further apart.

Since the output pressure of a PEMEL is around 30 bar [11, 22], additional compression is required to export the hydrogen to shore. The hydrogen compressor and export pipeline must be sized according to the distance to shore, operating pressure of the electrolyzer, flow of hydrogen, and pressure drop along the pipeline. A study done by North Sea Energy [23] estimated the required pipeline diameter and pressure assuming an output pressure of 68 bar and 20 m/s maximum travel speed. The results show

17

that for a 1 to 2 GW wind farm located 50 to 200 km from shore, the minimum diameter of the pipeline ranges from 0.25 to 0.41 m, while the minimum input pressures range from 83 to 100 bar.

To size the PEMEL, the nominal power does not need to be equal to the wind farm's nominal power since the wind farm might not spend large periods of time at nominal power. From an economic point of view, the most interesting approach might be to slightly undersize the electrolyzer since the revenue lost when the wind farm is at nominal power could be lower than the additional cost of a more powerful electrolyzer [6]. Furthermore, the energy used in purifying the water and compressing the hydrogen for transmission along with the wake and array losses lower the actual available power for the electrolyzer [24].

A backup power source must be provided for the electrolyzer in periods of shutdown when the electrolyzer must consume a small amount of power to remain operational. Periods of shutdown will not be common or last long, due to the PEMEL capability of being able to start operating at 1% nominal power, although with low efficiency.

Two electrolyzer configurations are possible: a single centralized electrolyzer fed by the whole wind farm or individual electrolyzers, one per wind turbine. The details of each configuration are given below. The main components for the centralized electrolyzer system are the same as for the individual electrolyzer system since the operating principle is similar. The components are:

- PEMEL and the supporting electronics
- AC-DC rectifiers (possibly already included in electrolyzer)
- Desalination unit and reservoir for desalinated water
- Seawater pumps
- Export pipeline
- Backup power source
- Communication equipment

2.2.1.A   Centralized Electrolyzer

In a centralized electrolyzer system, the individual installation of the wind turbines is the same as a typical offshore wind farm, with turbines in strategic places to minimize losses by the wake effect. The power produced by each individual turbine is transmitted to a central platform through regular underwater cables and while voltages can differ, newer and higher power turbines, such as the Haliade-X 13 MW [25], operate at 66 kV.

Once the electrical power reaches the central platform most of it can get rectified to DC, the other part is used to power the seawater pumps and hydrogen compressor in AC. The DC power is used mainly to produce hydrogen, but also to power the backup power source and the supporting systems. The produced hydrogen exits the electrolyzer at high purity and with a pressure of 30 bar, so the next

step is compressing it to the desired pipeline input pressure. After being compressed, the hydrogen is fed into the export pipeline where it gets transmitted to shore.

2.2.1.B   Individual Electrolyzer

When sufficient wind is present, most of the electricity is fed into the rectifiers to power the electrolyzers and possibly refill the backup power source. The remaining power is used to power the seawater pumps, which need AC electricity. In the case of no offshore compression, the produced hydrogen exits the electrolyzer and gets exported by a small dimension pipeline to a subsea collection manifold, that receives the hydrogen produced by each turbine-electrolyzer system and exports it to shore using a bigger diameter pipeline. However, if offshore compression is needed, the hydrogen exits the electrolyzer and gets exported by a small dimension pipeline to a collection manifold in a platform, compressed to a desired pressure, and exported to shore by a pipeline.

This approach becomes more viable as the nominal power of a turbine keeps increasing, since more powerful electrolyzers can be installed individually, and economies of scale can play their part [23]. At around 10 MW, the cost per kW of hydrogen production power starts decreasing at a much slower rate, especially after the year 2030. In [23], it is projected that the price per MW of a PEMEL will decrease from the current (2020) 0.75 M€/MW to 0.2 M€/MW by 2050.

Since bottom fixed and some floating options, such as a spar buoy, require significant modifications to be able to support all the extra infrastructure, the semi-submersible platform like the one used in WindFloat Atlantic is the best choice for the individual electrolyzer approach [10]. To make the platform suitable for all the equipment, modifications will need to take place such as creating a floor to put the equipment that also shields from the waves and possible water splashing, as well as modifying the buoys and ballast to accommodate the additional weight.

2.2.2   Onshore Electrolyzer Scenario

This approach is also known as a hybrid system, where the energy produced is transmitted to shore as electricity in conventional cables, once onshore the energy can be sold directly to the grid or used to produce hydrogen. The main advantage of this system is flexibility, when the market price for electricity is high the investor can sell electricity directly to the grid, when the market price is low, or grid level curtailment must occur the energy can be redirected to an electrolyzer to produce hydrogen. Curtailment occurs when the production of electricity is greater than the consumption, which leads to a need in reducing the production. Figure 2.10 contains an overview of the proposed system.
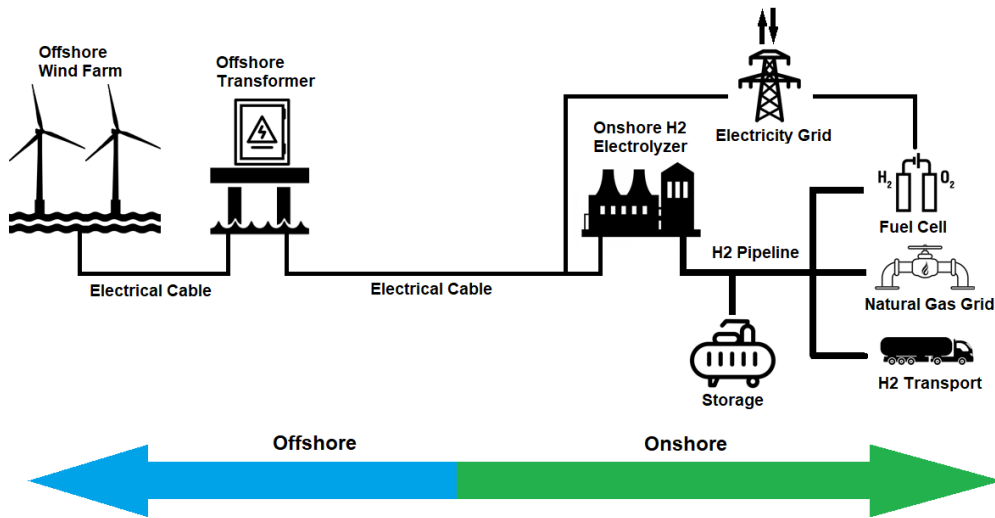
Figure 2.10: Onshore electrolyzer system

Since in this approach the electrolyzer will be onshore, it is possible to place the electrolyzer and all other sensitive equipment inside a building, where they can be sheltered from the elements but also provide a better work environment for the personnel responsible for the operation and maintenance. Furthermore, since access to the electrolyzer is much simpler than if it was offshore, the increased maintenance requirements and decreased power density of an AEL do not present as big of an obstacle, so the reduced CAPEX of this technology means both AEL and PEMEL are viable when the electrolyzer is installed on land.

HVDC is a more expensive technology that only becomes interesting when wind farms are located far from shore and/or have high nominal powers [26]. In the case of HVAC, longer lines imply more powerful line-reactive compensators to account for the capacitive losses, which in turn increases the cost. Since HVDC transmission does not show capacitive losses, only ohmic losses occur, the transmission losses and costs are significantly lower for HVDC. To summarize, transmission losses and costs are lower in the case of HVDC and even though the initial investment for HVDC transmission (stations and equipment) is higher than HVAC, the difference in cost diminishes when transmission distance increases. The breakeven distance for which HVDC becomes preferable is around 50-100 km for underground and underwater cables [26].

Regarding the source of water, the two possible options are connecting the electrolyzer to the fresh-water grid, an option that might not be viable due to environmental concerns in areas with recurring droughts, like southern Europe, or installation of a desalination unit next to the electrolyzer. Even though the water produced by a desalination unit is clean and the water in fresh-water grids has been previously treated, further treatment such as deionising the water is still required for both options before being used in electrolysis [15].

2.3   Hydrogen Utilization

One of the properties of hydrogen that makes it so interesting is the wide array of utilization cases, especially when combined with the continuously decreasing costs of electrolysis and forecasts for positive Net Present Value (NPV) on hydrogen electrolysis from renewable sources. Hydrogen electrolysis can also be a great way of reducing emissions, be it by working as energy storage to help when renewable resources are scarce, or by reducing emissions caused by other polluting ways of producing hydrogen. The use cases for hydrogen can be divided into 3 main areas: generating electricity, Power to Gas (P2G), and hydrogen as the end product.

2.3.1   Generating Electricity

Hydrogen represents today the best non-fossil fuel for some heavy vehicles that require large energy storage and fast recharge rates, such as long-haul trucks, buses, hybrid trains designed to operate in both electrified and non-electrified train tracks and even for a common car, since refilling the hydrogen tank takes a few minutes and gives around 600 km of range [27]. This application is denominated as Power to Mobility (P2M).

For grid applications, the fast response time of some fuel cells makes them adequate as dispatchable power plants for peak demand or for frequency control. This application is denominated as Power to Power (P2P). Furthermore, some solid oxide systems can operate with high efficiencies in both electrolyzer and fuel cell modes, however, it should be noted this technology has not reached the commercial level yet [12, 28].

Figure 2.11 contains a comparison of the main fuel cell technologies, where the first two are considered low temperature fuel cells and the remaining are high temperature fuel cells.

Fuel Cell Type	Common Electrolyte	Operating Temperature	Typical Stack Size	Electrical Efficiency (LHV)
Polymer Electrolyte Membrane (PEM)	Perfluorosulfonic acid	<120°C	<1 kW - 100 kW	60% direct H_2;[i] 40% reformed fuel[ii]
Alkaline (AFC)	Aqueous potassium hydroxide soaked in a porous matrix, or alkaline polymer membrane	<100°C	1 - 100 kW	60%[iii]
Phosphoric Acid (PAFC)	Phosphoric acid soaked in a porous matrix or imbibed in a polymer membrane	150 - 200°C	5 - 400 kW, 100 kW module (liquid PAFC); <10 kW (polymer membrane)	40%[iv]
Molten Carbonate (MCFC)	Molten lithium, sodium, and/or potassium carbonates, soaked in a porous matrix	600 - 700°C	300 kW - 3 MW, 300 kW module	50%[v]
Solid Oxide (SOFC)	Yttria stabilized zirconia	500 - 1000°C	1 kW - 2 MW	60%[vi]

Figure 2.11: Comparison of fuel cell technologies. Source: [29]

Both Alkaline Fuel Cell (AFC) and Proton Exchange Membrane Fuel Cell (PEMFC) have quick startup times, however PEMFC present greater power density, so they are the primary choice to equip hydrogen based vehicles. Due to this emerging market, intensive research and development into PEMFC is being performed by car and bus manufacturers, consequently cost reductions and increased durability are expected in the coming years.

Most stationary installations of fuel cells are high operating temperature [30], one example being the 50 MW Daesan Hydrogen-Fuel-Cell Power Generation that started operating in South Korea in 2020. The plant is composed of 114 Phosphoric Acid Fuel Cell (PAFC) fuel cells and will produce around 400,000 MWh of energy annually [31,32].

In the past few years, PAFC and Molten Carbonate Fuel Cell (MCFC) presented the highest growth rate, though this is expected to change due to several companies offering PEMFC in the order of 1-5 MW [30], some of them stackable modules.

2.3.2 Power to Gas

Hydrogen is a highly flammable gas, so it is possible to inject some hydrogen into the natural gas grid without significant modifications to the grid or the systems that use natural gas. This application is

denominated as P2G.

Some pilot projects already in operation blend up to 20% hydrogen in localized natural gas grids [33], such as small communities or universities. Several studies support the idea that a low concentration of hydrogen (up to 15-20%) in the natural gas grid does not significantly increase the risk associated with utilization of the gas [34, 35].

Another approach is being studied at several locations, including Central do Ribatejo in Portugal by EDP [36], where a 1 MW electrolyzer produces hydrogen during ramp down periods and stores it at 300 bar (storage capacity of 400 kg which is around 13 MWh). The project plans to study the injection of hydrogen in the natural gas grid and the co-combustion of hydrogen and natural gas at a regular gas turbine. This installation is part of an international project named FLEXnCONFU that aims to integrate hydrogen and ammonia in the electrical grid [37].

2.4   Day Ahead Forecasting

Due to the intermittent nature of renewable energy sources, some forecasting method is required to estimate the production of a certain power plant in order to participate in the electricity market. Furthermore, in electricity grids with a high renewable energy penetration, the uncertainty of not knowing how much energy certain power plants will produce can induce an additional level of difficulty in balancing the generation and consumption of electricity. By being able to estimate renewable energy generation for each energy source along with the expected consumption, it becomes easier to manage the grid. For example, if it's forecasted a low production for wind and solar energy, then dispatchable power plants such as hydroelectric damns or natural gas plants must be activated to compensate. Since natural gas plants need a certain amount of time to warm up before they can generate electricity, the ability to previously forecast their need to generate power at a certain time allows for time to ensure the plant can generate energy when it's needed.

When considering energy storage, forecasting energy generation and consumption means that the operation of the energy storage system can be optimised since there is an estimate on when an energy surplus will occur (leading to the storing of electricity), or when an energy deficit will occur (leading to the discharge of electricity).

Recently, deep learning neural networks have shown promising results in their ability to forecast wind speed/power production. Models based on Long Short-Term Memory (LSTM) [38, 39] and Convolutional Neural Network (CNN) [40, 41] are the most common and are occasionally used together [42] or with a data pre-processing procedure such as Variational Mode Decomposition (VMD) [39, 41]. VMD divides an input signal into k signals of different frequency (known as modes), which helps the neural network to identify and predict patterns, further increasing the forecasts' accuracy.

Not only can deep learning neural networks be used to forecast wind speed/power production, but also to forecast electricity prices [43]. Recently electricity price forecasting has become more challenging due to the increasing renewable energy penetration in the electricity grid and the associated generation capacity uncertainty that follows [44]. This challenge requires more complex models that make use of pre-processing methods like VMD combined with multi-layer neural networks, which can better identify patterns and generate reliable estimates.

2.5   Literature Review

The annual production of hydrogen in the EU is roughly 9.75 Mt, currently being produced using carbon-intensive methods, which would require 290 TWh of electricity if the hydrogen was produced solely from electrolysis, around 10% of current production in the EU. In 2020, G.Kakoulaki et al [45] concluded that the EU has enough renewable energy resources spread throughout member countries to satisfy the hydrogen demand solely using green hydrogen, thus decarbonising the sector.

Electrolyzers can play a role in adding flexibility to an electricity grid, so a technical analysis was conducted by D. Gusain et al [46] in order to study the use of electrolyzers as flexibility service providers. A model for large scale PEMEL was developed, along with the simulation of different use cases to assess: frequency regulation, flexibility provision and long term impact analysis. For the first use case the electrolyzer's response was adequate and even though the test had a 40 minute duration no cell degradation took place. For the second case, the electrolyzer is used to correct the difference between the expected power injection and the real power injected at a certain bus. The bus had a wind farm attached, so a forecast was made of the expected power produced throughout the day. The results showed the electrolyzer ensured that the real power was equal to the forecasted power, which means an electrolyzer can be used to provide flexibility to the grid operator. In the final case, the electrolyzer was run at constant current for a year, where a drop in efficiency of 0.8% was calculated. For a duration of 5 years, the efficiency drop increases to 3.5%. It was seen that the PEMEL is well suited to provide balancing services to the grid.

The sizing of electrolyzer has to weigh numerous factors, namely the power produced by the wind farm and if there is a grid connection to provide power to the electrolyzer during low wind periods. The main advantage of the grid connection is a more consistent hydrogen production rate and the main disadvantage is not being able to guarantee 100% carbon free hydrogen due to consuming power from the grid. José G. García Clúa et al [47] state that the ratio between the wind turbine's nominal wind speed (v_N) and the mean wind speed (v_m) of the installation site and the shape coefficient of a Weibull probability function k are the main influences in sizing the nominal powers of the electrolyzer and the wind turbine. The paper concludes that for $\frac{v_N}{v_m}$ lower than 1.67 the electrolyzer makes good use of the

available turbine power, however, the wind potential of the site isn't fully exploited. On the other hand, for $\frac{v_N}{v_m}$ greater than 1.77 the opposite happens. The recommended operation point is $\frac{v_N}{v_m}$ in the range of 1.67 to 1.77, since in this range a balance between making good use of the available turbine power and exploiting the wind potential of the location is struck.

A techno-economic analysis on grid-connected hydrogen production was performed by T. Nguyen et al [48], where several electricity pricing schemes and hydrogen storage solutions were analysed. The study concludes that a real time pricing scheme yields lower Levelized Cost Of Hydrogen (LCOH) since the electrolyzer can reduce consumption during periods of high energy price and that including storage is a good alternative to increase flexibility, especially when underground storage can be implemented. A capacity factor ranging between 0.9 and 1 was found to be optimal, since it minimizes consumption during peak hours but ensures a high utilization of the CAPEX. The lowest LCOH obtained is 2.49-2.74 €/kg for AEL (2.26-3.01 €/kg for PEMEL) with underground storage in a real time pricing scheme in Ontario, competitive with hydrogen produced using Steam Methane Reform (SMR) with carbon capture which is around 2.51-3.45 €/kg.

A similar study on offshore hydrogen production with underground storage was developed by Van Nguyen Dinh et al [24], where the CAPEX and OPEX used are consistent with the forecast for offshore wind power and electrolyzers in the year 2030. The results show that for a 101.3 MW wind farm off the coast of Ireland at a sell price of 5 €/kg, the Discounted Payback Period (DPB) considering storage for 2, 7, 21 and 45 days of average hydrogen production are 7.8, 8.6, 11.1 and 16.2 years, respectively.

The wind potential in Patagonia is enormous, anywhere from 4100 to 5200 full-load hours on average, which leads to a LCOE of electricity as low as 25.6 €/MWh. In 2018 Philipp-Matthias Heuser et al [49] analysed a link between Japan and Patagonia, where hydrogen is produced and liquefied in Patagonia and shipped to Japan. The analysis estimates that the LCOH is 2.16 €/kg at the output of the electrolyzer, with an increase of 0.57 €/kg after transport to shipping port and a further 0.58 €/kg to liquefy the hydrogen and store it in liquid form, which brings the final LCOH to 3.31 €/kg. The cost of transport to Japan is 1.13 €/kg, so the cost of hydrogen upon arrival in Japan is 4.44 €/kg.

With the increasing presence of renewable energy in the grid, higher levels of curtailment in renewable power plants will take place. Considering this reasoning, a study was conducted to compare 3 scenarios using an offshore wind farm [50]: sell all electricity to the grid, all electricity is converted to hydrogen or a hybrid system where electricity is sold to the grid when prices are high and converted to hydrogen when curtailment occurs or electricity prices are low. A model was developed for a 504 MW wind farm located 14.5 km from shore and all 3 scenarios were simulated. The results obtained were a LCOE in scenario 1 of 38.1 €/MWh for 0% curtailment and 47.6 €/MWh for 20% curtailment, while the LCOH for scenario 2 is 3.77 €/kg. For scenario 3, if the hydrogen price is 4 €/kg, adding hydrogen generation provides an equal or higher NPV only for curtailment levels higher than 17%. If the hydrogen

price is 4.25 €/kg, then the level of curtailment for which hydrogen generation becomes profitable is 10%.

Another article comparing the 3 scenarios described above was written by Pengfei Xiao et al [51] in 2020. Here the electricity price for the first and third scenarios varied from 80 €/MWh to 160 €/MWh, depending on the time of day, with the hydrogen price fixed at 6.27 €/kg in the scenarios where hydrogen is produced. The article concludes that the hybrid approach yields greater economic interest compared to the other scenarios, with most of the hydrogen being produced at night when the electricity price is lower.

A slightly different approach was taken by Peng Hou et al [52], where a 72 MW offshore wind farm was considered for the production of hydrogen, with 2 possible operating scenarios. In the first scenario, all of the energy gets converted to hydrogen in an electrolyzer, stored and then converted back to electricity in a fuel cell to be sold to the grid during peak hours. In the second scenario, the electricity generated by the wind turbines can be sold to the grid or fed into an electrolyzer, with the existing possibility of buying energy from the grid when prices are extremely low. The study concludes that the first scenario isn't economically viable due to the low round trip efficiency of the electrolyzer and fuel cell. However, for the second scenario, considering a 50% capacity factor for the electrolyzer, the DPB is 24.4, 5.5 and 2.6 years and the nominal power of the electrolyzer is 5.5, 13.5 and 23.4 MW, for a hydrogen price of 2, 5 and 9 €/kg, respectively.

A model to determine the most suitable electrolyzer technology and also to compare solar and wind as the energy source of a green hydrogen production system was developed by Christian Schnuelle et al [53]. Several scenarios were included in the article, such as onshore and offshore wind as well as selecting the nominal power of the electrolyzer as 40%, 60% or 80% of the respective power plant's nominal power. Considering a fixed electricity price dependent on the installation chosen and typical annual load duration curves, the authors state that AEL proved the most economically interesting option, mainly due to higher efficiencies and improved stack life which reduces the investment on replacing stacks and lower initial investment. The lowest LCOH achieved is 4.33 €/kg. Despite being more expensive, PEMEL offer an advantage regarding energy utilization, since they can operate at a lower power and better harness the renewable resources available.

In order to compare the subject of this thesis to other green hydrogen applications, two articles regarding hydrogen production using solar energy were analysed. The first considers various locations in Morocco [54], with different types of Photovoltaic (PV) panel installations, from fixed to 2-axis tracking and a CSP installation. Even though fixed PV panels produced the lowest LCOH of 4.74 €/kg, a better balance can be achieved using 1 axis tracking, which produces 30% more hydrogen at a small LCOH increase to 4.88 €/kg.

The second article analyses not only green hydrogen production using PV or CSP to harness the

solar energy in Chile, but also the existing technologies to transport hydrogen in a higher energy density: liquefied hydrogen and ammonia carrier [19]. The lowest LCOH in 2018, 1.82 €/kg is obtained using PV, a power purchase agreement and converting the electricity to hydrogen in an AEL. In 2025, LCOH reductions are expected to be around 20% to 34%, higher in PEMEL than AEL, to a minimum value of 1.39 €/kg. The cost of liquefying hydrogen (1.28 €/kg) is lower than the cost to convert to and from ammonia (total 2.04 €/kg), but due to the higher energy density and ease of transport a case can be made for ammonia as a means of transporting hydrogen.

Both of the articles agree that despite CSP with thermal storage allowing for a much higher capacity factor, which reduces the nominal power of the electrolyzer, the reduction in CAPEX in the electrolyzer is smaller than the increase in CAPEX by using CSP instead of PV.

Regarding the applications of hydrogen, Rodica Loisel et al [55] developed a model with an off-shore wind farm to simulate the economic viability of each application individually, then combining two applications, for example P2P and P2G, and a final scenario where all applications considered are implemented. In all scenarios, the electrolyzer's nominal power is considerably lower than the wind farm's nominal power, consequently most of the energy produced is sold directly to the electricity grid at whole-sale prices, with the remaining energy being reserved for secondary and tertiary reserves. The study concludes that the most economically interesting approach is P2G, with a hydrogen price of 4.2 €/kg, however, even the most profitable approach presents a negative NPV. It should be noted that combining many applications leads to a higher investment cost and ultimately reduces the project's profit.

Focusing on P2P, where fuel cells can play a role as long term energy storage and fast acting dispatchable power plants, a review of the main fuel cell technologies was conducted in 2018 [56]. After analysing each technology, the authors conclude that since fuel cells don't have great electrical efficiencies (40% to 55%), the best way to harvest their potential is to utilize the heat generated, either for heating in case of low temperature fuel cells (PEMFC and AFC) or Combined Heat and Power (CHP) in case of high temperature fuel cells (AFC, MCFC and Solid Oxide Fuel Cell (SOFC)). Integrating CHP yields increases of 10% to 30% in efficiency. In addition, micro gas turbines can be used to provide further heat to the combined cycle, which might also lead to increases in efficiency.

A challenge associated with a high percentage of renewable power in electricity grids is frequency containment, usually assured by big synchronous generators in traditional power plants due to their high inertia. PEMFC present high current density and fast response times, consequently might be an option to help maintain the grid frequency. In order to assess the role this technology can play in frequency containment, F. A. Alshehri et al [57] developed a dynamic model to simulate PEMFC, validated that the model's response resembles the response shown in existing literature and performed a comparison between Frequency Containment Reserve (FCR) composed by PEMFC or synchronous generators. The scenarios consist of a 50 MW disturbance for different system inertia with values 100%, 50% and 25%,

for both synchronous generators or PEMFC as FCR. For all scenarios, PEMFC provides the best nadir (lowest frequency recorded) and a faster rate of frequency stabilization, while the values representing Rate-of-Change-of-Frequency remain the same for both scenarios.

Continuing with the analysis for the viability of grid-connected fuel cells, an assessment was conducted in 2013 [58]. The authors of the assessment conclude that the start up time of the fuel cell must be taken into account (around 10 minutes). Furthermore, the dynamic loading on the system severely influences the longevity of the fuel cells, a load ranging from 0-100% presented a much lower power output after 100 operating hours than a load ranging from 40-100% after 400 operating hours. As long as some requirements and the operating conditions mentioned above are respected, grid-connected fuel cells are viable.

Table 2.3 contains a summary of the LCOH observed throughout the literature review. LCOH is calculated by adding all the expenses of the project (CAPEX and OPEX correctly adjusted according to the rate of return) and dividing by the amount of hydrogen produced by the electrolyzer in kg. The cost of hydrogen is mainly influenced by the electricity cost and the cost of the required infrastructure, which means AEL typically has a lower LCOH than PEMEL due to the lower cost. The same applies to the electricity source, the lower LCOH values are observed in locations with low electricity prices, such as the electricity grid in Ontario [48], solar PV in Chile [19] or onshore wind in Patagonia [49].

Electricity Source	AEL [€/kg]	PEMEL [€/kg]
Grid	2.49-2.74 [48]	2.26-3.01 [48]
Solar PV	2.04-5.00 [19, 53]	2.71-7.98 [19, 53, 54]
Solar CSP	3.03 [19]	3.79-8.5 [19, 54]
Onshore Wind	4.33 [53]	2.73-6.61 [49, 53]
Offshore Wind	9.17 [53]	3.77-11.75 [24, 50, 53, 55]

Table 2.3: Summary of LCOH

Focusing on the day ahead forecasting, Toubeau et al [38] developed a bidirectional LSTM to forecast wind power generation, PV generation, electricity price and total system load. The model generates either a Gaussian distribution or a non-parametric predictive distribution to characterize the uncertainty of the prediction errors. Instead of returning a single forecasted value for each of the 24 hours of the following day, the developed model returns loss quantiles for the pairs: 1-99%, 5-95%, 10-90%, 25-75%, making it possible to assess the difficulty and uncertainty for the different forecasted variables since tighter quantile intervals lead to lower uncertainty, representing an easier variable to forecast. The authors conclude the developed model yields the most accurate forecasts of any tested method (including the tool used by the system operator to forecast the four variables), with the best results (lowest error and tightest quantile intervals) for the PV generation and total system load.

A spatiotemporal approach for wind speed forecasting was taken by Hong et al [40], consisting of a 2D CNN that utilizes not only the previous wind speed data for the target location, but also the previous

wind speed data for locations in the vicinity of the target location. More specifically, in the case study the target location is Fuhai, an offshore wind farm near Taiwan, and the other 6 locations used as input to the developed model are in China, South Korea and Philippines. The results show that using the 2D CNN with the data from the target and adjacent locations provides considerably lower forecasting errors than using a 1D CNN with only the target location data. The model was also compared to various combinations of other popular neural networks used in wind speed forecasting, namely the Multilayer Feedfoward Neural Network (MFNN) and LSTM. In this comparison, the developed model still presented the best forecasting accuracy, with a Mean Average Percent Error (MAPE) around 7-15% depending on the season.

A hybrid system consisting of wavelet packet decomposition, CNN and a CNN combined with a LSTM was developed by Liu et al [42] for short term wind speed forecasting, named the WPD-CNNLSTM-CNN. The wind speed data is from the northeast of China, has a time step of 10 minutes and forecasts were made for 10, 20 and 30 minutes. Firstly the wind data is decomposed in wavelets, the lowest frequency one is analysed by a CNN followed by a LSTM and the remaining wavelets are analysed by a CNN. The performance of the model was compared to other commonly used forecasting methods and it was concluded that the WPD-CNNLSTM-CNN provided the lowest errors, with a MAPE ranging from roughly 1.6% to 4.1% for a 1-step and 3-step prediction, respectively.

VMD is another method often used to decompose a signal into modes and was used in the following two articles to aid in hourly day ahead forecasting. The first analysed the performance of a recursive LSTM that generates each of the 24 hourly values individually, using the previously calculated values to forecast the following value and a direct LSTM, where all 24 values are forecasted at the same time [39]. For each mode there is a neural network to identify patterns and perform the forecasts based on that single mode, with the final result being the sum of the output of all neural networks. The model aims to forecast wind power generation and the results show that while both LSTM configurations provide adequate accuracy, the direct LSTM has a MAPE of 10% for 24 hour day ahead forecasting, compared to 22% for the recursive LSTM.

In the second article [41], a 1D CNN was chosen to process the modes and generate the wind speed forecasts. Two data sets (both with a time step of 10 minutes) were used to ensure that the model works for several locations. The time horizon of the predictions is 32 time steps, which for these data sets means that the farthest prediction is 5 hours and 20 minutes ahead. The developed model presents considerably lower forecasting errors when compared to similar forecasting tools for both data sets, with a MAPE of around 20%, meaning it can be used in wind speed forecasting.

For electricity price forecasting similar methods to the ones mentioned above can also be used, where a simple time series forecasting is done based on previous values. Nonetheless, better results might be achieved if the forecasted renewable energy generation for the following day was used as an

input in forecasting the electricity prices, since electricity prices are influenced by renewable energy generation (higher renewable energy generation leads to lower electricity prices and vice versa). Zhang et al [43] developed a model that not only uses previous electricity prices, but also forecasted wind and solar energy generation to forecast hourly day ahead electricity prices. In total there were 4 models developed, the first 3 independently forecast electricity price, wind generation and solar generation only using their respective time series previous values, while the final model takes the output of the 3 other models and uses the renewable energy forecasts to refine the forecasted electricity prices. The authors conclude the developed model can accurately predict electricity prices, presenting a Mean Average Error (MAE) of 3.74 €/MWh.

3

Proposed Models

The proposed models are presented in this chapter, starting with a brief overview on how the simulations were conducted, how each component was modelled, how the systems were optimised to maximize revenue and how the economic analysis was performed. The simulation is performed for both hydrogen producing systems as well as for a system representing a conventional offshore wind farm.

The data regarding the project's location was obtained in http://windatlas.xyz for two locations off the coast of Galicia, Spain. These locations were chosen since they present some of the highest wind speeds close to shore in the Iberian Peninsula. The first location is 25 km off the coast (latitude 43.93, longitude -8.21) and the second is 50 km (latitude 44.14, longitude -8.32). By performing the simulation in two locations, an analysis on how distance to shore affects the systems can be conducted. The data consists of:

- Wind Speed → The wind speed in m/s at every hour from 2015 to 2019, rounded to the first decimal place.

- Distance to Shore

- Measuring Height → The height at which the wind speed was measured, which is around 100 m.

- Prandtl Number → Used in Prandtl's law to calculate the wind speed at a different height than the measuring height.

For the pricing data, the hydrogen's sale price is considered constant throughout the project's lifetime and the day ahead market price for electricity is obtained in MIBEL for the same years as the recorded wind speed data, along with the positive and negative imbalance prices for each hour.

3.1   Simulation Overview

The simulation is performed to assess if the integration of hydrogen into offshore wind farms is economically interesting from the perspective of an investor. It contains an optimisation model and an economic model applied to the three systems: offshore electrolyzer system, onshore electrolyzer system and a conventional wind farm. The hydrogen produced can either be directly sold as hydrogen or used in the fuel cell, generating electricity to sell in the electricity market.

The optimisation model takes a different approach to the singularities of each system, always coordinating the operation of the system with the goal of maximizing revenue. In the economical analysis, performance metrics are calculated to provide an easy assessment regarding the profitability of each system. Using cost projections for 2030 and 2050, the simulation also aims to provide an insight into the future of hydrogen production from offshore wind energy.

The conventional wind farm is composed only by the wind farm and the electrical transmission system, without any hydrogen integration. Thus, it is useful in establishing a comparison between the hydrogen producing systems and a normal wind farm, acting as a benchmark. In the simulations, hydrogen integration is preferable whenever hydrogen producing systems yield higher profit than the conventional wind farm, providing an easy assessment method.

Regarding the hydrogen producing systems, one crucial factor is sizing the electrolyzer and fuel cell since a larger electrolyzer/fuel cell will result not only in higher revenues but also in higher initial investment and maintenance costs. This sizing should be done as a ratio of the wind farm's nominal power, on account that a higher powered wind farm should be accompanied by a higher powered electrolyzer and vice-versa. The ratio that maximizes NPV is denominated as optimal ratio.

The optimal ratio's calculations aren't trivial, so a trial and error approach was taken where several combinations for the sizing of the electrolyzer and fuel cell were tested and the ones that yielded the highest NPV were selected as the optimal ratios. Considering that the conditions that influence the value of the optimal ratios are hydrogen price, electricity price and wind speed, the ratios must be calculated for every hydrogen price present in the analysis.

The remaining components (desalination unit, compressor, storage and pipeline) are sized according to their performance requirements. For example, the desalination unit and compressor are sized taking into account the maximum water flow required to feed the electrolyzer and maximum hydrogen production rate, respectively.

The first steps for all three systems are the same: calculating the number of required turbines to achieve the desired nominal power of the wind farm, simulating the wind power production and forecasting day ahead wind power production and electricity prices. In order to calculate the required number of turbines, the nominal power of the wind farm is divided by the nominal power of the chosen wind turbine, then the resulting value is rounded up to ensure the wind farm has the desired nominal power. For example, if the desired power is 100 MW and the chosen turbine has a nominal power of 9.5 MW, then the number of turbines is $\frac{100}{9.5} \approx 11$ and the wind farm's nominal power is $11 \times 9.5 = 104.5$ MW.

From this point onwards, the simulation differs depending on the system. For the onshore electrolyzer system the next steps are:

- Sizing the electrolyzer, fuel cell and desalination unit

- Sizing the compressor and storage

- Calculating electrical losses

- Onshore electrolyzer optimisation

For the offshore electrolyzer system the next steps are:

33

- Sizing the electrolyzer, fuel cell and desalination unit

- Sizing the pipeline

- Sizing the compressor and storage

- Calculating hydrogen production

- Offshore electrolyzer optimisation

Finally, for the conventional wind farm the only necessary step is to calculate the electrical losses, due to the fact that there is no hydrogen production so all electricity gets sold to the grid. The optimisations for the onshore and offshore electrolyzer are detailed in chapters 3.3.1 and 3.3.2, respectively.

With all the technical aspects calculated, the economic analysis can be done. In this analysis the revenue streams and expenses are calculated, along with performance metrics used to assess the economically viability of each system and to compare the systems amongst themselves. The economic model is further detailed in chapter 3.4.

3.2 Component Modelling

3.2.1 Wind Farm

A 9.5 MW offshore wind turbine from Vestas was selected, it has a hub height of 110 m and its power curve is available in The Wind Power. Even though more efficient turbines capable of achieving higher capacity factors will certainly be available in the future, this wind turbine model was used in the projections for 2030 and 2050. Effectively, this is a conservative approach that affects all systems, which means the comparisons made in this thesis should be applicable to future (more efficient) wind farms.

To calculate the wind speed at the rotor height, Prandtl's law is used according to equation 3.1.

$$u_{hub} = u_{meas} \cdot \frac{log(h_{hub}/z_0)}{log(h_{meas}/z_0)} \tag{3.1}$$

where u_{hub} is the wind speed at the height of the wind turbine's hub, u_{meas} is the wind speed at the height the wind speed was measured, h_{hub} is the height of the wind turbine's hub, h_{meas} is the height at which the wind speed was measured and z_0 is the Prandtl number.

Afterwards, the wind speed at the rotor height is converted to the generated electrical power for a single turbine using the turbine's power curve. The final step is to multiply this value by the number of turbines and by 0.95 to represent, among others, wake losses and the losses in the collector system. Repeating this process for every hour of the recorded data, a time series of the energy in MWh generated by the wind farm is obtained.

3.2.2 Electrolyzer

Due to the reasons stated in chapter 2.2.1, the chosen electrolyzer is a PEMEL. The important parameters are the electrolyzer's specific energy consumption, $c_{sp,el}$ (in kWh/kg), specific water consumption, $c_{wa,el}$ (in m³/kg), nominal power (in MW), operating range (in % of nominal power) and the lifetime of the stack (in years). The operating range is the minimum and maximum power at which the electrolyzer can operate, for most PEMEL it's 1-100% of the nominal power, however, it can vary for different technologies.

The modelled electrolyzer is Hydrogenics' PEMEL [22] and its technical specifications can be found in table 3.1. The specific consumption and the stack's lifetime in 2030 and 2050 was estimated according to projections for a typical PEMEL in the same time frame. The only exception is the stack's lifetime in 2030, where the average value between the lifetime of the stack in 2020 and 2050 was considered on account of no information being found regarding the stack's lifetime in 2030. The operating range and water consumption was considered the same for the 3 time periods since no future projections were found, considering that technologies tend to improve over time this is a conservative approach that won't lead to overly optimist results.

Table 3.1: Electrolyzer's technical specifications

Component	Present	2030	2050
specific energy consumption [kWh/kg]	53.28 [22]	47 [15]	45 [15]
specific water consumption [m³/kg]	0.01554 [22]		
operating range [%]	1-100 [22]		
stack lifetime [years]	8 [15]	10 [15]	12 [15]

Several parameters were calculated to aid in modelling the electrolyzer and simplifying the optimisation framework. The first parameter is maximum hydrogen production rate (H_{max-p} in kg/h) of the electrolyzer, which is a useful feature to size other components of the system and is calculated using equation 3.2.

$$H_{max-p} = \frac{P_{el} \cdot R_{max}}{c_{sp,el}} \quad \text{[kg/h]} \tag{3.2}$$

where P_{el} is the electrolyzer's nominal power, R_{max} is the upper bound of the operating range and $c_{sp,el}$ is the electrolyzer's specific energy consumption in MWh/kg. The other parameters are maximum and minimum operating power ($P_{el_{max}}$ and $P_{el_{min}}$, respectively), calculated using equations 3.3 and 3.4.

$$P_{el_{max}} = P_{el} \cdot R_{max} + H_{max-p} \cdot c_{sp,cp} \quad \text{[MW]} \tag{3.3}$$

$$P_{el_{min}} = P_{el_{max}} \cdot \frac{R_{min}}{R_{max}} \quad \text{[MW]} \tag{3.4}$$

where P_{el} is the electrolyzer's nominal power, R_{max} and R_{min} are the upper and lower bound of the operating range, respectively, H_{max-p} is the maximum hydrogen production rate and $c_{sp,cp}$ is the compressor's specific energy consumption. These parameters will be used in the optimisation framework since they represent the maximum and minimum power for which the electrolyzer can produce hydrogen.

With the previous variables calculated, the hydrogen production based on the power provided to the electrolyzer in each time step can be calculated according to equation 3.5.

$$\text{hydrogen produced} = \begin{cases} 0, & P_{in} < P_{el_{min}} \\ \frac{P_{in}}{c_{sp,el}+c_{sp,cp}}, & P_{el_{min}} \leq P_{in} < P_{el} \\ H_{max-p}, & P_{in} \geq P_{el} \end{cases} \quad \text{[kg]} \tag{3.5}$$

where P_{in} is the power being fed into the electrolyzer, $P_{el_{min}}$ is the electrolyzer's minimum operating power, $c_{sp,el}$ and $c_{sp,cp}$ is the specific energy consumption of the electrolyzer and compressor, respectively and P_{el} is the electrolyzer's nominal power. The compressor's consumption must be considered since the hydrogen is compressed as soon as it exits the electrolyzer and the energy to do so also comes from the wind farm, slightly reducing the amount of energy available for the electrolyzer.

3.2.3 Electrical Transmission losses

The electrical transmission system was modeled as a constant loss of 3.5% of the transmitted energy [21]. This approximation was considered due to the low impact that the transmission losses have on the techno-economic analysis and that the models for electrical transmission systems aren't trivial, which would have added complexity and negatively impacted the simulation's execution time.

3.2.4 Compressor

At least one compressor is needed in each of the hydrogen producing systems. For the offshore electrolyzer system, the compressor increases the hydrogen's pressure once it leaves the electrolyzer and injects it into the transmission pipeline. For the onshore electrolyzer system it compresses the hydrogen in order to store or sell it. Regarding the compressor's specific energy consumption, $c_{sp,cp}$, the typical value for compressing the hydrogen from 30 to 100 bar is around 1 kWh/kg [19], so this value was considered in the simulation. The compressor's nominal power (P_{cp} in MW) can easily be calculated using equation 3.6.

$$P_{cp} = c_{sp,cp} \cdot H_{max-p} \quad \text{[MW]} \tag{3.6}$$

where $c_{sp,cp}$ is the compressor's specific energy consumption and H_{max-p} is the electrolyzer's maximum hydrogen production rate.

3.2.5 Pipeline

In order to calculate the required pipeline's diameter, equation 3.7 was used, obtained in [59].

$$D = \sqrt[5]{7.569 \cdot 10^5 \cdot Z \cdot T_{in} \cdot L \cdot d \cdot \lambda \cdot \left(\frac{p_b}{T_b}\right)^2 \cdot \frac{Q_n^2}{p_{in}^2 - p_{out}^2}} \quad \text{[m]} \tag{3.7}$$

In this equation, D is the pipeline's diameter in m, Z is the hydrogen's compressibility factor (roughly 1.02), T_{in} is the hydrogen's temperature at the inlet of the pipeline (assumed 15 ℃), L is the pipeline's length (either 25 km or 50 km, depending on the chosen location), d is hydrogen's relative density at the outlet pressure, λ is the linear friction coefficient (around 5.3x10^{-12}), p_b and T_b are the base pressure (101325 Pa) and temperature (288 K), respectively, Q_n is the maximum hydrogen flow in Nm^3/s and p_{in} and p_{out} are the pressures at the inlet (90 bar) and outlet (70 bar) of the pipeline, respectively.

The relative density is obtained by dividing the density of the hydrogen at the outlet by ρ_b (the air density at 1 atm of pressure and at 15 ℃), which is around 1.225 kg/m^3. In hydrogen's case, for pressures under 100 bar the increase in density is roughly linear to the increase in pressure, so a linear relation is assumed between a theoretical density of 0 kg/m^3 if the hydrogen's pressure is 0 bar until a density 7.8 kg/m^3 if the pressure is 100 bar [16]. Effectively, this approximation means that the density of hydrogen at a given pressure is the pressure in bar times 0.078 (denominated density coefficient and expressed as f_ρ), so the relative density can be calculated using equation 3.8.

$$d = \frac{p_{out} \cdot f_\rho}{\rho_b} \tag{3.8}$$

The maximum hydrogen flow can be obtained using equation 3.9, where H_{max-p} is the electrolyzer's maximum hydrogen production rate. The constant 3600 is used to convert H_{max-p} from kg/h to kg/s and the constant 11.1 is to convert from kg/s to Nm^3.

$$Q_n = \frac{H_{max-p} \cdot 11.1}{3600} \quad \text{[Nm}^3\text{/s]} \tag{3.9}$$

Once the pipeline's diameter is obtained, its value converted into inches. To ensure the pipeline isn't undersized, the value in inches is rounded up and presented as an even number. Since the pipeline also acts as a means of storage, the amount of hydrogen (M_p in kg) that can be stored is calculated using equation 3.10.

$$M_p = p_{out} \cdot f_\rho \cdot V_p \quad \text{[kg]} \tag{3.10}$$

where p_{out} is the pressure at the outlet of the pipeline (70 bar), f_ρ is the density coefficient (0.078) and V_p is the pipeline's volume in m^3 obtained using equation 3.11.

$$V_p = L \cdot \pi \cdot \frac{D^2}{4} \ \ [\text{m}^3] \tag{3.11}$$

where L is the pipeline's length in m and D is the pipeline's diameter in m.

3.2.6 Storage Tanks

The storage tanks are sized based on the desired amount of hydrogen to store, the storage pressure and in the offshore electrolyzer system the amount of hydrogen that can be stored in the pipeline (expressed as M_p in kg). The pipeline's storage capacity is considered when sizing the storage tanks due to the significant amount of storage that a large pipeline can provide. The maximum storage amount of hydrogen is quantified as the electrolyzer's hydrogen production if the electrolyzer is running at nominal power during n days, where n is set at 1 day. Then, this amount is converted to kg of hydrogen (expressed as M) using equation 3.12.

$$M = 24 \cdot n \cdot H_{max-p} \ \ [\text{kg}] \tag{3.12}$$

where H_{max-p} is the electrolyzer's maximum hydrogen production rate in kg/h. Afterwards, the required volume (expressed as V in m^3) for the storage tanks is obtained with equation 3.13, where p_s is the storage pressure (100 bar), f_ρ is the density coefficient (0.078) and M_p is the pipeline's storage capacity in kg.

$$V = \frac{M - M_p}{p_s \cdot f_\rho} \ \ [\text{m}^3] \tag{3.13}$$

The reserve capacity is the amount of hydrogen that the storage tanks need to have in order to sell hydrogen and is specified in % of the maximum storage capacity. For example, if the reserve capacity is set at 50%, no hydrogen will be sold until the storage tanks are 50% full so that the system always has a reserve of hydrogen in case it needs to generate electricity using the fuel cell. The fuel cell can be used as long as there is enough hydrogen stored, even if the stored hydrogen is less than the reserve capacity.

3.2.7 Fuel Cell

The modeling of the fuel cell takes into account two parameters: the nominal power and an efficiency curve. Since this fuel cell will mainly operate during peak electricity prices and to compensate forecast errors, the chosen technology is the PEMFC and the efficiency curve implemented in the model is a generic efficiency curve for a PEMFC (figure 3.1).
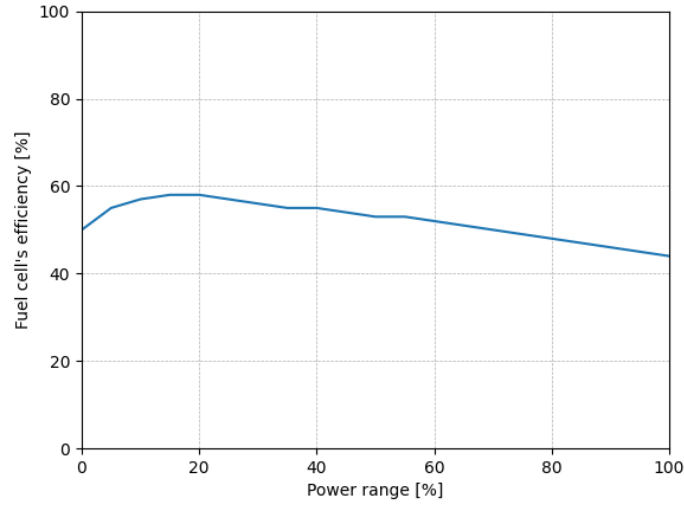
Figure 3.1: Fuel Cell's efficiency curve. Source: [60]

The fuel cell's maximum hydrogen consumption rate (H_{max-c} in kg/h) is useful when optimising the operation of the hydrogen producing systems. Its value is calculated based on the nominal power and full load efficiency, as is represented in equation 3.14.

$$H_{max-c} = \frac{P_{fc}}{\eta_{100\%} \cdot H_{LHV}} \quad \text{[kg/h]} \tag{3.14}$$

where P_{fc} is the fuel cell's nominal power, $\eta_{100\%}$ is the fuel cell's efficiency at full load (0.43) and H_{LHV} is hydrogen's lower heating value (0.03333 MWh/kg)

3.2.8 Desalination Unit

The average consumption for a Reverse Osmosis desalination unit is around 4 kWh/m³ [61] and knowing that a PEMEL's water consumption is around 0.01554 m³/kg [22], the energy spent desalinating water to produce 1 kg of hydrogen is 0.062 kWh. Since the modelled electrolyzer's specific consumption is at most 53 kWh/kg (lower values are considered for 2030 and 2050), the desalination unit's consumption is several orders of magnitude lower and therefore wasn't included in the model.

The economic attribute is the most relevant part to the simulation and is the reason the desalination unit was modelled. In order to size the unit, the maximum amount of water the electrolyzer needs per day (W_{daily} in m³/day) is calculated according to equation 3.15.

$$W_{daily} = 24 \cdot c_{wc,el} \cdot H_{max-p} \quad \text{[m³/day]} \tag{3.15}$$

where $c_{wc,el}$ is the electrolyzer's specific water consumption (0.01554 m³/kg) and H_{max-p} is the

39

electrolyzer's maximum hydrogen production rate in kg/h.

3.3   Hourly Optimisation

Considering that both hydrogen production systems can generate either hydrogen or electricity, an optimisation algorithm needs to be developed to control how the production of each resource occurs. The main objective of the algorithm is to always maximize the revenue based on current wind power production, electricity price and many other factors.

This optimisation is also crucial in highlighting the added flexibility of integrating hydrogen in offshore wind farms since the systems can be controlled in real time to minimize regulation costs. Regulation costs in the day ahead market occur whenever there is an imbalance between the electricity bidded the previous day and the actual electricity sold to the grid, which is mainly due to the uncertainty of forecasting wind power production. The hydrogen production systems have the ability to regulate their electricity output (with some restrictions) to ensure the electricity sold matches the electricity bid and no regulation costs are paid.

For the onshore electrolyzer system, two optimisation algorithms were developed. The first represents the day ahead operation and uses the forecasts to determine what the electricity bid should be. The second algorithm represents the real time operation and uses the previously placed bid, the real power production and electricity price to determine how to distribute the wind farm's electricity between selling electricity to the grid and producing hydrogen.

Since this optimisation isn't trivial and requires calculating a significant amount of variables, the algorithms were implemented as a Mixed-Integer Linear Program (MILP). This method consists of defining an objective function to maximize or minimize, the problem's variables and the constraints between the variables. One constraint is, for example, the relation between electricity fed into the electrolyzer and the amount of hydrogen produced. This optimisation is done on an hourly basis due to the fact that the actual electricity production is only known in real time, so for every hour of the simulation the day ahead MILP and real time MILP are used.

On the other hand, for the offshore electrolyzer system only a real time algorithm was developed, since all electricity sold to the grid is generated in the fuel cell, which can easily be adjusted to match the previous day bid. Considering that this optimisation is simpler than the onshore electrolyzer system's optimisation, no MILP was implemented for this system.

3.3.1   Onshore Electrolyzer System

The first step is to establish the electricity bids for the entire simulation time frame using the day ahead optimisation model. This model takes into consideration the forecasts for electricity price and energy

production and calculates the optimal bidding strategy to maximize revenue using a MILP. From the calculations, the electricity bid for each hour is saved to be used in the real time optimisation. The objective function is the maximization of the revenue at a given hour, defined in expression 3.16, and the constraints are defined in equations 3.17-3.21.

$$\text{max revenue} = sp_h^{for} \cdot bid_h + ph \cdot hp_h \tag{3.16}$$

$$ep_h^{for} = ee_h + bid_h \tag{3.17}$$

$$hp_h \leq \frac{ee_h}{c_{sp,el} + c_{sp,cp}} + H_{max-p} \cdot (1 - y_{ee}) \tag{3.18}$$

$$hp_h \leq H_{max-p} \cdot y_{ee} \tag{3.19}$$

$$ee_h < P_{el_{min}} + P_{el_{max}} \cdot y_{ee} \tag{3.20}$$

$$ee_h \geq P_{el_{min}} - P_{el_{max}} \cdot (1 - y_{ee}) \tag{3.21}$$

In the previous equations sp_h^{for} is the forecasted day ahead electricity price at hour h, bid_h is the day ahead market electricity bid at hour h (it can take a negative value when buying electricity from the grid to produce hydrogen is profitable), ph is the price of hydrogen, hp_h is the hydrogen produced at hour h, ep_h^{for} is the forecasted electricity production at hour h, ee_h is the energy fed into the electrolyzer at hour h, y_{ee} is a binary value that is 0 when ee_h is lower than the electrolyzer's minimum operating power and 1 if it's higher, as can be seen in Appendix A, H_{max-p} is the electrolyzer's maximum hydrogen production rate and $P_{el_{max}}$ and $P_{el_{min}}$ are the maximum and minimum powers for which the electrolyzer can produce hydrogen. The range of values each variable can take are defined in equations 3.22 - 3.24.

$$0 \leq hp_h \leq H_{max-p} \tag{3.22}$$

$$0 \leq ee_h \leq P_{el_{max}} \tag{3.23}$$

$$-P_{el_{max}} \leq bid_h \leq P_{el_{max}} \tag{3.24}$$

With the electricity bids determined, the final step is to perform the real time optimisation, which uses the actual wind power production and electricity price along with all other relevant information to decide how to operate the system. In order to transform this problem into a MILP, the objective function (equation 3.25) and the constraints (equations 3.26 - 3.44) were defined.

$$\text{max revenue} = sp_h \cdot es_h + ph \cdot (hp_h - hc_h) - RC_h \tag{3.25}$$

$$es_h = ep_h - ee_h + efc_h \tag{3.26}$$

$$imb_h = es_h - bid_h \tag{3.27}$$

$$ss_h = ss_{h-1} + hp_h - hc_h - hs_h \tag{3.28}$$

$$hp_h \leq \frac{ee_h}{c_{sp,el} + c_{sp,cp}} + H_{max-p} \cdot (1 - y_{ee}) \tag{3.29}$$

$$hp_h \leq H_{max-p} \cdot y_{ee} \tag{3.30}$$

$$hs_h \geq ss_h - ss_{res} - ss_{max} \cdot (1 - y_{ss}) \tag{3.31}$$

$$hs_h \leq ss_{max} \cdot y_{ss} \tag{3.32}$$

$$RC_h \geq imb_h \cdot (sp_h - sp_h^+) - 1000 \cdot P_{Park} \cdot (1 - y_{imb}) \tag{3.33}$$

$$RC_h \geq imb_h \cdot (sp_h + sp_h^-) - 1000 \cdot P_{Park} \cdot y_{imb} \tag{3.34}$$

$$efc_h \leq \frac{0.55 \cdot hc_h \cdot h_{LHV}}{1000} + 1000 \cdot P_{fc} \cdot y_{fc} \tag{3.35}$$

$$efc_h \leq \frac{0.477 \cdot hc_h \cdot h_{LHV}}{1000} + 1000 \cdot P_{fc} \cdot (1 - y_{fc}) \tag{3.36}$$

$$imb \leq 2 \cdot P_{Park} \cdot y_{imb} \tag{3.37}$$

$$imb \geq -2 \cdot P_{Park} \cdot (1 - y_{imb}) \tag{3.38}$$

$$\frac{efc_h}{P_{fc}} \leq 0.63 + y_{fc} \tag{3.39}$$

$$\frac{efc_h}{P_{fc}} \geq 0.63 + (1 - y_{fc}) \tag{3.40}$$

$$ss_h \leq ss_{res} + ss_{max} \cdot y_{ss} \tag{3.41}$$

$$ss_h \geq ss_{res} - ss_{max} \cdot (1 - y_{ss}) \tag{3.42}$$

$$ee_h < P_{el_{min}} + P_{el_{max}} \cdot y_{ee} \tag{3.43}$$

$$ee_h \geq P_{el_{min}} - P_{el_{max}} \cdot (1 - y_{ee}) \tag{3.44}$$

From the wind and pricing data along with the previously calculated electricity bids, information regarding electricity produced (ep_h), electricity bid (bid_h), electricity price (sp_h), positive imbalance price (sp_h^+) and negative imbalance price (sp_h^-) is already known. These 5 values are fixed for each hour of the simulation, so they are considered constants by the real time optimisation model. The remaining constants have the same value throughout the optimisation, they are hydrogen price (ph), electrolyzer and compressor specific energy consumption ($c_{sp,el}$ and $c_{sp,cp}$), maximum hydrogen production rate (H_{max-p}), hydrogen storage reserve (ss_{res}), maximum hydrogen storage (ss_{max}), wind farm's nominal power (P_{Park}), hydrogen's lower heating value (h_{LHV}), fuel cell's nominal power (P_{fc}) and maximum and minimum powers for which the electrolyzer can produce hydrogen ($P_{el_{max}}$ and $P_{el_{min}}$). The variables are

electricity sold at hour h (es_h), hydrogen sold at hour h (hs_h), energy fed into the electrolyzer at hour h (ee_h), electricity produced by the fuel cell at hour h (efc_h), hydrogen produced at hour h (hp_h), hydrogen consumed by the fuel cell at hour h (hc_h), current amount of hydrogen stored at hour h (ss_h), previous amount of hydrogen stored at hour h-1 (ss_{h-1}), electricity imbalance at hour h (imb_h) and regulation costs at hour h (RC_h).

Certain operations performed in the optimisation framework of the onshore electrolyzer system aren't linear, more specifically, the fuel cell's energy generation, regulation costs, storage management and hydrogen production. Considering that the optimisation problem is solved as a MILP, all constraints must be linear, so in order to implement these 4 calculations binary variables were defined. A more detailed explanation can be found in Appendix A, but in essence binary variables work by selecting which constraints actually dictate how a certain variable should be calculated. The constraints for each binary variable are defined in equations 3.37 - 3.44.

The range of values each variable can take are defined in equations 3.45 - 3.51, where H_{max-p} is the fuel cell's maximum hydrogen consumption. The only variables without limitations to their values are regulation costs (can be a positive or negative value) and electricity sold since it can be a negative value when the electricity price is low enough that buying electricity to generate hydrogen is profitable.

$$hs_h \geq 0 \tag{3.45}$$

$$0 \leq ee_h \leq P_{el_{max}} \tag{3.46}$$

$$0 \leq efc_h \leq P_{fc} \tag{3.47}$$

$$0 \leq hp_h \leq H_{max-p} \tag{3.48}$$

$$0 \leq hc_h \leq H_{max-c} \tag{3.49}$$

$$0 \leq ss_h \leq ss_{max} \tag{3.50}$$

$$-P_{Park} \leq imb_h \leq P_{Park} \tag{3.51}$$

Both MILPs were implemented in Python using Pulp and three solvers were tested: CBC, GLPK and Gurobi. Gurobi was considerably faster than the rest, so it's the clear choice to use in the simulations.

3.3.2 Offshore Electrolyzer System

The offshore electrolyzer optimisation is much simpler then its onshore counterpart since all electricity generated is fed into the electrolyzer and the previously stored hydrogen acts as a buffer to compensate any forecast errors regarding electricity production in the fuel cell. This optimisation is also done on an hourly basis, where the first step is to assess the hydrogen storage and store all hydrogen produced

until the storage reaches the required reserve capacity, only then can hydrogen be sold or fed into the fuel cell.

When there is a surplus of hydrogen, the optimal ratio between hydrogen sold compared to hydrogen fed into the fuel cell that maximizes revenue is calculated and the respective values for electricity and hydrogen sold are saved to be used in the economic analysis. This decision is based on the forecasted electricity price, so the electricity bid is placed in the day ahead market. Considering that the energy source is a fuel cell, the electricity generation can perfectly match the bid since the fuel cell's power can be easily adjusted.

3.4 Economic Model

The economic model uses the results from the technical analysis and evaluates the project from an economic point of view by calculating revenue, expenses and the performance metrics to evaluate each system. This analysis uses the following economic parameters regarding the expected project's return and loan conditions:

- Rate of return (default 7%)

- Project's lifetime (default 25 years)

- Initial investment (default 20%)

- Loan duration (default 20 years)

- Loan interest rate (default 5%)

The process for the economic analysis is similar for all systems, first electricity and hydrogen revenues are calculated then the yearly revenue is obtained by adding both revenue streams for entire year. The yearly revenue is extended until it has a length equal to the project's lifetime, for example if the wind and pricing data has a time frame of 3 years and the project's lifetime is 5 years, the yearly revenue (R_n) would be $[R_1, R_2, R_3, R_1, R_2]$.

In order to calculate the CAPEX and OPEX, standard values (in €/MW, €/kg, etc) are used to quickly estimate the investment required for each component based on its dimension. For each system the total CAPEX and yearly OPEX costs are calculated taking into account the components that each system has. For example, for the conventional wind farm the CAPEX is calculated as described in equation 3.52, where $CAPEX_{WT}$ and $CAPEX_{ET}$ are the CAPEX for the wind turbines and electrical transmission system, respectively, in €/MW.

$$CAPEX = CAPEX_{WT} \cdot P_N + CAPEX_{ET} \cdot P_N \ \ [€] \tag{3.52}$$

Table 3.2 contains all of the CAPEX values used in the model. Regarding the pipeline's CAPEX for 2020, it is calculated using equation 3.53 obtained in [62], where D is the pipeline's diameter in mm and the result is in €/m.

$$CAPEX_{Pipeline} = 0.0022 \cdot D^2 + 0.86 \cdot D + 247.5 \ [\text{€/m}] \tag{3.53}$$

No cost projections for 2030 and 2050 were found for the pipeline's CAPEX, however, in [6] it was considered that the pipeline's CAPEX decreased 1% every year, so this measure was adopted in this thesis. In practice, the pipeline's CAPEX in 2030 and 2050 is the 2020 value multiplied by 0.99^{10} and 0.99^{30}, respectively. While in [6] this 1% yearly decrease was only considered for the pipeline, in this thesis the same procedure was applied to the storage tanks since it is a conservative approach and no CAPEX projections for 2030 and 2050 were found.

The compressor's CAPEX reduction was also derived from [6], where a 30% reduction was considered for 2030 and 70% for 2050. Regarding the fuel cell, CAPEX values were found for 2020 and 2030, however, since no values were found for 2050, a 1% yearly decrease from the 2030 CAPEX was considered.

The electrical transmission system's CAPEX was obtained in [63]. In this paper, a techno-economic analysis is performed for floating offshore wind farms in 5 locations off the coast of California, providing detailed costs of each component. Considering that the electrical transmission system's cost is directly related to the distance to shore, a linear relation between distance to shore and total electrical system cost can be calculated using the data from the 5 locations. The paper also presents cost projections until 2050, so a linear relation can be calculated for each of the considered years in this thesis. The linear relations between distance to shore (d in km) and CAPEX of the electrical transmission system (shortened to ETS in tables and equations) for 2020, 2030 and 2050 are:

$$CAPEX_{ETS}^{2020} = 6.111 \cdot d + 217.5 \ [\text{k€/MW}] \tag{3.54}$$

$$CAPEX_{ETS}^{2030} = 5.247 \cdot d + 183.5 \ [\text{k€/MW}] \tag{3.55}$$

$$CAPEX_{ETS}^{2050} = 4.735 \cdot d + 166.4 \ [\text{k€/MW}] \tag{3.56}$$

Table 3.2: CAPEX values for all components

Component	CAPEX		
	2020	2030	2050
Floating OWF	4.532 M€/MW [6]	2.354 M€/MW [6]	1.533 M€/MW [6]
Central platform	223 k€/MW [6]	188 k€/MW [6]	125 k€/MW [6]
Electrolyzer	700 k€/MW [15,48,50]	395 k€/MW [15]	175 k€/MW [15]
Desalination unit	1700 €/(m^3/day) [64]	1420 €/(m^3/day) [64]	907 €/(m^3/day) [64]
Compressor	3.9 M€/MW [49]	2.72 M€/MW [6,49]	1.18 M€/MW [6,49]
Pipeline	equation 3.53 [62]	0.99^{10}*equation 3.53 [6,62]	0.99^{30}*equation 3.53 [6,62]
Storage	439 €/kg [19]	397 €/kg [6,19]	325 €/kg [6,19]
Fuel cell	1600 k€/MW [65]	425 k€/MW [65]	340 k€/MW [6,65]
ETS	equation 3.54 [63]	equation 3.55 [63]	equation 3.56 [63]

Regarding the OPEX values, whenever the cost was expressed as a percentage of CAPEX for 2020 and no sources were found for 2030 and 2050, the value for 2020 was considered for the remaining years. Table 3.3 contains all of the OPEX values used in the model, except for the central platform and electrical transmission system whose OPEX is already included in the floating offshore wind farm's OPEX.

The fuel cell's OPEX was considered equal to the electrolyzer due to their similar structure and components. The OPEX for the electrolyzer consists of a flat 2% of CAPEX every year plus the cost of replacing the stack every 8 to 12 years. Since no information was found regarding the stack's lifetime in 2030, the average value between the stack's lifetime in 2020 and 2050 was considered as the correct lifetime for 2030. The cost of the stack for 2030 is considered to be 200 k€/MW. This value was achieved by assuming the same CAPEX reduction in the electrolyzer between 2020 (700 k€/MW) and 2030 (395 k€/MW), as can be seen in equation 3.57. The same procedure was applied to desalination unit's OPEX for 2030 and 2050.

$$OPEX_{stack}^{2030} = \frac{395}{700} \cdot 350 = 200 \ [\text{k€/MW}] \tag{3.57}$$

Table 3.3: OPEX values for all components

Component	OPEX		
	2020	2030	2050
Floating OWF	197 k€/MW/year [6]	102 k€/MW/year [6]	66.4 k€/MW/year [6]
Central platform	-		
Electrolyzer	2%CAPEX/year [19] + 350 k€/MW/8 years [15]	2%CAPEX/year [19] + 200 k€/MW/10 years [15]	2%CAPEX/year [19]+ 88 k€/MW/12 years [15]
Desalination unit	0.25 €/m^3 [66]	0.21 €/m^3 [64,66]	0.13 €/m^3 [64,66]
Compressor	4%CAPEX/year [48,49]		
Pipeline	4%CAPEX/year [62]		
Storage	4%CAPEX/year [19]		
Fuel cell	2%CAPEX/year [15]		
ETS	-		

The economic model also provides numeric metrics to assess the viability of all the proposed systems and to facilitate the comparison between them. Two types of metrics are calculated, the first are metrics to evaluate and quantify the profitability project as a whole and the second are to evaluate the cost of production of each commodity, also know as levelized cost.

3.4.1 Investment Distribution

In order to better understand how the investment is divided among the components of each system, the CAPEX and OPEX distributions of both hydrogen producing systems were calculated. The systems were sized with the same dimensions used to plot the LCOH curves in chapter 5.3, which are an electrolyzer ratio of 95% and 100% for the offshore electrolyzer system and onshore electrolyzer system, respectively. In both systems the fuel cell was sized to 5%, according to the reasoning presented in 5.4.

Figure 3.2 contains the CAPEX distribution of the offshore electrolyzer system for 2020 and 2030. The legend of the figure has the color and name of each component, along with the respective percentages for 2020 (the first value) and 2030 (the second value).

Figure 3.2: CAPEX distribution for the offshore electrolyzer system for the location 25 km from shore. Electrolyzer ratio 95% and fuel cell ratio 5%.

The total CAPEX in 2020 is around 611 M€ and in 2030 it drops by 44% to 344 M€. For both scenarios, the offshore wind farm represents over 70% of the CAPEX, representing the high investment requirements of this technology. Even though all components are less expensive in 2030, some constitute a bigger percentage of the investment in 2030 when compared to 2020, such as the central platform, storage tanks and pipeline. This is caused by the significant cost reduction in more recent and not yet matured technologies, such as floating offshore wind farms and PEMEL.

Figure 3.3 contains the CAPEX distribution of the onshore electrolyzer system for 2020 and 2030.

Similar to the previous figure, the legend of the figure has the color and name of each component, along with the respective percentages for 2020 (the first value) and 2030 (the second value).
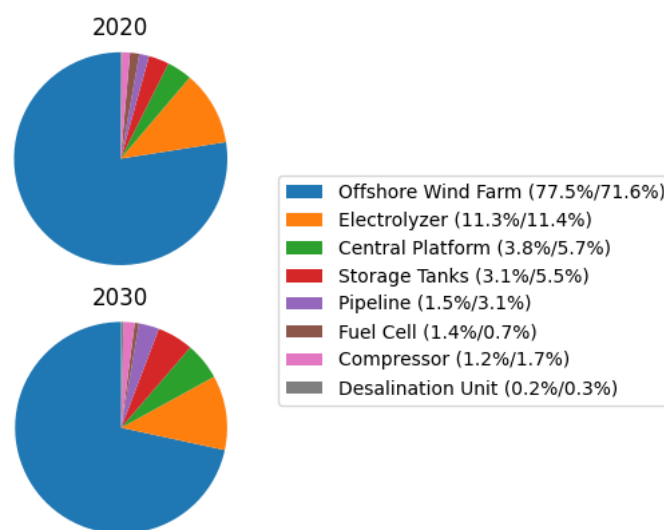

Figure 3.3: CAPEX distribution for the onshore electrolyzer system for the location 25 km from shore. Electrolyzer ratio 100% and fuel cell ratio 5%.

The total CAPEX in 2020 is roughly 623 M€ and in 2030 it's around 350 M€, a 44% cost reduction. Similar to the offshore electrolyzer system, the offshore wind farm composes over 70 % of the investment required, with the electrolyzer being the second most expensive component.

Through the analysis of the CAPEX distributions of both systems, a conclusion present in some articles of the literature review is verified. This conclusion states that the LCOH of green hydrogen is mainly influenced by the cost of renewable electricity, more specifically, the CAPEX of the offshore wind farm is 70% of the entire system CAPEX.

Another important remark is that the two most expensive components used in the simulations (floating offshore wind farm and PEMEL), are extremely recent technologies that aren't yet implemented on a large scale. This elevates the uncertainty surrounding the actual cost of developing either of the hydrogen producing systems, especially the accuracy of the cost projections, hence a sensitivity analysis like the one presented in chapter 5.5 needs to be performed.

Looking at the OPEX distributions, the cost of replacing the PEMEL stack isn't included since it only occurs every 8-12 years depending on the simulation's year and its cost is similar to the yearly OPEX for the entire system. Figure 3.4 and figure 3.5 contain the yearly OPEX for the offshore electrolyzer system and onshore electrolyzer system, respectively.
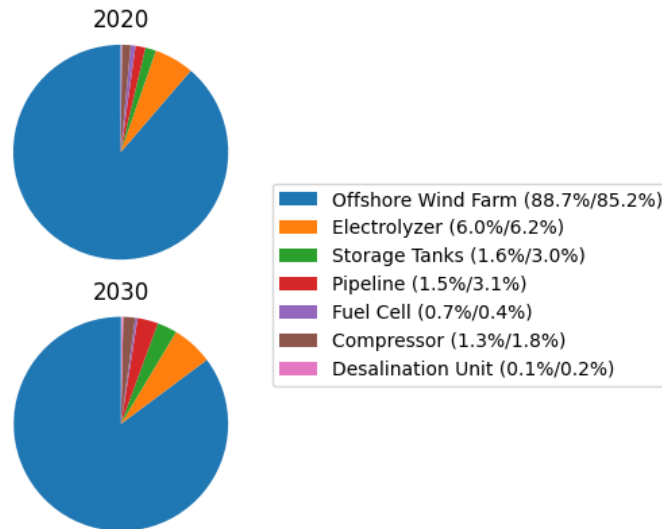
Figure 3.4: OPEX distribution for the offshore electrolyzer system for the location 25 km from shore. Electrolyzer ratio 95% and fuel cell ratio 5%.
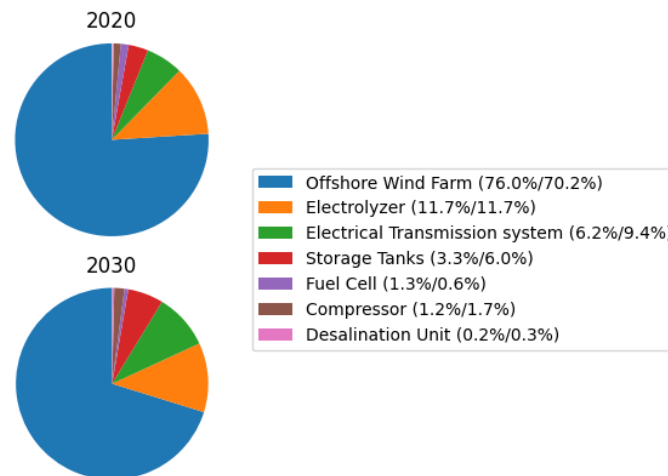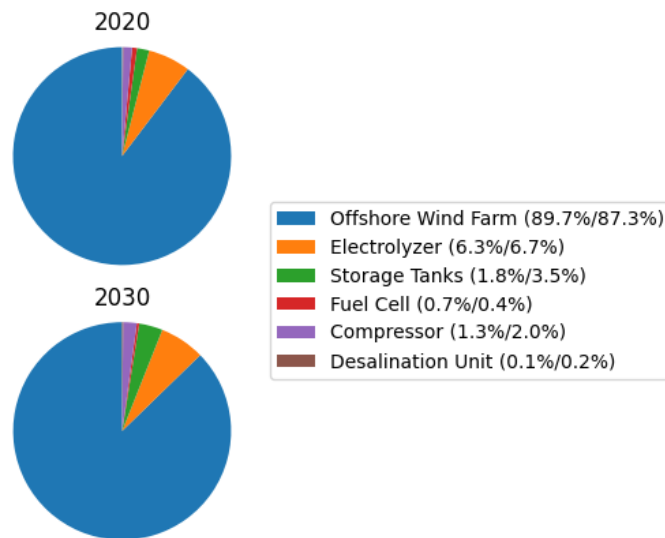

Figure 3.5: OPEX distribution for the onshore electrolyzer system for the location 25 km from shore. Electrolyzer ratio 100% and fuel cell ratio 5%.

The OPEX for the offshore wind farm represents almost the entirety of the total system OPEX, over 85% for all distributions presented above. The second more significant cost is the maintenance of PEMEL, hovering around 6% of the total system OPEX. Similar to the CAPEX distributions, the two more expensive technologies regarding maintenance and operation costs are the floating offshore wind farm and PEMEL, reinforcing the uncertainty of actual cost of implementing these systems and the need for a sensitivity analysis.

3.4.2 Performance Metrics

When performing an economic analysis, it's important to ascertain if the investment is entirely paid by equity or if a loan is requested, meaning part of the investment comes from equity and the remainder from the loan. In the case where a loan has been requested, annuities must be payed according to the loan's value, duration and interest rate. Another aspect to consider is adjusting the revenues, CAPEX and OPEX values according to the rate of return so everything is in the same year, since revenue/expenses can't be compared across several years.

The equations to adjust total revenue, total CAPEX and total OPEX according to the rate of return are 3.58, 3.59 and 3.60, respectively, where N is the project's lifetime in years, R_n is the revenue for year n, R_t is the total revenue, I_t is the total investment, I_i is the initial investment in %, a is the rate of return, $OPEX_y$ is the yearly amount spent on OPEX, a_{loan} is the loan's interest rate and N_{loan} is the loan's duration. The yearly revenue R_n is calculated using equation 3.61, where $R_n^{H_2}$ and R_n^E are the revenues from selling hydrogen and electricity in year n, respectively, and RC_n is the regulation cost in year n. When calculating the total OPEX, the second sum in equation 3.60 represents the cost of replacing the electrolyzer stack (I_s), which only occurs every N_{stack} years. The number of times the stack is replaced is $\frac{N}{N_{stack}}$ rounded down to an integer. The annuity of the loan can be calculated using equation 3.62.

$$R_t = \sum_{n=1}^{N} \frac{R_n}{(1+a)^n} \ \text{[€]} \tag{3.58}$$

$$CAPEX_{total} = I_t \cdot I_i + \sum_{n=1}^{N_{loan}} \frac{annuity}{(1+a)^n} \ \text{[€]} \tag{3.59}$$

$$OPEX_{total} = \sum_{n=1}^{N} \frac{OPEX_y}{(1+a)^n} + \sum_{n=1}^{N/N_{stack}} \frac{I_s}{(1+a)^{n \cdot N_{stack}}} \ \text{[€]} \tag{3.60}$$

$$R_n = R_n^{H_2} + R_n^E - RC_n \ \text{[€]} \tag{3.61}$$

$$annuity = (1 - I_i) \cdot I_t \cdot \frac{a_{loan} \cdot (1 + a_{loan})^{N_{loan}}}{(1 + a_{loan})^{N_{loan}} - 1} \ \text{[€]} \tag{3.62}$$

To assess the profitability of a project, the two metrics chosen are NPV and Internal Rate of Return (IRR). NPV subtracts all the expenses from the revenue generated throughout the lifetime of the project, properly adjusted according to the project's rate of return, as can be seen in equation 3.63. A NPV of 0 € denotes that the specified rate of return was exactly the achieved rate of return of the project, a positive value implies that the project will exceed the expected return and a negative value implies the project is not economically viable at the specified rate of return.

$$NPV = R_t - CAPEX_{total} - OPEX_{total} \ \text{[€]} \tag{3.63}$$

The IRR on the other hand is the maximum rate of return on the project, providing an estimate on the return on the investment made in the project. Essentially, the IRR is the rate of return for which the NPV is 0, meaning its value can be obtained through an iterative procedure where the rate of return is increased from 0 in increments of 0.5% until the NPV is negative. A linear interpolation (equation 3.64) is then performed, where a_1 is the highest rate of return that yields a positive NPV (NPV_1) and a_2 is the lowest rate of return that yields a negative NPV (NPV_2).

$$IRR = 100 \cdot (a_1 - (a_2 - a_1)\frac{NPV_1}{NPV_2 - NPV_1}) \ \ [\%] \tag{3.64}$$

3.4.3 Levelized Cost

The levelized cost is the average cost of producing a certain product for a plant over the course of its lifetime. Only the LCOH is calculated for the hydrogen producing systems, mainly due to the amount of electricity generated in the offshore electrolyzer system and that in the onshore electrolyzer system electricity is both sold and bought, so there isn't a clear definition on how to calculate LCOE in these circumstances. These values are calculated by dividing the total expenses of the plant throughout its lifetime by the total amount of hydrogen (in kg) or electricity (in MWh) generated by the plant also throughout its lifetime. It should be noted that the electricity purchase expenses incurred to produce hydrogen must be considered when calculating LCOH.

The equations to calculate the LCOH and LCOE are equation 3.65 and equation 3.66, respectively, where H_{2_n} is the amount of hydrogen generated in kg in year n, E_n^g is the total amount of electricity generated in MWh in year n, E_n^p is the total amount of electricity purchased in MWh in year n to produce hydrogen, N is the project's lifetime and a is the project's rate of return.

$$LCOH = \frac{CAPEX_{total} + OPEX_{total} + \frac{E_n^p}{(1+a)^n}}{\sum_{n=1}^{N} \frac{H_{2_n}}{(1+a)^n}} \ \ [\text{€/kg}] \tag{3.65}$$

$$LCOE = \frac{CAPEX_{total} + OPEX_{total}}{\sum_{n=1}^{N} \frac{E_n^g}{(1+a)^n}} \ \ [\text{€/MWh}] \tag{3.66}$$

One important remark is that both hydrogen producing systems can also generate electricity, even more so the onshore electrolyzer system that is directly connected to the grid. This can reduce the significance of the levelized costs of electricity and hydrogen since the system generates both products, so the total expenses weren't spent to produce a single product.

The effect is especially present when low amounts of a certain product are produced when compared to the other product, which leads to dividing the total expenses of the project by the small amount of product. For example, if the electricity price is always extremely high and the hydrogen price is low, the

onshore electrolyzer will prioritize selling electricity over producing hydrogen, so the LCOH is going to have a relatively high value. While this is technically correct, it doesn't translate the reality of the entire system since, in this example, most of the revenue comes from electricity.

4

Day Ahead Forecasting

4.1 Theoretical Background

Since the day ahead bids in MIBEL must be placed before 12:00 CET the previous day, a forecast of electricity production and electricity price at each hour is necessary to reduce regulation costs and help to better optimise the operation of the systems. To do so, a neural network was chosen due to its ability to learn and detect patterns in time series forecasting. More specifically, a neural network based on a Convolutional Neural Network (CNN), which are heavily used in image processing to detect patterns, however, they also have the ability to be used in time series forecasting.

When it comes to a CNN, a convolution is a multiplication of a set of weights (known as a filter or kernel) with the input data. A dot product is used to multiply a filter-sized patch of the input and the filter, consisting of the element-wise multiplication between the patch of the input and the filter, which is then summed, producing a single value. Convolutional layers work by calculating the dot product of n filters of a certain size to an input sequence, generating a single number based on the sequence of numbers encapsulated by the filter. Then, the filter is moved across the entire input sequence with a specified stride, so the output of each convolutional layer is composed of the result of all dot products.

For time series forecasting, the 1D CNN is often used which means the convolutional layers only need to apply the filters in one dimension. Figure 4.1 shows an example of a 1D convolutional layer, where a filter of size K is applied to an input sequence. If the input sequence had a length of T and the convolution's stride was 1, then the first dimension of the output would be the number of possible positions of a filter in the input sequence (T-K + 1) and the second dimension would be the number of filters, F.
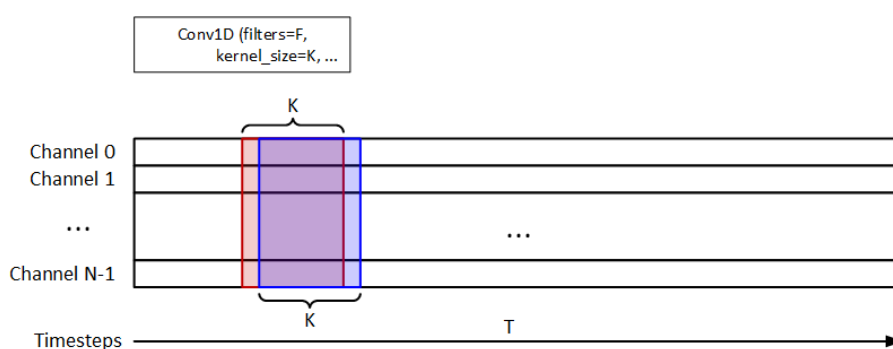
Figure 4.1: 1D convolutional layer

The remaining layers used in the neural network are the fully connected layer, the flatten layer and the upsampling layer. Appendix B provides additional information regarding the mentioned layers.

In terms of pre-processing the data, one important step is to normalize the entire data set, which means rescaling the data from the original range so that all values are within the range of 0 and 1. This operation can be done by applying equation 4.1, where x is the value to rescale, max is the

maximum value in the data set and min is the minimum. Normalization's advantages are, among others, accelerating the training of the network and allowing for the use of greater learning rates.

$$x_{norm} = \frac{x - min}{max - min} \tag{4.1}$$

Instead of using as an input the actual values of wind power and electricity price, a decomposition of the input signal into secondary and simpler signals is performed to greatly improve the forecasts' accuracy. These secondary signals are known as modes and the sum of all modes is equal to the original signal. To serve as an example, figure 4.2 contains a signal that isn't immediately recognizable, however, when the signal is decomposed into modes (figure 4.3) it's easy to observe that the original signal is merely the sum of a cosine and a sine of different frequencies.

Figure 4.2: Original signal in the mode decomposition example

Figure 4.3: Modes obtained in the mode decomposition example

In this thesis, the chosen decomposition technique is VMD. When using VMD, the normalization of the data should by applied after the decomposition to each mode obtained from the original signal.

4.2   Implementation

The developed model consists of an adaptation from an article included in the literature review [41]. The authors designed and trained a 1D CNN that forec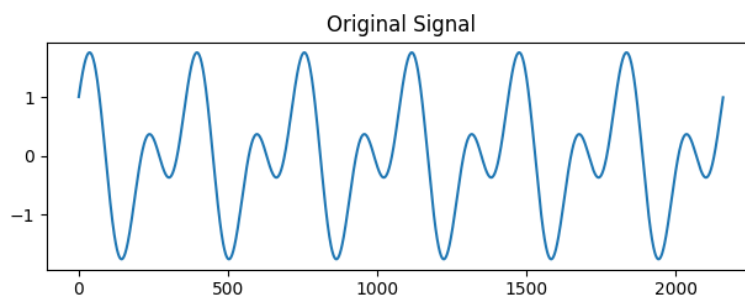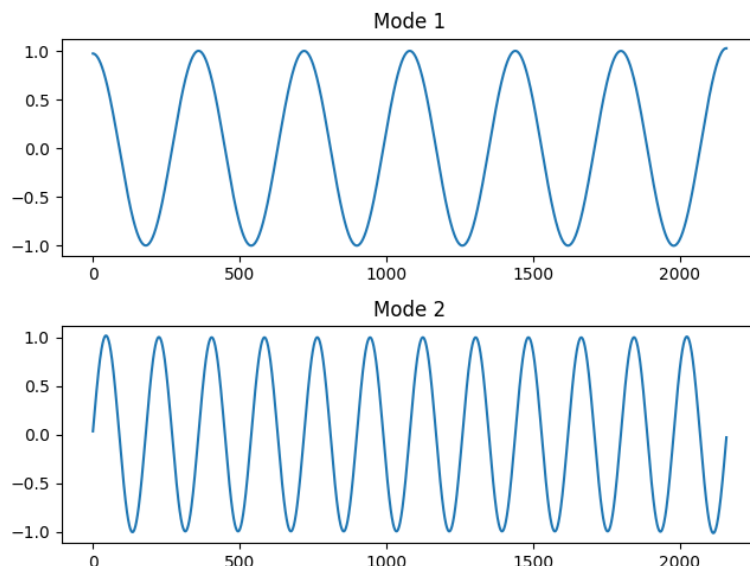asts wind power production with a horizon of 32 time steps. Since each time step of the wind data is 10 minutes, the model generates forecasts for the next 5 hours and 20 minutes. The neural network is composed of 3 consecutive convolutional layers, a flatten layer, a fully connected layer, an upsampling layer, a convolutional layer followed by another upsampling layer and convolutional layer. The wind power production is pre-processed before being used as an input for the neural network: first the input signal is decomposed into 4 modes using VMD and then the data is normalized.

Two structural changes were implemented to make the model more suitable to the scenario at hand, the first was changing the final layers of the neural network so that it outputs 24 values instead of 32, one for each hour of the following day. The second adaptation was changing the number of modes the model received as an input. When deciding on how many modes to use in VMD a balance must be struck between accurate signal decomposition and computation time, so a test was conducted to assess the accuracy of applying VMD with varying number of modes to both data sets.

A higher number of modes leads to a more accurate decomposition, however, the computation time and memory usage increase significantly. The chosen number of modes was 10, since it provides a MAPE of under 3% in the decomposition of electricity prices data set and under 7% for the wind power production data set. The MAPE is calculated using equation 4.2, where every value in the original signal is compared to the sum of the equivalent value of all modes, repeating this step for the entire data set.

$$MAPE_{VMD} = 100 \cdot \sum_{t=0}^{n} \frac{(\sum_{i=1}^{10} mode[i][t]) - signal[t]}{n} \; \text{[\%]} \tag{4.2}$$

The model is a CNN that receives 64 hours of input data and returns the 24 hours of the following day, with a small distinction between forecasting wind power production and electricity prices. Taking into account that the day ahead bids in MIBEL must be placed before 12:00 CET the previous day, the forecast must be made with a 12 hour gap between present time and the first forecasted value. For example, if the present day was January 1st and the objective was to forecast wind power production for January 2nd then the forecast will be made at 12:00 in January 1st (hour h) and will use as input the last 64 hours $[h - 64; h]$, with the prediction being the 24 hours of January 2nd, which is $[h + 12; h + 36]$.

There are two possible approaches when forecasting wind power production, either forecasting the wind power directly or forecasting the wind speed and then converting the results to power production using the wind turbine's power curve. Both approaches were tested and the most accurate forecasts were obtained when forecasting the wind power production directly, hence it is the chosen method in this thesis.

In the case of electricity price forecasting, the present day electricity prices are set the previous day (December 31st in the example) for the 24 hours of January 1st, so even though the forecast will be made at 12:00, the prices for the remainder of the day are already known and are used in the forecast. This corresponds to the same time frame of prediction $[h+12; h+36]$, however the input is now $[h-52; h+12]$.

An example of VMD applied on 64 hours of wind power production (figure 4.4) can be seen in figure 4.5.
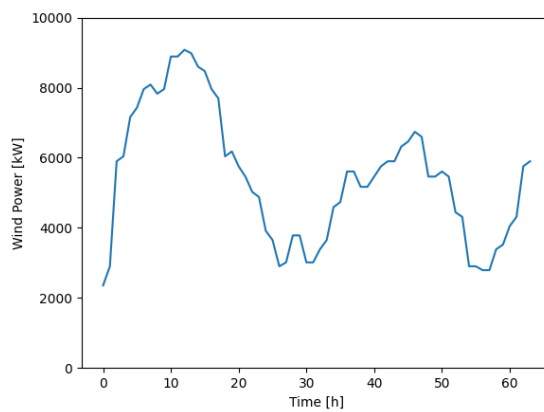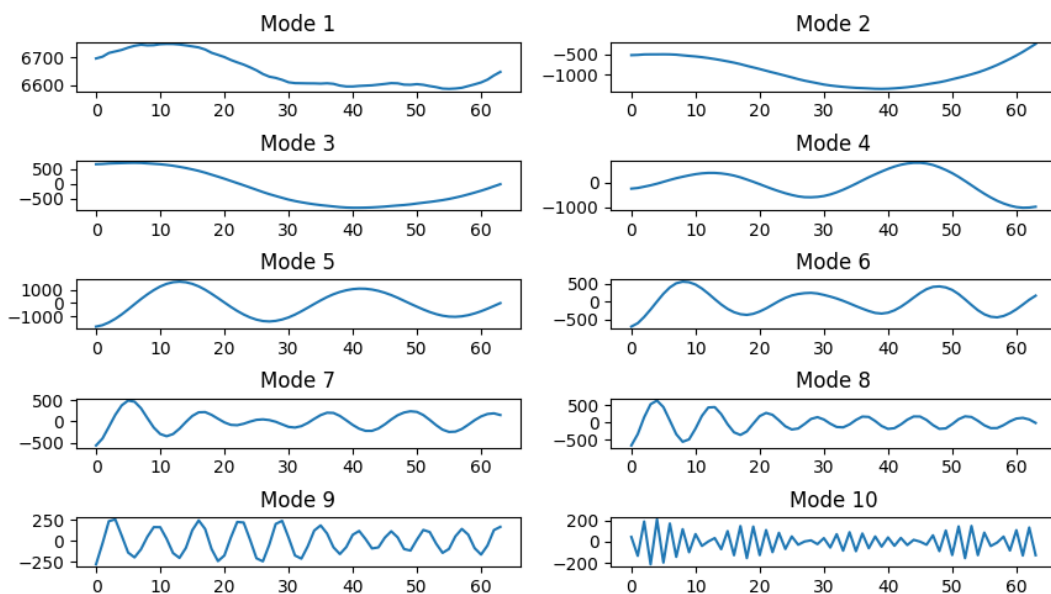

Figure 4.4: Original signal

Figure 4.5: 10 mode VMD

When training a neural network, the parameters that regulate how the learning process is conducted are called hyperparameters, which have to be manually adjusted until the neural network is functioning at the required level. These hyperparameters include:

- The overall structure of the neural network (number of layers, number of units per layer, etc)

- Number of epochs

- Batch size

- Optimiser (controls the learning rate)

- Loss function

Hyperparameter tuning isn't an exact science with a method to estimate the best value for each hyperparameter. Instead, the values can be adjusted manually after analysing the previous training attempts of the neural network. The other option is implementing a grid search, where every combination is tested and the one that leads to the lowest errors is selected. In this thesis the hyperparameters were tuned manually using a trial and error approach, since grid searching is an extremely inefficient method and good results were obtained with the manually adjusted hyperparameters.

The overall structure of the neural network wasn't altered except for the final convolutional layer, where a filter of size 9 is required to convert the output's length from 32 to 24. The number of epochs must be large enough to give the neural network time to learn, but not too large so that it induces overfitting. Overfitting is when the neural network becomes overly tailored to the training set, which leads to considerably worse results when applied to a new data set. The chosen number of epochs was 5 for the electricity price model and 25 for the wind power production model. The difference can be attributed to the fact that wind power production is harder to forecast, as is shown in chapter 4.3. The batch size was set at 64 and the chosen optimiser was $Adam$.

The loss function controls how the neural network weighs the errors it has made, attributing a loss value to each prediction which influences how the neural network rates the results of previous attempts. The chosen loss function was the mean square error, a commonly used function since it prioritizes minimizing bigger errors over smaller ones.

The model was implemented in Python, using Pandas to manage the data sets, Keras for the neural network and vmdpy library [67] to implement VMD.

4.3 Performance

When working with time series forecasting, a baseline test is often done to assess the difficulty in forecasting the desired data set and to provide a measure of the developed model's performance compared to a simpler method. In this thesis the chosen baseline test is repeating the values for the previous day, quantifying the repetitiveness of the data set by comparing the values to be forecasted with the previous day values.

The performance metrics chosen to evaluate the model are Root Mean Square Error (RMSE), MAE and MAPE. RMSE is useful to determine if the forecasting error is roughly constant throughout the data set or if there are certain moments where the forecasting error is substantially bigger than the average, which would mean that the model isn't always reliable. It is calculated according to equation 4.3, where n is the number of samples, $\hat{y}_i$ is a forecasted value and y_i it the actual value.

$$RMSE = \sqrt{\sum_{i=1}^{n} \frac{(\hat{y}_i - y_i)^2}{n}} \tag{4.3}$$

MAE is calculated according to equation 4.4 and is the average value of the forecasting error across the data set. When compared to RMSE, it is useful to determine the mean error as well as if the error is roughly constant, since a similar value of MAE and RMSE implies a roughly constant error without a meaningful amount of large errors.

$$MAE = \frac{1}{n} \sum_{i=1}^{n} |\hat{y}_i - y_i| \tag{4.4}$$

MAPE is calculated according to equation 4.5 and represents the average forecasting error in %, providing a simple and understandable manner to evaluate and compare models.

$$MAPE = \frac{100}{n} \sum_{i=1}^{n} \frac{|\hat{y}_i - y_i|}{y_i} \ [\%] \tag{4.5}$$

4.3.1 Wind Power Production

The wind speed data sets were obtained in Wind Atlas off the coast of Galicia, Spain (the first one 25 km from shore and the second 50 km from shore). The data set consists of hourly wind speeds from 2010 to 2019, with the first 5 years being used to train the neural network and the final 5 years as the test set since the techno-economic simulation is also ran in the same time frame. Due to the different wind profiles of each location, the training of 2 neural networks was necessary so that each one can be trained for only one location.

The neural networks were trained using the 9.5 MW offshore wind turbine [68] so that it can easily be scaled to the desired wind farm's dimension by multiplying the forecasted values by the number of wind turbines, resulting in wind power production forecast for the entire wind farm. Despite being rare, in certain tests the forecasted values were slightly negative or higher than the turbine's nominal power. Since both scenarios are impossible, any value above the wind turbine's nominal power is rounded down to the turbine's nominal power and any negative value is rounded to 0.

An example of the predictions and actual values of wind power production for 6 randomly selected days from the test set located 25 km from shore can be observed in figure 4.6 and the performance

metrics for both test sets can be found in table 4.1.
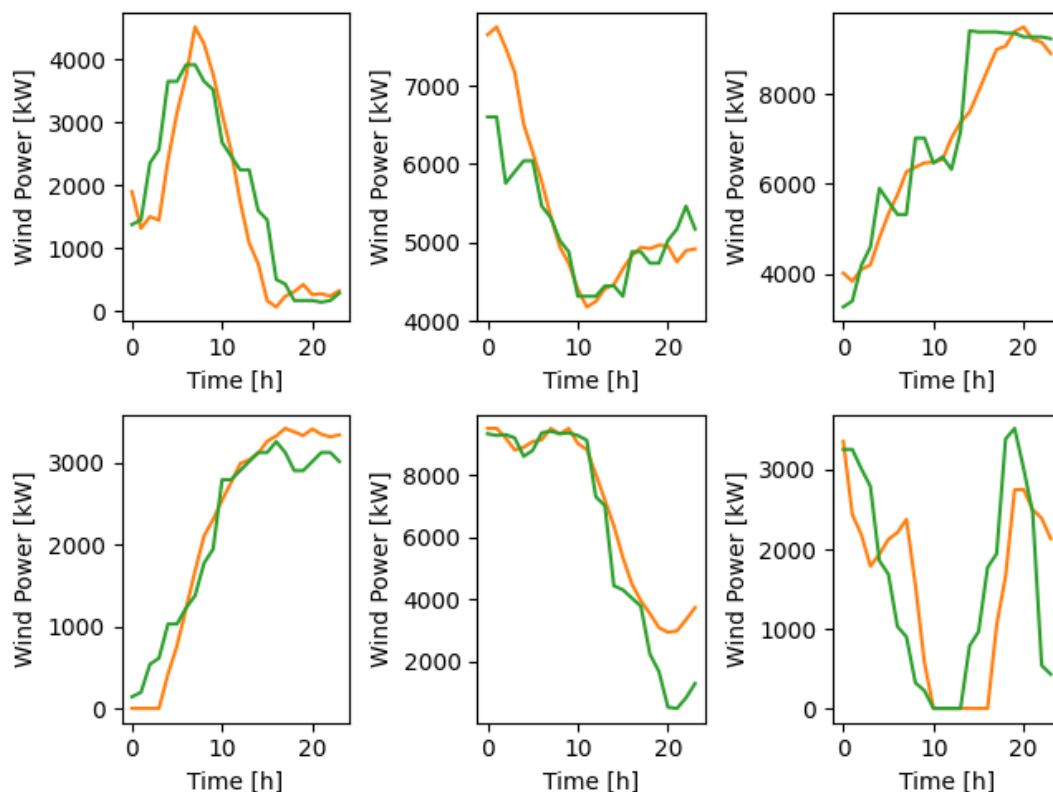
Figure 4.6: Wind power production forecast sample for a 9.5 MW Vestas offshore wind turbine in the location 25 km from shore (Green line is actual power production and orange is forecasted)

Table 4.1: Performance metrics for wind power production forecast

Model		RMSE [kW]	MAE [kW]	MAPE [%]
25 km from shore	Neural Network	859	592	33
	Baseline	4274	3218	232
50 km from shore	Neural Network	665	443	23
	Baseline	4323	3242	220

The baseline test has a MAPE of over 200% in both cases, meaning that the wind power production of a certain day isn't similar to the wind power production of the previous day. The neural networks provide much better forecasts, with errors several times lower than the baseline test. A MAE of 592 kW for the location 25 km from shore indicates that on average, the forecasts are within 0.6 MW of the actual power production. The neural network provides more accurate forecasts for the location furthest from shore, mainly due to the more consistent wind with less abrupt changes and higher mean wind speed.

The examples in figure 4.6 show that the model accurately tracks the wind power production throughout the day, having the most difficulty when sudden power production changes occur, as is the case in the third image around hour 13. For the location furthest from shore the results are even better, so any

conclusion drawn from figure 4.6 can be applied to both locations.

4.3.2 Electricity Price

The electricity price data set was obtained in REN's website [69] and contains the MIBEL's electricity prices from 2010 to 2019. The first 5 years were used as the training set and the remaining 5 years as the test set in order to match the time frame of the techno-economic simulation.

In MIBEL the electricity price for Spain and Portugal is the same as long as there is no congestion in the electricity transmission between both countries. If there isn't enough transmission capacity to transport the required amount of power from one country to the other then a market split occurs and the electricity price between both countries is no longer equal. Whenever a market split occurred, the electricity price considered in the forecasting model and overall simulation was Spain's price since the wind farm is located on Spanish waters.

An example of the predictions and actual values of the electricity price for 6 randomly selected days from the test set can be observed in figure 4.7 and the performance metrics for the test set can be found in table 4.2.
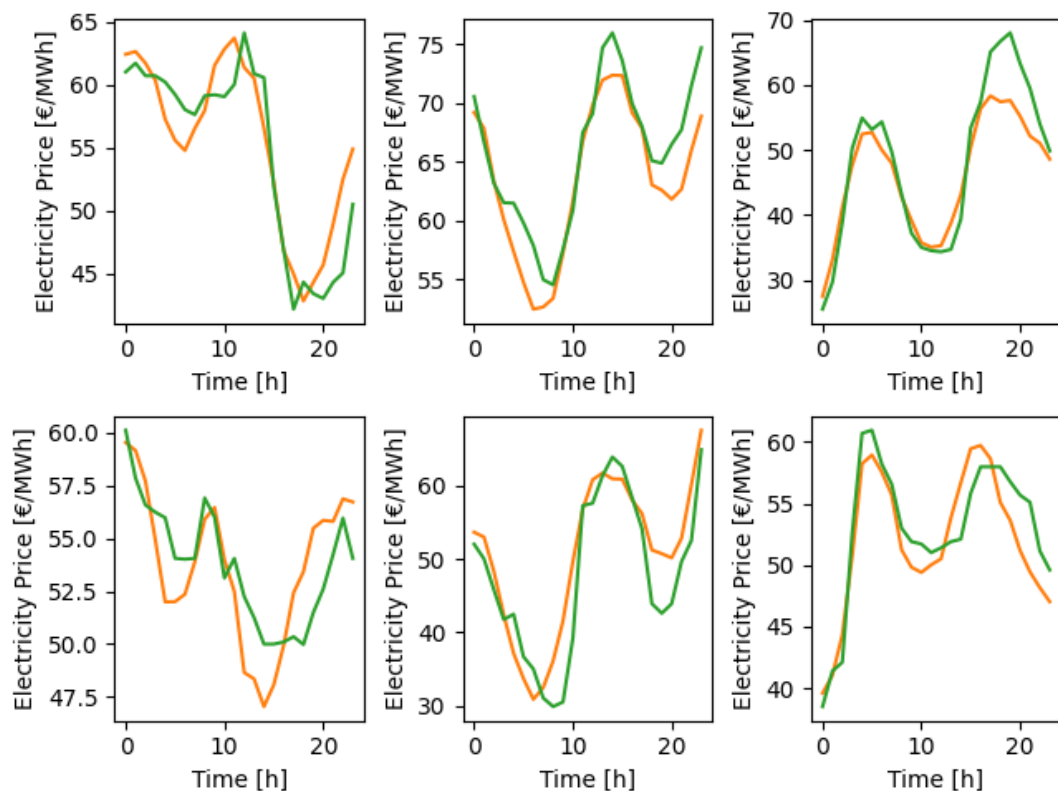

Figure 4.7: Electricity price forecast sample (Green line is actual electricity price and orange is forecasted)

61

Table 4.2: Performance metrics for electricity price forecast

Model	RMSE [€/MWh]	MAE [€/MWh]	MAPE [%]
Neural Network	3.19	2.31	6
Baseline	8.54	5.88	18

Unlike the baseline test for wind power production, the baseline test for the electricity price forecasting presents relatively low errors, indicating that electricity price is easier to predict and setting a higher standard for the neural network. The errors are low enough to even be used in the simulation, however, the developed model is able to forecast the electricity prices with a greater accuracy. Considering that it has an average error of 2.31 €/MWh and a MAPE of around 6%, this neural network provides substantially better results than the baseline test and the neural network for wind power production forecasting.

An important feature of MIBEL that leads to more uncertain electricity prices is the high renewable energy penetration, since renewable energy is an intermittent source that generates electricity at low prices when there are enough renewable resources to generate electricity, mainly wind and rain.

5

Results and Discussion

In this chapter the conditions applied in the simulation are presented, along with the results from the economic analysis for 2020, 2030 and 2050. From a technical point of view, the optimal sizing ratios for the electrolyzer and fuel cell as well as the optimisation algorithm for the onshore electrolyzer system are discussed.

5.1 Simulation Conditions

Simulations were run with a hydrogen price ranging from 2-10 €/kg in order to assess the sensibility of each system to a change in hydrogen price. The model tests several ratios of the electrolyzer and fuel cell's nominal powers compared to the wind farm's nominal power. Since one of the goals is to compare the two hydrogen producing systems between themselves and also against a conventional wind farm without hydrogen production, the specifications shared by the systems were the same when possible. Table 5.1 contains the specifications of each system.

Table 5.1: Specifications of each system

Component	Offshore Elec.	Onshore Elec.	Conventional Wind Farm
Wind Farm Nominal Power	104.5 MW		
Turbines	Vestas V164-9.5		
Electrolyzer	Hydrogenics Hylyzer (PEM)		-
Storage Required	1 day		-
Storage Reserve	50%		-
Storage Pressure	100 bar		-
Pipeline Output Pressure	70 bar	-	
Transmission Losses	-	3.5%	
Rate of Return	7%		
Project's Lifetime	25 years		
Initial Investment	20%		
Loan Duration	20 years		
Loan's Interest Rate	5%		

To give some context regarding the wind data, the analysed wind farm has a capacity factor of 44.1% for the closest location and 47.3% for the furthest location, which are high but inline with wind farms in similar wind conditions.

The yearly average electricity prices in the day ahead market in Spain from 2015 to 2019 range from 39.72 to 57.29 €/MWh, with an average of 49.45 €/MWh. The average regulation cost for a positive imbalance (denominated as sp_h^+ in section 3) is 75.2% of the day ahead price and for a negative imbalance (denominated as sp_h^- in section 3) is -127.2%. In practice, this leads to paying on average 25-27% of the day ahead electricity price per MWh of imbalance.

5.2 Optimal Ratios

The sizing of the electrolyzer and fuel cell is relative to the wind farm's nominal power and depends on several factors, from electricity and hydrogen price to capital cost of the components. The ratios that lead to the highest NPV (effectively striking the balance between increased revenue and increased cost) are denominated as optimal ratios. To calculate the optimal ratios, every ratio from 0-100% in increments of 5% is tested for both the electrolyzer and fuel cell as well as for every hydrogen price considered.

The fuel cell is sized to its minimum size of 5% of the offshore wind farm's nominal power in every scenario for both systems. Even though not installing a fuel cell would lead to a higher NPV, this minimum value was imposed so that the fuel cell's operation could be analysed (further discussed in chapter 5.4).

Due to the similarities in the electrolyzer's optimal ratios for both locations considered, only the ratios for the offshore wind farm located 25 km from shore are presented in this chapter (table 5.2). The remaining ratios for the hydrogen prices between 6-10 €/kg and for wind farm located 50 km from shore are presented in appendix C.

Table 5.2: Electrolyzer's optimal ratios for the location 25 km from shore

System	Hydrogen Price [€/kg]	Year		
		2020	2030	2050
Offshore Electrolyzer	2	60%	90%	90%
	3	80%	90%	95%
	4	90%	90%	95%
	5	90%	90%	95%
	6	90%	95%	95%
Onshore Electrolyzer	2	5%	5%	5%
	3	5%	100%	100%
	4	100%	100%	100%
	5	100%	100%	100%
	6	100%	100%	100%

In the offshore electrolyzer system, the electrolyzer should be sized to 90-95% of the wind farm's nominal power, with the exception of the two lowest hydrogen prices in 2020. For these prices, the investment cost for an electrolyzer in the 90-95% range is greater than the increase in revenue from the increased hydrogen production capacity. Since the wind farm isn't always at nominal power, the electrolyzer's power isn't the limiting factor on hydrogen production during periods of low wind speed.

Comparing an electrolyzer sized to 90% and another sized to 95%, the more powerful one can only produce more hydrogen whenever the wind farm's output is above 90% of its nominal power. Given that the chosen locations have high wind speeds, the wind farm is regularly above 90%, nonetheless, the additional revenue might not be enough to counter the increased cost of a more powerful electrolyzer. Consequently, the electrolyzer is sized to 95% when the hydrogen price is higher and/or the investment

for a more powerful electrolyzer is lower (as the cost projections for 2030 and 2050 point towards). Ideally the electrolyzer isn't sized with a ratio of 100%, not only due to the reasons stated above, but also due to the wake and collector system losses of the wind farm that lower the actual available power to the electrolyzer.

5.3   Economic Analysis

The final step in the simulation is the economical analysis, where the LCOE, NPV and IRR are calculated and discussed. Firstly, the LCOE for the conventional wind farm is presented in figure 5.1, providing a way to assess the cost of generating electricity in the chosen locations. This curve was obtained using curve fit in Python using the LCOE values for 2020, 2030 and 2050.
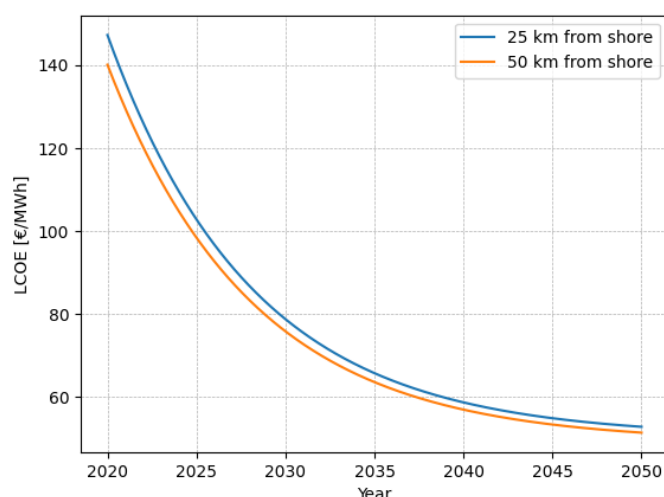
Figure 5.1: LCOE of the conventional wind farm at both distances considered

The LCOE in 2020 is above 140 €/MWh for both locations, as is to be expected considering that there were less than 62 MW of floating wind at the end of 2020. However, there is a significant drop of 30% in LCOE from 2020-2025 and a further 16% from 2025-2030. In the 20 years after 2030, the LCOE's rate of descent decreases, although it still drops by 17.5%. The location 50 km from shore provides the lowest LCOE, leading to the conclusion that (in these locations), the benefit of stronger wind speeds encountered further away from shore overcome the additional cost in the electrical transmission system.

The same procedure used to obtain the LCOE curve for the conventional wind farm was also used for the LCOH curves for both hydrogen producing systems. The LCOH curve for the offshore electrolyzer and onshore electrolyzer systems are presented in figures 5.2a and figure 5.2b, respectively.

Taking into account that the LCOH in both systems is dependent on the electrolyzer ratios, a ratio of

95% was chosen in the offshore electrolyzer system (the difference in LCOH if the ratio is 90% is under 0,5%). For the onshore electrolyzer system, a ratio of 100% was chosen since it is the most common optimal ratio. The fuel cell was sized with a ratio of 5%.

(a) Offshore electrolyzer

(b) Onshore electrolyzer

Figure 5.2: LCOH of the hydrogen producing systems at both distances considered

The LCOH for the offshore electrolyzer system (figure 5.2a) follows a similar trend to the one observed in the conventional wind farm's LCOE, only with an even more substantial reduction throughout the years considered in the simulation. It drops by 34% from 2020-2025, by a further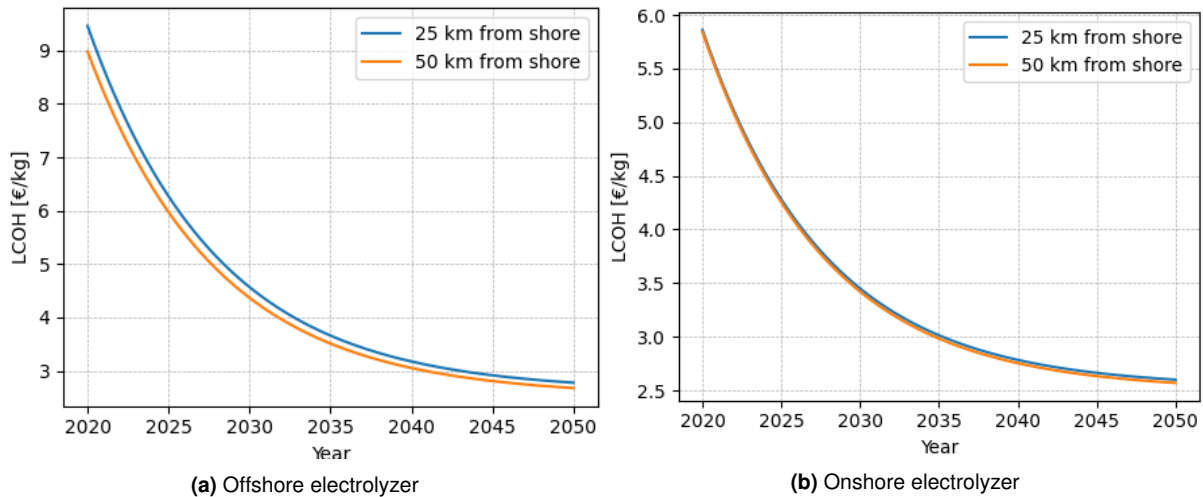 18% from 2025-2030 and in the final 20 years from 2030 to 2050 it drops another 18.5%. This reduction is greater than the conventional wind farm's LCOE due to the decline in the investment costs in PEMEL. As expected, the location further away from shore is able to produce hydrogen at a lower LCOH.

Regarding the onshore electrolyzer system, its LCOH is always lower than the offshore electrolyzer system, mainly due to its ability to purchase electricity from the grid. Therefore, the electricity isn't necessarily generated by renewable resources and the hydrogen produced by this system can't be denominated as green hydrogen.

The LCOH difference between the systems is over 3 €/kg in 2020, however in 2030 and 2050 this difference lowers to roughly 1 €/kg and 0.20 €/kg, respectively. The LCOH reduction is greater from 2020-2025, where it drops by 27%, slowing down between 2025-2030 with a 19.5% reduction. In the final 20 years the LCOH drops by a further 25%. Similarly to the other systems, the location further away from shore is able to generate the lower LCOH, despite only having a difference of 0.03 €/kg, not as significant as the 0.48€/kg difference for the offshore electrolyzer in 2020.

Throughout this chapter, only the simulations for hydrogen prices of 2, 4 and 6 €/kg are presented, with appendix D containing all simulations with hydrogen prices ranging from 2-10 €/kg.

Table 5.3 contains the revenue for both hydrogen producing systems for the location closest to shore. Since the quantity of hydrogen produced in the offshore electrolyzer system isn't dependent on hydrogen

price, the increase in revenue from a higher hydrogen price is directly proportional to the increase in hydrogen price (hydrogen price increases 25% from 4 €/kg to 5 €/kg, then the revenue also increases by 25%).

There are only two case where this direct proportionality isn't applicable, the first is if the hydrogen fuel cell was used, however, as is further discussed in chapter 5.4, the fuel cell is never used in this system. The second is that a more powerful electrolyzer leads to a higher hydrogen production, which only has a small impact in the revenue of each simulation since, for most scenarios, the electrolyzer is sized to 90% or 95% of the conventional wind farm.

Due to these reasons, only the revenue for a hydrogen price of 4 €/kg is presented, the remaining revenues for both locations can be consulted in appendix D. Additionally, the revenue for the conventional wind farm also is also only located in the mentioned appendix since its value is constant throughout the simulated years.

Table 5.3: Yearly revenue for the location 25 km from shore

System	Hydrogen Price [€/kg]	Yearly revenue [€]					
		2020		2030		2050	
		H2	Electricity	H2	Electricity	H2	Electricity
Offshore Electrolyzer	4	30.4M	0	34.4M	0	36.3M	0
Onshore Electrolyzer	2	0.39M	18.5M	0.63M	18.3M	0.74M	18.2M
	4	67M	-25.6M	77.1M	-26.9M	80.7M	-27M
	6	103M	-27.1M	116M	-27.2M	121M	-27.3M

The revenue analysis for the offshore electrolyzer system is straightforward, a more powerful electrolyzer and a higher hydrogen price lead to an increase in revenue. The other factor affecting revenue is the overall efficiency of the system. Comparing 2020 and 2030, the wind farm's losses and compressor consumption are the same, however, the electrolyzer's specific consumption is 11.6% lower (considering the compressor's consumption of 1 kWh/kg). The theoretical revenue in 2030 would then be $\frac{1}{1-0.116} \times 30.4$, which is 34.4 M€, the same value obtained in the simulations.

The onshore electrolyzer's sources of revenue vary greatly depending on the hydrogen price: for 2 €/kg the revenue is mostly from selling electricity, for prices higher than 3-4 €/kg, depending on the year, the revenue comes mostly from selling hydrogen. Furthermore, whenever hydrogen is the main source of revenue, more electricity is sold than bought as is represented on table 5.3 by the negative electricity revenue.

The decision to sell electricity or produce hydrogen can be defined by comparing the monetary value of the electricity required to produce 1 kg of hydrogen to the price of hydrogen. For example, in 2020 to produce 1 kg of hydrogen, the electrolyzer and compressor use 0.05428 MWh/kg. If the hydrogen price is 3 €/kg, then, for an electricity price lower than $\frac{3}{0.05428} = 55.27$ €/MWh, hydrogen production

yields higher revenue, however, for prices higher than 55.27 €/MWh (denominated as the threshold sale value), selling electricity is the more profitable alternative. In this example, if the electricity price is lower than 55.27 €/MWh, not only would the system direct all generated electricity to the electrolyzer, it would also purchase electricity from the grid to maximise the hydrogen production.

Figure 5.3a contains forecasts and actual values for both wind power production and electricity price and figure 5.3b contains the hydrogen production and electricity transactions with the grid for a hydrogen price of 3 €/kg.
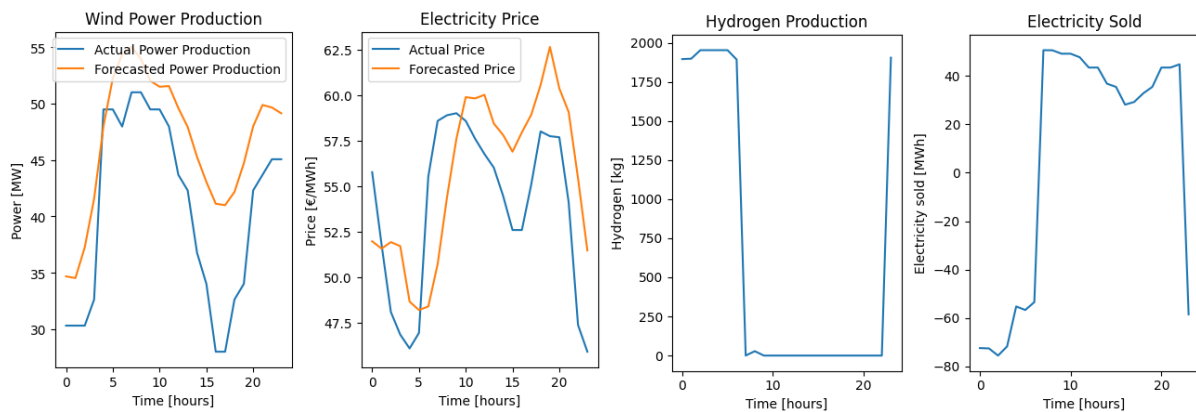
(a) Forecasts and actual values of wind power production and electricity prices

(b) Hydrogen production and electricity transactions for the onshore electrolyzer system

Figure 5.3: Sensitivity analysis for the conventional wind farm in 2030 for the location 25 km from shore

As expected, when the electricity price is below the threshold, the system purchases electricity to produce hydrogen, when it's above the threshold the system sells electricity, although it's not always the case since regulation costs also influence the revenue. This means that if a bid was placed to sell a certain amount of electricity and if the most profitable option turns out to be not selling any electricity, then regulation costs must be payed.

One of two possible scenarios can occur: either producing hydrogen and paying the regulation costs is more profitable than complying with the previously placed bid, or the added expense of regulation costs means the more profitable option is to comply with the previously placed bid. An example of the latter can be seen around hour 15, where the forecasted price is above the threshold, so a bid was placed on the day ahead market to sell the electricity produced during that hour.

However, the actual electricity price was below the threshold, so the better option would have been to produce hydrogen during that hour if there were no regulation costs. Since there are regulation costs, the added revenue from producing hydrogen instead of selling electricity wouldn't have been enough to compensate paying the additional regulation costs, so in the end the final option is to sell the electricity. Situations like this highlight the importance of accurate forecasting in order to maximize revenue from a system where critical operational decisions must be made.

The economic assessment of the three systems for different hydrogen prices can be seen in table 5.4 (for the location 25 km from shore), and in table 5.5 (for the location 50 km from shore).

Table 5.4: Economic assessment for the location 25 km from shore

System	Hydrogen Price [€/kg]	NPV [€]			IRR [%]		
		2020	2030	2050	2020	2030	2050
Offshore Electrolyzer	2	-651M	-256M	-82.3M	-	-	-
	4	-486M	-56M	129M	-	0.58	31.24
	6	-309M	145M	340M	-	24.61	72.08
Onshore Electrolyzer	2	-489M	-157M	-33M	-	-	0.89
	4	-374M	119M	325M	-	22.05	67.41
	6	22.6M	571M	796M	8.51	77.72	155
Conventional Wind Farm	-	-474M	-152M	-31M	-	-	1.22

The first remark to make is that the onshore electrolyzer system is always more economically interesting than the offshore electrolyzer system, mainly due to its ability to purchase electricity. The NPV of the offshore electrolyzer system is only positive for a hydrogen price higher than 6 €/kg in 2030 and 4 €/kg in 2050. On the other hand, the onshore electrolyzer system shows a positive NPV for hydrogen prices above 6 €/kg in 2020, 4 €/kg in 2030 and 2050.

Even though the results only show positive NPV for higher hydrogen prices or in future years, the conventional wind farm in these locations also yields a negative NPV in all simulated years, indicating that floating offshore wind farms are still relatively expensive to build and might not be profitable in the coming years in the Iberian Peninsula. It should be noted that cost projections are far from certain and small variations greatly impact the economic assessment of future years (as is detailed in chapter 5.5).

Table 5.5: Economic assessment for the location 50 km from shore

System	Hydrogen Price [€/kg]	NPV [€]			IRR [%]		
		2020	2030	2050	2020	2030	2050
Offshore Electrolyzer	2	-655M	-256M	-77M	-	-	-
	4	-476M	-40.5M	150M	-	2.54	34.29
	6	-286M	177M	376M	-	28.03	76.63
Onshore Electrolyzer	2	-486M	-152M	-26.5M	-	-	2.37
	4	-371M	125M	331M	-	21.52	65.29
	6	25.9M	576M	803M	8.69	75.53	148.35
Conventional Wind Farm	-	-470M	-147M	-24M	-	-	2.68

As is the case with the conventional wind farm, for the offshore electrolyzer system the location further from shore is always more economically interesting from a point of view of the NPV and IRR (with the exception of 2020 with a hydrogen price of 2 €/kg). The onshore electrolyzer system always yields higher NPV in the location furthest from shore, however, in 2030 and 2050 for hydrogen prices higher than 4 €/kg, the IRR is higher on the location closest to shore.

The cases where the NPV is higher on one location and lower on another highlight the difference between the two metrics: NPV translates to amount of profit (higher if the wind farm is 50 km from shore), and IRR translates the return on the investment (higher if the wind farm is 25 km from shore due to the lower investment costs). These cases occur for scenarios where the electrolyzer is running at nominal power for most of the year.

5.4 Fuel Cell Operation

The fuel cell can operate whenever its operation is profitable, as long as there is enough hydrogen stored to supply the fuel cell. Theoretically, this allows the fuel cell to operate during high electricity prices, maximizing revenue in relation to hydrogen consumed.

There are two downsides of using the fuel cell: the low fuel cell efficiency and the high hydrogen price when converted to €/MWh. The modelled fuel cell has a maximum efficiency of 58%, so the electricity price must be at least $\frac{1}{0.58} = 1.72$ higher than the hydrogen price in €/MWh. Even for the simulation with the lowest hydrogen price of 2 €/kg, it is still equivalent to 60 €/MWh considering hydrogen's lower heating value of 0.03333 MWh/kg, so the minimum threshold electricity price for which the fuel cell should produce electricity is roughly $1.72 \times 60 = 103.2$ €/MWh.

The highest electricity price registered in the MIBEL day ahead market from 2015 to 2019 was 101.99 €/MWh, lower than the threshold value calculated above. In the offshore electrolyzer system, the fuel cell is never used since the electricity price doesn't reach a high enough value to make the electricity generated by the fuel cell more valuable than the hydrogen used to generate it.

On the other hand, there are two scenarios where the fuel cell is used in the onshore electrolyzer system when the hydrogen price is 2 €/kg. The first is when the electricity price is high (over 70-80 €/MWh) and there is a negative imbalance, which can me mitigated by the fuel cell. By using the fuel cell to generate electricity, not only does that increase the revenue from selling the extra amount of electricity but also saves on that portion of the regulation costs caused by the imbalance. The sum of these two parts is, in some circumstances, higher than the 103.2 €/MWh threshold.

The other scenario is when electricity price is at a normal value, however, there is a high negative imbalance regulation cost. The scenarios where the high regulation cost is several times above the average regulation cost are rare, nonetheless, they are still present in the studied time period in MIBEL. Same as with the previous scenario, the sum of the revenue of the electricity generated by the fuel cell and the regulation costs (in this scenario higher than normal) can lead to a value greater than the 103.2 €/MWh threshold.

Despite the onshore electrolyzer system occasionally using the fuel cell, it's still extremely rare and the increased revenue is orders of magnitude lower than the total revenue. The simulation where the

fuel cell has the biggest revenue is when the hydrogen price is 2 €/kg, the wind farm is located 50 km from shore and the electrolyzer and fuel cell are sized to 5% of the offshore wind farm's nominal power. The yearly fuel cell's revenue is, on average, 1511 €, an extremely low value when compared to the entire yearly revenue of over 20 M€.

5.5 Sensitivity Analysis

In the sensitivity analysis, certain parameters of the system were changed to ascertain how these changes affect the results from the economic analysis, for both locations. The analysis regarding 2030 for the location 25 km from shore is presented and discussed in this chapter, the analyses for the remaining years and the location further from shore can be found in appendix E.

The parameters that were changed are capacity factor, rate of return and CAPEX. Starting with the offshore wind farm's capacity factor, in [6] a capacity factor of 54% was used in 2030, so the energy production of the wind farm was scaled to a similar capacity factor while maintaining the same nominal power. In order to provide a perspective on how the systems are impacted, a lower capacity value was also simulated. In the end, the lower capacity factor was set at 34.98% and the higher capacity factor was set at 53.18% (as a reminder, the capacity factor in the techno-economic analysis is 44.1%).

The project's rate of return was changed from 7% to 6% and 8%, on the other hand, the CAPEX was increased and decreased by 10% and afterwards 20%. By varying the component cost, the cost uncertainties raised by using recent technologies (floating offshore wind and PEMEL) can be studied and their effects quantified.

The economic parameters recalculated during the sensitivity analysis were the NPV and either LCOE for the conventional wind farm without hydrogen production or LCOH for the hydrogen producing systems. The results from the sensitivity analysis for the conventional wind farm are present in figures 5.4a and 5.4b, respectively.
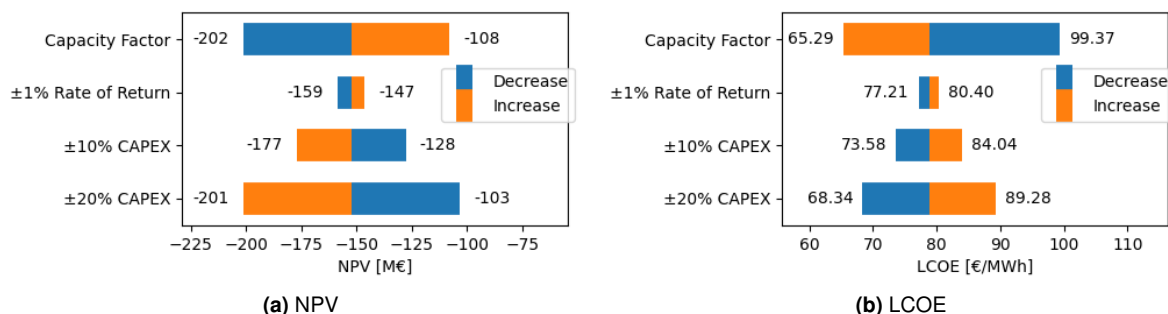

(a) NPV

(b) LCOE

Figure 5.4: Sensitivity analysis for the conventional wind farm in 2030 for the location 25 km from shore

As can be seen, even though the change in capacity factor was around 20% of the previous value,

it has a significant impact on both parameters which translates to the importance of selecting a location with high wind speeds. Regarding the CAPEX analysis, there is a noticeable impact even if its value is only changed by 10%. Considering that these cost projections for 2030 were estimated in 2019-2020, a 10-20% error margin is reasonable since cost reduction is heavily dependent on the amount of investment in the technology (in this case floating offshore wind).

Figures 5.5 and 5.6 contain the results from the sensitivity analysis for offshore electrolyzer system and onshore electrolyzer system, respectively.
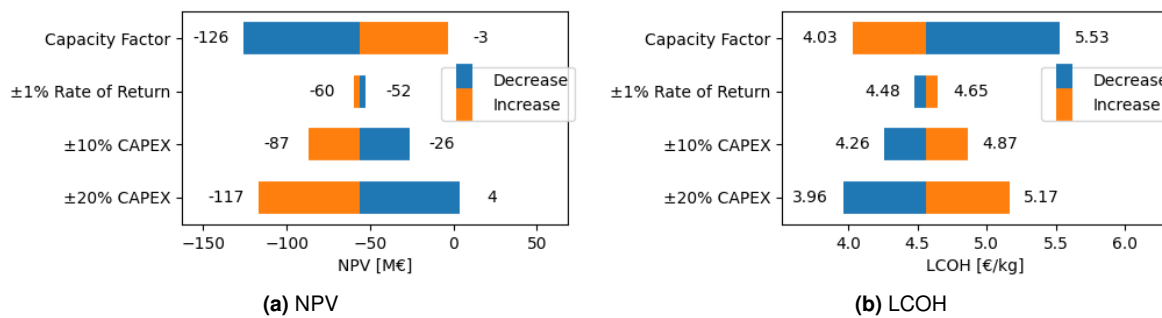

(a) NPV

(b) LCOH

Figure 5.5: Sensitivity analysis for the offshore electrolyzer system in 2030 for the location 25 km from shore

(a) NPV

(b) LCOH
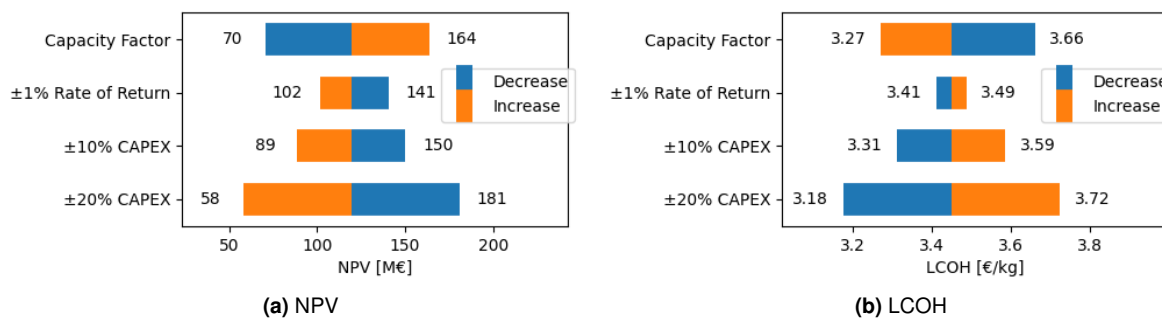
Figure 5.6: Sensitivity analysis for the onshore electrolyzer system in 2030 for the location 25 km from shore

The same observations made regarding the sensitivity analysis of the conventional wind farm can be applied to both hydrogen producing systems. However, a change in the capacity factor has a greater impact on the offshore electrolyzer system than the onshore electrolyzer system, mainly due to the fact that the latter system can purchase electricity from the grid, so it isn't as dependent on the electricity generated in the offshore wind farm.

Furthermore, even increasing the capacity factor by 20% leads to a slightly negative NPV in the offshore electrolyzer system for a hydrogen price of 4 €/kg, while a 20% reduction in CAPEX has a similar effect. Looking at the LCOH for the offshore electrolyzer system, the biggest reduction is 14.8% if the CAPEX drops by 20%, achieving a value lower than in a scenario where the capacity factor increases by 20%.

Regarding the onshore electrolyzer system, for both a 10% and 20% variation in CAPEX, there is a significant change in the overall profitability of the system. Comparing the scenario where CAPEX rises by 20% to the scenario where CAPEX drops by 20%, despite there being an appreciable difference in LCOH, the NPV is three times higher in the latter scenario. Comparing the LCOH sensitivity between both systems, for every change in the analysed parameters the offshore electrolyzer system's LCOH always has a more significant variation relative to its initial value.

6

Conclusion

In this thesis, a techno-economic analysis on two hydrogen producing systems and a floating offshore wind farm without hydrogen production was performed. The first hydrogen producing system is the offshore electrolyzer system, where the PEMEL is located near the turbines and all electricity is used to produce hydrogen that is transported to shore via a pipeline. The second system is the onshore electrolyzer system, where PEMEL is located on land and all electricity generated by the wind farm is transmitted to shore using a conventional subsea cable. Once the electricity is onshore, it can either be sold directly to the grid or fed into the electrolyzer to produce hydrogen, depending on market conditions. Both systems also have a fuel cell that can generate electricity from hydrogen when electricity prices are high and/or to prevent paying regulation costs.

In order to perform the simulations, each component was individually modelled and combined to construct the systems. Considering that the hydrogen producing systems can generate either hydrogen or electricity, an hourly optimisation algorithm was implemented to manage the operation of the systems. This algorithm maximizes instantaneous revenue, taking into consideration, among others, the previously placed electricity bid, electricity price, hydrogen price and the offshore wind farm's instant power.

Additionally, as a means to simulate the day ahead market, a forecasting model was developed to forecast electricity price and wind power production for the following day. This model uses the previous 64 hours of data to generate a forecast for the 24 hours of the following day, allowing for the implementation of the day ahead electricity market, relevant due to the economic impact of regulation costs that can be minimized by the hydrogen producing systems. The fuel cell integrated into both systems can be regulated so that its electricity production matches the bid placed in the day ahead market, while on the onshore electrolyzer system, electricity can be directed to/from the electrolyzer to compensate for any imbalances (it can also use the fuel cell if needed).

The simulations were conducted considering that the systems were implemented in Galicia, Spain, for a location 25 km from shore and another 50 km from shore, enabling the study on how distance affects each system. The simulation was run using wind speed and electricity price data from 2015 to 2019, for a fixed hydrogen price. Several hydrogen prices were tested, starting at 2 €/kg to 10 €/kg. With the aim of assessing how green hydrogen production using offshore wind energy might develop in the coming years, the simulations were also performed for 2030 and 2050, using cost projections and expected electrolyzer efficiency gain available in the literature.

In the hydrogen producing systems, the electrolyzer and fuel cell were sized as a ratio of the wind farm's nominal power, with the ratio that lead to the highest NPV denominated as optimal ratio. For the offshore electrolyzer system, the electrolyzer should be sized with a ratio of 90-95% depending on hydrogen price and the year (with the exception of prices lower than 4 €/kg in 2020, where the ratio should be around 60-80%). On the other hand, for the onshore electrolyzer system, the electrolyzer

should be sized to 5% for a hydrogen price of 2 €/kg for all years and also in 2020 for a hydrogen price of 3 €/kg. For every other scenario, the best configuration is sizing the onshore electrolyzer to the same nominal power as the wind farm.

The high investment cost in floating wind technology can be observed when analysing the conventional wind farm without hydrogen production, which is only profitable in 2050 with an IRR of 2.68% and 1.22% for the locations 50 km from shore and 25 km from shore. It should be noted that for these two locations, the higher wind speeds further from shore compensate the added cost of assembling a longer transmission system. Looking at the LCOE, for 2020, 2030 and 2050 it is 140.11 €/MWh, 75.88 €/MWh and 51.47 €/MWh, respectively.

It's important to highlight that the systems were implemented in the Iberian Peninsula, where offshore wind power production is very rare due to the deep waters. Therefore, floating wind turbines are the only option and are presently at a much higher cost compared to fixed bottom wind turbines, since it's a much more recent technology, with only 62 MW installed at the end of 2020 [4]. Furthermore, no support policy for renewable energies (such as feed-in tariff or contract for differences) was considered.

The fuel cell is never used in the offshore electrolyzer system, it's only used in the onshore electrolyzer system when the hydrogen price is 2 €/kg in scenarios with a high electricity price and a forecasting error that would lead to paying regulation costs. Its revenue doesn't even cover the yearly OPEX, due to the high value of hydrogen compared to electricity in €/MWh and the low efficiency of the fuel cell ($<$60%).

The offshore electrolyzer system for the location 50 km from shore has an LCOH of 8.98 €/kg, 4.37 €/kg and 2.68 €/kg for 2020, 2030 and 2050, with the location 25 km from shore having slightly higher LCOH. This system is only economically viable for high hydrogen prices, mainly owing to the high investment cost in constructing a floating offshore wind farm. In 2030 for the location 50 km from shore, a hydrogen price of 4 €/kg yields a NPV of -40.5 M€ and a hydrogen price of 5 €/kg yields an NPV of 68 M€ (IRR is 14.87%). For the same location in 2050, a hydrogen price of 2 €/kg leads to an NPV of -77 M€ and a hydrogen price of 3 €/kg leads to an NPV of 36.4 M€ (IRR is 13.41%).

In the scenarios where the electrolyzer in the onshore electrolyzer system is sized to 100% of the wind farm's nominal power, the system purchases more electricity to generate hydrogen than it sells, so its primary revenue stream is the sale of hydrogen. When compared to its offshore counterpart, purchasing electricity helps the system to achieve a lower LCOH of 5.84 €/kg, 3.42 €/kg and 2.57 €/kg for 2020, 2030 and 2050, respectively, for the location 50 km from shore. At this location, in 2030 for a hydrogen price of 3 €/kg the project has an NPV of -90 M€ and for a hydrogen price of 4 €/kg, the NPV is 125 M€ (with an IRR of 21.52%). In 2050, a hydrogen price of 2 €/kg results in a NPV of -26.5 M€ and a hydrogen price of 3 €/kg results in a NPV of 103 M€ (IRR is 24.6%).

The lower LCOH of the onshore electrolyzer system translates to this system always being more

economically interesting than the offshore electrolyzer system, however, there is an important distinction that separates them. While the energy source of the offshore electrolyzer system is only the renewable energy generated in the offshore wind farm, the onshore electrolyzer system also purchases electricity from the grid, so its energy source might not be 100% renewable as the source of its electricity can't be determined. Thus, only the hydrogen produced by the offshore electrolyzer system can be denominated as green hydrogen.

Looking at the distribution of the investment costs, between 70-77% of the CAPEX is for the offshore wind farm, with the second most expensive component being the electrolyzer, which is around 11% when sized to 95% or 100% of the wind farm's nominal power. In terms of OPEX, the offshore wind farm represents at least 85% of the total system OPEX, with the electrolyzer representing 6-7%. The high percentage of the investment costs being allocated towards the offshore wind farm is in agreement with the literature review, where several authors concluded that the LCOE of the energy source is the most significant factor in determining the LCOH of a green hydrogen system.

One important remark is that floating offshore wind farms and PEMEL are not widely implemented technologies, so the cost projections indicate a drastic cost reduction over the next decade. For the location 50 km from shore between 2020 and 2030, the LCOH drops by 51% for the offshore electrolyzer system and 41% for the onshore electrolyzer system, with the LCOE for the conventional wind farm without hydrogen production dropping by 46%.

On the other hand, a consequence of implementing not yet matured technologies is the uncertainty surrounding the cost projections, which can be addressed using a sensitivity analysis. Through this analysis, the impact of a change in certain parameters is quantified by varying the parameters and determining how the economic analysis is affected. Focusing on 2030 on a scenario with a hydrogen price of 4 €/kg for the location 25 km from shore, an increase in the capacity factor from 44.1% to 53.8% (considered a conservative approach for offshore wind farms in 2030 [6]) and a decrease in CAPEX of 20% yield similar results.

In the offshore electrolyzer system, the capacity factor increase leads to an increase in NPV from -56 M€ to -3 M€ and a decrease in LCOH from 4.56 €/kg to 4.03 €/kg. In the case of a 20% reduction in the CAPEX's cost projections, the NPV increases to 4 M€ and LCOH decreases to 3.96 €/kg. For the onshore electrolyzer system, the capacity factor increase changes the NPV from 119 M€ to 164 M€ and the LCOH from 3.45 €/kg to 3.27 €/kg, with the 20% CAPEX reduction yielding an NPV 181 M€ and an LCOH 3.18 €/kg.

Conversely, decreasing the capacity factor by the same margin (to around 35%) and increasing the CAPEX by 20% lead to opposite results in the same proportion: lower NPV and higher LCOH. While the change in capacity factor and CAPEX's cost projections are significant, in the roughly 10 years linking present day to 2030 these technologies will most likely suffer an extreme growth. Since the cost

reductions and efficiency gains are directly tied to their adoption in the coming years, accurate cost projections are, at best, hard to determine.

When it comes to posteriorly improving the elaborated work, a few alterations can be made to enhancing the developed model. First, during the lifetime of the hydrogen producing systems, the hydrogen price is kept constant and several prices are tested. A more realistic hydrogen market could be implemented, possibly based on the policies and incentives that will guide the green hydrogen field in the coming years.

Currently, there is only one small scale offshore wind farm in the Iberian Peninsula, the 25 MW WindFloat Atlantic located 20 km off the coast of Viana do Castelo, Portugal. There aren't more wind farms mainly due to the deeper waters and lower wind speeds when compared to locations where offshore wind farms are widely installed, such as the North Sea. A follow up study considering a location in the North Sea, where bottom fixed wind turbines can be installed and higher wind speeds can be harnessed, will surely lead to a more economically viable green hydrogen producing system.

In this work, only the day ahead market was modelled as it corresponds to the market where most electricity transactions occur. However, the modelling of the intraday market along with the balancing market would be a more realistic scenario, especially when considering the flexibility of the hydrogen producing systems in the balancing market.

The final possible improvement is to model the electrolyzer with an efficiency curve instead of a single specific consumption value, improving the model's representation of how an electrolyzer operates. This would lead to more realistic electrolyzer behaviour, especially in the optimisation algorithm as this would add another layer of complexity.

Bibliography

[1] IEA, "Key world energy statistics 2020," 2020, [Accessed 10 May 2021]. [Online]. Available: https://www.iea.org/reports/key-world-energy-statistics-2020

[2] M. Panfilov, "4 - underground and pipeline hydrogen storage," in *Compendium of Hydrogen Energy*, ser. Woodhead Publishing Series in Energy, R. B. Gupta, A. Basile, and T. N. Veziroğlu, Eds. Woodhead Publishing, 2016, pp. 91–115 https://doi.org/10.1016/B978-1-78242-362-1.00004-3

[3] B. Miao, L. Giordano, and S. H. Chan, "Long-distance renewable hydrogen transmission via cables and pipelines," *International Journal of Hydrogen Energy*, 2021 https://doi.org/10.1016/j.ijhydene.2021.03.067

[4] WindEurope, "Offshore wind in europe: Key trends and statistics 2020," 2021. [Online]. Available: https://windeurope.org/intelligence-platform/product/offshore-wind-in-europe-key-trends-and-statistics-2020/ [Accessed 10 May 2021].

[5] European Marine Observation and Data Network (EMODnet). [Online]. Available: https://portal.emodnet-bathymetry.eu/ [Accessed 10 May 2021].

[6] Offshore Renewable Energy (ORE) Catapult, "Offshore wind and hydrogen: Solving the integration challenge," September 2020, [Accessed 10 May 2021]. [Online]. Available: https://ore.catapult.org.uk/?orecatapultreports=offshore-wind-and-hydrogen-solving-the-integration-challenge

[7] Airborne Wind Europe, "High-altitude wind energy map published," [Accessed 10 May 2021]. [Online]. Available: https://airbornewindeurope.org/resources/high-altitude-wind-energy-map-published-2/

[8] WindEurope, "Offshore wind in europe: Key trends and statistics 2017," 2018. [Online]. Available: https://windeurope.org/intelligence-platform/product/the-european-offshore-wind-industry-key-trends-and-statistics-2017/ [Accessed 10 May 2021].

[9] Equinor, "Hywind scotland." [Online]. Available: https://airbornewindeurope.org/resources/high-altitude-wind-energy-map-published-2/ [Accessed 10 May 2021].

[10] ERM, "Dolphyn hydrogen phase 1 – final report," October 2019. [Online]. Available: https://assets.publishing.service.gov.uk/government/uploads/system/uploads/attachment_data/file/866375/Phase_1_-_ERM_-_Dolphyn.pdf [Accessed 10 May 2021].

[11] IRENA, "Hydrogen from renewable power: Technology outlook for the energy transition," September 2018, [Accessed 10 May 2021]. [Online]. Available: https://irena.org/publications/2018/Sep/Hydrogen-from-renewable-power

[12] A. Buttler and H. Spliethoff, "Current status of water electrolysis for energy storage, grid balancing and sector coupling via power-to-gas and power-to-liquids: A review," *Renewable and Sustainable Energy Reviews*, vol. 82, pp. 2440 – 2454, 2018 https://doi.org/10.1016/j.rser.2017.09.003

[13] Y. Guo, G. Li, J. Zhou, and Y. Liu, "Comparison between hydrogen production by alkaline water electrolysis and hydrogen production by PEM electrolysis," *IOP Conference Series: Earth and Environmental Science*, vol. 371, p. 042022, December 2019 https://doi.org/10.1088/1755-1315/371/4/042022

[14] McPhy, "Augmented mclyzer." [Online]. Available: https://mcphy.com/en/equipment-services/electrolyzers/augmented/ [Accessed 10 May 2021].

[15] IRENA, "Green hydrogen cost reduction: Scaling up electrolysers to meet the 1.5ºc climate goal," International Renewable Energy Agency, Abu Dhabi, December 2020. [Online]. Available: https://irena.org/publications/2018/Sep/Hydrogen-from-renewable-power [Accessed 10 May 2021].

[16] J. Andersson and S. Grönkvist, "Large-scale storage of hydrogen," *International Journal of Hydrogen Energy*, vol. 44, no. 23, pp. 11 901 – 11 919, 2019 https://doi.org/10.1016/j.ijhydene.2019.03.063

[17] H. Dagdougui, R. Sacile, C. Bersani, and A. Ouammi, "Chapter 4 - hydrogen storage and distribution: Implementation scenarios," in *Hydrogen Infrastructure for Energy Applications*, H. Dagdougui, R. Sacile, C. Bersani, and A. Ouammi, Eds. Academic Press, 2018, pp. 37 – 52. ISBN 978-0-12-812036-1 https://doi.org/10.1016/B978-0-12-812036-1.00004-4

[18] O. Kruck, F. Crotogino, R. Prelicz, and T. Rudolph, "Overview on all known underground storage technologies for hydrogen," *Project HyUnder–Assessment of the Potential, the Actors and Relevant Business Cases for Large Scale and Seasonal Storage of Renewable Electricity by Hydrogen Underground Storage in Europe. Report D*, vol. 3, 2013. [Online]. Available: hyunder.eu/wp-content/uploads/2016/01/D3.1_Overview-of-all-known-underground-storage-technologies.pdf [Accessed 10 May 2021].

[19] F. I. Gallardo, A. Monforti Ferrario, M. Lamagna, E. Bocci, D. Astiaso Garcia, and T. E. Baeza-Jeria, "A techno-economic analysis of solar hydrogen production by electrolysis in the north of chile and the case of exportation from atacama desert to japan," *International Journal of Hydrogen Energy*, 2020 https://doi.org/10.1016/j.ijhydene.2020.07.050

[20] N. Barberis Negra and J. Todorovic and T. Ackermann, "Loss evaluation of hvac and hvdc transmission solutions for large offshore wind farms," *Electric Power Systems Research*, vol. 76, no. 11, pp. 916 – 927, 2006 https://doi.org/10.1016/j.epsr.2005.11.004

[21] A. Papadopoulos, S. Rodrigues, E. Kontos, T. Todorcevic, P. Bauer, and R. T. Pinto, "Collection and transmission losses of offshore wind farms for optimization purposes," in *2015 IEEE Energy Conversion Congress and Exposition (ECCE)*, 2015 https://doi.org/10.1109/ECCE.2015.7310601 pp. 6724–6732.

[22] Hydrogenics, "Large scale pem electrolysis: technology status and upscaling strategies." [Online]. Available: http://hybalance.eu/wp-content/uploads/2019/10/Large-scale-PEM-electrolysis.pdf [Accessed 10 May 2021].

[23] North Sea Energy, "A vision on hydrogen potential from the north sea," 2019. [Online]. Available: https://north-sea-energy.eu/static/29bef9235ee0548a2425dea4356a2f1e/NSE3-D1.6-D1.7-D1.8-Offshore-Hydrogen-Roadmap-linked-to-national-hydrogen-grid.pdf [Accessed 10 May 2021].

[24] V. N. Dinh, P. Leahy, E. McKeogh, J. Murphy, and V. Cummins, "Development of a viability assessment model for hydrogen production from dedicated offshore wind farms," *International Journal of Hydrogen Energy*, 2020 https://doi.org/10.1016/j.ijhydene.2020.04.232

[25] General Electric, "Switch it up: This tech helps take the world's largest offshore wind turbine to a new level." [Online]. Available: https://www.ge.com/news/reports/switch-tech-helps-take-worlds-largest-offshore-wind-turbine-new-level [Accessed 10 May 2021].

[26] A. Alassi, S. Bañales, O. Ellabban, G. Adam, and C. MacIver, "Hvdc transmission: Technology review, market trends and future outlook," *Renewable and Sustainable Energy Reviews*, vol. 112, pp. 530–554, 2019 https://doi.org/10.1016/j.rser.2019.04.062

[27] Toyota, "2021 Toyota Mirai." [Online]. Available: https://www.toyota.com/mirai/ [Accessed 29 May 2021].

[28] A. Wood, H. He, T. Joia, and C. C. Brown, "Reversible solid oxide fuel cell development at versa power systems," *ECS Transactions*, vol. 66, no. 3, p. 23, 2015.

[29] US Department of Energy, "Comparison of fuel cell technologies," 2016. [Online]. Available: https://www.energy.gov/eere/fuelcells/comparison-fuel-cell-technologies

[30] E. Weidner, R. Ortiz Cebolla, and J. Davies, "Global deployment of large capacity stationary fuel cells," 2019 http://dx.doi.org/10.2760/372263

[31] "Doosan starts installation of hydrogen-fueled 50 MW fuel cell power plant in South Korea," *Fuel Cells Bulletin*, vol. 2018, no. 8, p. 1, 2018 https://doi.org/10.1016/S1464-2859(18)30270-0

[32] Fuel Cells Works, "Daesan Hydrogen Fuel Cell Power Plant Completed with Help of Doosan Fuel Cells." [Online]. Available: https://fuelcellsworks.com/news/daesan-hydrogen-fuel-cell-power-plant-completed-with-help-of-doosan-fuel-cells/ [Accessed 10 May 2021].

[33] HyDeploy. [Online]. Available: https://hydeploy.co.uk/ [Accessed 10 May 2021].

[34] M. W. Melaina, O. Antonia, and M. Penev, "Blending hydrogen into natural gas pipeline networks: A review of key issues," March 2013 https://doi.org/10.2172/1068610

[35] C. J. Quarton and S. Samsatli, "Power-to-gas for injection into the gas grid: What can we learn from real-life projects, economic assessments and systems modelling?" *Renewable and Sustainable Energy Reviews*, vol. 98, pp. 302–316, 2018 https://doi.org/10.1016/j.rser.2018.09.007

[36] EDP, "Flexnconfu: Power-to-x to increase the flexibility of thermal plants." [Online]. Available: https://www.edp.com/en/innovation/flexnconfu-power-to-increase-the-flexibility-of-thermal-plants [Accessed 10 May 2021].

[37] FLEXnCONFU. [Online]. Available: https://flexnconfu.eu/demonstration/ [Accessed 10 May 2021].

[38] J.-F. Toubeau, J. Bottieau, F. Vallée, and Z. De Grève, "Deep learning-based multivariate probabilistic forecasting for short-term scheduling in power markets," *IEEE Transactions on Power Systems*, vol. 34, no. 2, pp. 1203–1215, 2019 https://doi.org/10.1109/TPWRS.2018.2870041

[39] X. Shi, X. Lei, Q. Huang, S. Huang, K. Ren, and Y. Hu, "Hourly day-ahead wind power prediction using the hybrid model of variational model decomposition and long short-term memory," *Energies*, vol. 11, no. 11, 2018 https://doi.org/10.3390/en11113227

[40] Y.-Y. Hong and T. R. A. Satriani, "Day-ahead spatiotemporal wind speed forecasting using robust design-based deep learning neural network," *Energy*, vol. 209, p. 118441, 2020 https://doi.org/10.1016/j.energy.2020.118441

[41] J. Zhou, H. Liu, Y. Xu, and W. Jiang, "A hybrid framework for short term multi-step wind speed forecasting based on variational model decomposition and convolutional neural network," *Energies*, vol. 11, no. 9, 2018 https://doi.org/10.3390/en11092292

[42] H. Liu, X. Mi, and Y. Li, "Smart deep learning based wind speed prediction model using wavelet packet decomposition, convolutional neural network and convolutional long short term memory network," *Energy Conversion and Management*, vol. 166, pp. 120–131, 2018 https://doi.org/10.1016/j.enconman.2018.04.021

[43] W. Zhang, F. Cheema, and D. Srinivasan, "Forecasting of electricity prices using deep learning networks," in *2018 IEEE PES Asia-Pacific Power and Energy Engineering Conference (APPEEC)*, 2018 https://doi.org/10.1109/APPEEC.2018.8566313 pp. 451–456.

[44] J. Lago, G. Marcjasz, B. De Schutter, and R. Weron, "Forecasting day-ahead electricity prices: A review of state-of-the-art algorithms, best practices and an open-access benchmark," *Applied Energy*, vol. 293, p. 116983, 2021 https://doi.org/10.1016/j.apenergy.2021.116983

[45] G. Kakoulaki, I. Kougias, N. Taylor, F. Dolci, J. Moya, and A. Jäger-Waldau, "Green hydrogen in europe – a regional assessment: Substituting existing production with electrolysis powered by renewables," *Energy Conversion and Management*, p. 113649, 2020 https://doi.org/10.1016/j.enconman.2020.113649

[46] D. Gusain, M. Cvetković, R. Bentvelsen, and P. Palensky, "Technical assessment of large scale pem electrolyzers as flexibility service providers," in *2020 IEEE 29th International Symposium on Industrial Electronics (ISIE)*, 2020 https://doi.org/10.1109/ISIE45063.2020.9152462 pp. 1074–1078.

[47] J. G. García Clúa, R. J. Mantz, and H. De Battista, "Optimal sizing of a grid-assisted wind-hydrogen system," *Energy Conversion and Management*, vol. 166, pp. 402 – 408, 2018 https://doi.org/10.1016/j.enconman.2018.04.047

[48] T. Nguyen, Z. Abdin, T. Holm, and W. Mérida, "Grid-connected hydrogen production via large-scale water electrolysis," *Energy Conversion and Management*, vol. 200, p. 112108, 2019 https://doi.org/10.1016/j.enconman.2019.112108

[49] P.-M. Heuser, D. S. Ryberg, T. Grube, M. Robinius, and D. Stolten, "Techno-economic analysis of a potential energy trading link between patagonia and japan based on co2 free hydrogen," *International Journal of Hydrogen Energy*, vol. 44, no. 25, pp. 12 733 – 12 747, 2019 https://doi.org/10.1016/j.ijhydene.2018.12.156

[50] S. McDonagh, S. Ahmed, C. Desmond, and J. D. Murphy, "Hydrogen from offshore wind: Investor perspective on the profitability of a hybrid system including for curtailment," *Applied Energy*, vol. 265, p. 114732, 2020 https://doi.org/10.1016/j.apenergy.2020.114732

[51] P. Xiao, W. Hu, X. Xu, W. Liu, Q. Huang, and Z. Chen, "Optimal operation of a wind-electrolytic hydrogen storage system in the electricity/hydrogen markets," *International Journal of Hydrogen Energy*, vol. 45, no. 46, pp. 24 412 – 24 423, 2020 https://doi.org/10.1016/j.ijhydene.2020.06.302

[52] P. Hou, P. Enevoldsen, J. Eichman, W. Hu, M. Z. Jacobson, and Z. Chen, "Optimizing investments in coupled offshore wind -electrolytic hydrogen storage systems in denmark," *Journal of Power Sources*, vol. 359, pp. 186 – 197, 2017 https://doi.org/10.1016/j.jpowsour.2017.05.048

[53] C. Schnuelle, T. Wassermann, D. Fuhrlaender, and E. Zondervan, "Dynamic hydrogen production from pv & wind direct electricity supply – modeling and techno-economic assessment," *International Journal of Hydrogen Energy*, vol. 45, no. 55, pp. 29 938 – 29 952, 2020 https://doi.org/10.1016/j.ijhydene.2020.08.044

[54] S. Touili, A. Alami Merrouni, Y. El Hassouani, A. illah Amrani, and S. Rachidi, "Analysis of the yield and production cost of large-scale electrolytic hydrogen from different solar technologies and under several moroccan climate zones," *International Journal of Hydrogen Energy*, vol. 45, no. 51, pp. 26 785 – 26 799, 2020 https://doi.org/10.1016/j.ijhydene.2020.07.118

[55] R. Loisel, L. Baranger, N. Chemouri, S. Spinu, and S. Pardo, "Economic evaluation of hybrid offshore wind power and hydrogen storage system," *International Journal of Hydrogen Energy*, vol. 40, no. 21, pp. 6727 – 6739, 2015 https://doi.org/10.1016/j.ijhydene.2015.03.117

[56] S. V. M. Guaitolini, I. Yahyaoui, J. F. Fardin, L. F. Encarnação, and F. Tadeo, "A review of fuel cell and energy cogeneration technologies," in *2018 9th International Renewable Energy Congress (IREC)*, 2018 https://doi.org/10.1109/IREC.2018.8362573 pp. 1–6.

[57] F. A. Alshehri, J. L. R. Torres, A. Perilla, B. W. Tuinema, M. A. M. M. van der Meijden, P. Palensky, and F. Gonzalez-Longatt, "Generic model of pem fuel cells and performance analysis in frequency containment period in systems with decreased inertia," in *2019 IEEE 28th International Symposium on Industrial Electronics (ISIE)*, 2019 https://doi.org/10.1109/ISIE.2019.8781346 pp. 1810–1815.

[58] P. A. Bernstein, M. Heuer, and M. Wenske, "Fuel cell system as a part of the smart grid," in *2013 IEEE Grenoble Conference*, 2013 https://doi.org/10.1109/PTC.2013.6652334 pp. 1–4.

[59] T. Wlodek, S. Kuczyński, A. Olijnyk, M. Łaciak, and A. Szurlej, "Thermodynamic and technical issues of hydrogen and methane-hydrogen mixtures pipeline transmission," *Energies*, vol. 12, p. 569, February 2019 https://doi.org/10.3390/en12030569

[60] Kurtz, Jennifer, Sam Sprik, Genevieve Saur, and Shaun Onorato. 2019., "Fuel cell electric vehicle durability and fuel cell performance," Golden, CO: National Renewable Energy Laboratory. NREL/TP-5400-73011. [Online]. Available: https://www.nrel.gov/docs/fy19osti/73011.pdf [Accessed 10 May 2021].

[61] M. T. Mito, X. Ma, H. Albuflasa, and P. A. Davies, "Reverse osmosis (ro) membrane desalination driven by wind and solar photovoltaic (pv) energy: State of the art and challenges for large-scale implementation," *Renewable and Sustainable Energy Reviews*, vol. 112, pp. 669–685, 2019 https://doi.org/10.1016/j.rser.2019.06.008

[62] M. Reuß, T. Grube, M. Robinius, P. Preuster, P. Wasserscheid, and D. Stolten, "Seasonal storage and alternative carriers: A flexible hydrogen supply chain model," *Applied Energy*, vol. 200, pp. 290–302, 2017. [Online]. Available: https://www.sciencedirect.com/science/article/pii/S0306261917305457 https://doi.org/10.1016/j.apenergy.2017.05.050

[63] Beiter, Philipp, Walter Musial, Patrick Duffy, Aubryn Cooperman, Matt Shields, Donna Heimiller, and Mike Optis. 2020., "The cost of floating offshore wind energy in california between 2019 and 2032," Golden, CO: National Renewable Energy Laboratory. NREL/TP-5000-77384. [Online]. Available: https://www.nrel.gov/docs/fy21osti/77384.pdf [Accessed 10 May 2021].

[64] U. Caldera and C. Breyer, "Learning curve for seawater reverse osmosis desalination plants: Capital cost trend of the past, present, and future," *Water Resources Research*, vol. 53, no. 12, pp. 10 523–10 538, 2017 https://doi.org/10.1002/2017WR021402

[65] IEA, "The future of hydrogen," 2019, [Accessed 10 May 2021]. [Online]. Available: https://www.iea.org/reports/the-future-of-hydrogen

[66] M. Kettani and P. Bandelier, "Techno-economic assessment of solar energy coupling with large-scale desalination plant: The case of morocco," *Desalination*, vol. 494, p. 114627, 2020. [Online]. Available: https://www.sciencedirect.com/science/article/pii/S0011916420313059 https://doi.org/10.1016/j.desal.2020.114627

[67] V. R. Carvalho, M. F. Moraes, A. P. Braga, and E. M. Mendes, "Evaluating five different adaptive decomposition methods for eeg signal seizure detection and classification," *Biomedical Signal Processing and Control*, vol. 62, p. 102073, 2020 https://doi.org/10.1016/j.bspc.2020.102073

[68] The Wind Power, "MHI Vestas Offshore - V164/9500." [Online]. Available: https://www.thewindpower.net/turbine_en_1476_mhi-vestas-offshore_v164-9500.php [Accessed 10 May 2021].

[69] REN, "Spot Market Prices - Portugal and Spain." [Online]. Available: https://www.mercado.ren.pt/EN/Electr/MarketInfo/MarketResults/OMIE/Pages/Prices.aspx [Accessed 10 May 2021].

[70] SuperDataScience, "Convolutional Neural Networks (CNN): Step 3 - Flattening." [Online]. Available: https://www.superdatascience.com/blogs/convolutional-neural-networks-cnn-step-3-flattening [Accessed 10 May 2021].

A

Binary Variables in MILP

As the name suggests, a MILP must be composed by linear constraints and objective function, which induces a degree of difficulty when implementing an efficiency curve, as is the case of the fuel cell. To solve this, the efficiency curve was decomposed into two values: if the fuel cell is operating below 63% of the nominal power (denominated as the dividing threshold), then its efficiency is 55%, otherwise it's 47.7%. These values were determined by changing the dividing threshold from 1% to 99% and computing the mean efficiencies above and below the threshold. Then, the error associated with representing an efficiency curve was calculated as:

$$Error = \sum_{n=0}^{trh} |\eta_{below} - \eta_{curve}[n]| + \sum_{n=trh}^{100} |\eta_{above} - \eta_{curve}[n]| \qquad (A.1)$$

where n is the fuel cell's load (0-100% of nominal power), trh is the dividing threshold, η_{below} and η_{above} are the efficiency below and above the dividing threshold, respectively, and η_{curve} is the fuel cell's efficiency curve. The dividing threshold that yields the lowest error is 63%, so it was the selected threshold.

In order to implement the fuel cell's efficiency to either 55% or 47.7% depending on the operating

load, a binary variable is defined to "select" which constraint actually constrains the efficiency. In the case of the fuel cell, when the binary variable y_{fc} is 0 the efficiency should be 55% and when y_{fc} is 1 the efficiency should be 47.7%. The constraints that set the fuel cell's electricity production are equations 3.35 and 3.36, which apply the efficiency value to the energy value of the hydrogen being fed into the fuel cell. If this binary variable is 0, then equation 3.36 sets the fuel cell's electricity production to a value lower than 1000 times the fuel cell's nominal power, effectively this constraint provides no useful information and in a certain way is ignored. However, equation 3.35 sets the electricity production of the fuel cell to 55% of the energy of the hydrogen being fed into the fuel cell, which is the intended objective. If y_{fc} is 1 then the opposite occurs, equation 3.35 is "ignored" and equation 3.36 sets the fuel cell's efficiency to 47.7%.

A similar method is used for the other non-linear calculations of the model. When calculating regulation costs, the equation used is either 3.33 if the imbalance is positive or 3.34 if the imbalance is negative, so the binary variable y_{imb} was defined to select the correct equation depending on the imbalance. Regarding storage, hydrogen can only be sold when the current stored hydrogen is higher then the reserve storage capacity, so the variable y_{ss} was defined to indicate when hydrogen can be sold. The final non-linear calculation is hydrogen production in the electrolyzer, since the power directed to the electrolyzer should either be 0 if hydrogen production isn't favorable or between maximum and minimum powers for which the electrolyzer can produce hydrogen ($P_{el_{max}}$ and $P_{el_{min}}$). Variable y_{ee} was defined to indicate when the power directed to the electrolyzer is insufficient to produce hydrogen and when it's a value that will lead to producing hydrogen.

To summarize, the binary variables are defined according to equations A.2 - A.5, where imb is the difference between electricity sold to the grid and the day ahead market bid, efc_h is the electricity generated by the fuel cell, P_{fc} is the fuel cell's nominal power, ss_h is the current amount of hydrogen stored, ss_{res} is the hydrogen storage reserve and ee_h is the energy fed into the electrolyzer.

$$y_{imb} = \begin{cases} 0, & imb \leq 0 \\ 1, & imb > 0 \end{cases} \tag{A.2}$$

$$y_{fc} = \begin{cases} 0, & efc_h/P_{fc} \leq 0.63 \\ 1, & efc_h/P_{fc} > 0.63 \end{cases} \tag{A.3}$$

$$y_{ss} = \begin{cases} 0, & ss_h \leq ss_{res} \\ 1, & ss_h > ss_{res} \end{cases} \tag{A.4}$$

$$y_{ee} = \begin{cases} 0, & ee_h < P_{el_{min}} \\ 1, & ee_h \geq P_{el_{min}} \end{cases} \tag{A.5}$$

B
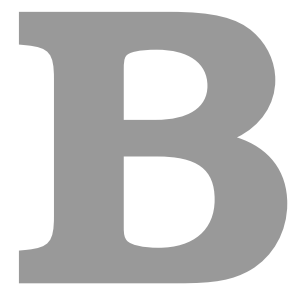
Neural Network Layers

The goal of the neural network is to generate a 1D array with a length of 24, one value for each hour of the following day. Even when working with 1D CNNs, if the number of filters is greater than 1 and the size of the filters is lower than the size of the input (which is almost always the case), then the output of the convolutional layers is 2 dimensional. To convert a 2 dimensional object into a 1 dimensional object, a flatten layer can be used. This layer simply takes every value in the 2 dimensional object and places it into a single dimension, which means that by flattening an object with dimensions $x \times y$, a 1 dimension array with length $x + y$ is created (illustrated on figure B.1).
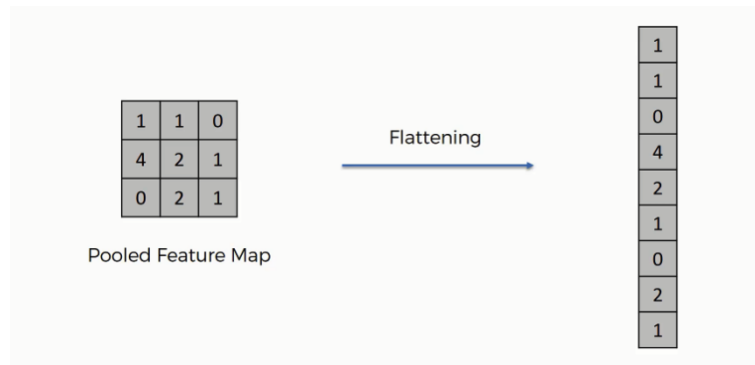
Figure B.1: Flatten layer. Source [70]

After a flattening layer, a fully connected layer is often used to provide a buffer between the learned features and the output, with the intent of interpreting the learned features before making a prediction. As the name suggests, in a fully connected layer all neurons of one layer are connected to all neurons in the following layer. Figure B.2 presents an example of a fully connected layer, which is essentially, one layer of a Multilayer Perceptron (MLP) neural network.

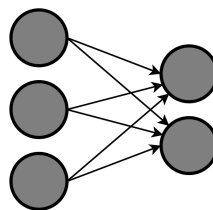**Figure B.2:** Fully connected layer

The use of convolutional layers inevitably leads to in a reduction in the input's dimension. The up-sampling layer can increase the dimension by repeating the input values, as can be seen in figure B.3.
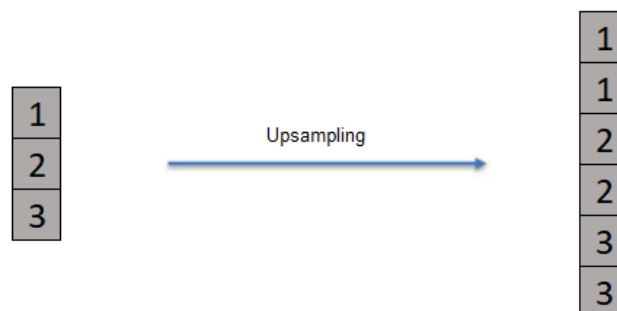

Figure B.3: Upsampling layer

C

Optimal Ratios

The electrolyzer's optimal ratios for the wind farm in both considered locations are presented in this appendix.

Table C.1: Electrolyzer's optimal ratios

System	Hydrogen Price [€/kg]	25 km from shore			50 km from shore		
		2020	2030	2050	2020	2030	2050
Offshore Electrolyzer	2	60%	90%	90%	65%	90%	95%
	3	80%	90%	95%	75%	90%	95%
	4	90%	90%	95%	90%	95%	95%
	5	90%	90%	95%	90%	95%	95%
	6	90%	95%	95%	95%	95%	95%
	7	95%	95%	95%	95%	95%	95%
	8	95%	95%	95%	95%	95%	95%
	9	95%	95%	95%	95%	95%	95%
	10	95%	95%	95%	95%	95%	95%
Onshore Electrolyzer	2	5%	5%	5%	5%	5%	5%
	3	5%	100%	100%	5%	100%	100%
	4	100%	100%	100%	100%	100%	100%
	5	100%	100%	100%	100%	100%	100%
	6	100%	100%	100%	100%	100%	100%
	7	100%	100%	100%	100%	100%	100%
	8	100%	100%	100%	100%	100%	100%
	9	100%	100%	100%	100%	100%	100%
	10	100%	100%	100%	100%	100%	100%

D

Economic Analysis

In this appendix the results from the economic analysis are presented in more detail for hydrogen prices from 2-10 €/kg.

Table D.1: Yearly revenue for the location 25 km from shore

| System | Hydrogen Price [€/kg] | Yearly revenue [€] | | | | | |
| | | 2020 | | 2030 | | 2050 | |
		H2	Electricity	H2	Electricity	H2	Electricity
Offshore Electrolyzer	2	12.1M	0	17.2M	0	18M	0
	3	21.6M	0	25.8M	0	27.2M	0
	4	30.4M	0	34.4M	0	36.3M	0
	5	38M	0	43M	0	45.4M	0
	6	45.6M	0	52.2M	0	54.5M	0
	7	53.9M	0	60.9M	0	63.6M	0
	8	61.6M	0	69.6M	0	72.7M	0
	9	69.3M	0	78.4M	0	81.8M	0
	10	77M	0	87.1M	0	90.8M	0
Onshore Electrolyzer	2	0.39M	18.5M	0.63M	18.3M	0.74M	18.2M
	3	1.7M	17.5M	49.7M	-17.8M	54.9M	-20.9M
	4	67M	-25.6M	77.1M	-26.9M	80.7M	-27M
	5	85.4M	-27M	96.9M	-27.2M	101M	-27.3M
	6	103M	-27.1M	116M	-27.2M	121M	-27.3M
	7	120M	-27.1M	136M	-27.2M	142M	-27.3M
	8	137M	-27.1M	155M	-27.2M	162M	-27.3M
	9	154M	-27.1M	174M	-27.2M	182M	-27.3M
	10	171M	-27.1M	194M	-27.2M	202M	-27.3M
Conventional Wind Farm	-	-	18.8M	-	18.8M	-	18.8M

Table D.2: Yearly revenue for the location 50 km from shore

| System | Hydrogen Price [€/kg] | Yearly revenue [€] | | | | | |
| | | 2020 | | 2030 | | 2050 | |
		H2	Electricity	H2	Electricity	H2	Electricity
Offshore Electrolyzer	2	13.5M	0	18.4M	0	19.5M	0
	3	19M	0	27.6M	0	29.2M	0
	4	32.6M	0	37.3M	0	39M	0
	5	40.7M	0	46.7M	0	48.7M	0
	6	49.5M	0	56M	0	58.5M	0
	7	57.8M	0	65.4M	0	68.2M	0
	8	66.1M	0	74.7M	0	77.9M	0
	9	74.3M	0	84M	0	87.7M	0
	10	82.6M	0	93.4M	0	97.4M	0
Onshore Electrolyzer	2	0.38M	20M	0.62M	19.8M	0.73M	19.7M
	3	1.7M	19M	49.7M	-16.3M	54.9M	-19.3M
	4	66.9M	-24.1M	77.2M	-25.4M	80.7M	-25.5M
	5	85.4M	-25.5M	96.9M	-25.7M	101M	-25.8M
	6	103M	-25.6M	116M	-25.7M	121M	-25.8M
	7	120M	-25.6M	136M	-25.7M	142M	-25.8M
	8	137M	-25.6M	155M	-25.7M	162M	-25.8M
	9	154M	-25.6M	174M	-25.7M	182M	-25.8M
	10	171M	-25.6M	194M	-25.7M	202M	-25.8M
Conventional Wind Farm	-	-	20.3M	-	20.3M	-	20.3M

Table D.3: Economic assessment for the location 25 km from shore

System	Hydrogen Price [€/kg]	NPV [€]			IRR [%]		
		2020	2030	2050	2020	2030	2050
Offshore Electrolyzer	2	-651M	-256M	-82.3M	-	-	-
	3	-573M	-156M	23M	-	-	11.22
	4	-486M	-56M	129M	-	0.58	31.24
	5	-397M	44M	234M	-	12.19	51.63
	6	-309M	145M	340M	-	24.61	72.08
	7	-220M	246M	446M	-	37.32	92.62
	8	-131M	347M	551M	-	50	113.29
	9	-41M	448M	657M	4.28	62.64	134.05
	10	48M	549M	762M	10.21	75.29	154.91
Onshore Electrolyzer	2	-489M	-157M	-33M	-	-	0.89
	3	-485M	-95.3M	96M	-	-	24.43
	4	-374M	119M	325M	-	22.05	67.41
	5	-177M	345M	561M	-	49.8	111.26
	6	22.6M	571M	796M	8.51	77.72	155
	7	222M	796M	1032M	22.39	105.47	198.68
	8	421M	1022M	1268M	36.62	133.14	242.32
	9	620M	1248M	1504M	50.73	160.79	285.96
	10	819M	1474M	1740M	64.7	188.41	329.58
Conventional Wind Farm	-	-474M	-152M	-31M	-	-	1.22

Table D.4: Economic assessment for the location 50 km from shore

System	Hydrogen Price [€/kg]	NPV [€]			IRR [%]		
		2020	2030	2050	2020	2030	2050
Offshore Electrolyzer	2	-655M	-256M	-77M	-	-	-
	3	-570M	-149M	36.4M	-	-	13.41
	4	-476M	-40.5M	150M	-	2.54	34.29
	5	-381M	68M	263M	-	14.87	55.43
	6	-286M	177M	376M	-	28.03	76.63
	7	-190M	285M	489M	-	41.3	97.92
	8	-94M	394M	603M	0.97	54.51	119.31
	9	2M	502M	716M	7.12	67.69	140.8
	10	98M	611M	829M	13.48	80.87	162.37
Onshore Electrolyzer	2	-486M	-152M	-26.5M	-	-	2.37
	3	-482M	-90M	103M	-	-	24.6
	4	-371M	125M	331M	-	21.52	65.29
	5	-173M	350M	567M	-	48.68	106.86
	6	25.9M	576M	803M	8.69	75.53	148.35
	7	225M	802M	1039M	22.18	102.21	189.8
	8	424M	1028M	1275M	36.03	128.84	231.22
	9	623M	1253M	1510M	49.77	155.43	272.64
	10	823M	1479M	1746M	63.38	182.0	314.04
Conventional Wind Farm	-	-470M	-147M	-24M	-	-	2.68

E

Sensitivity Analysis

In this appendix the results from the sensitivity analysis for 2020, 2030 and 2050 are presented for both locations, except for the location 25 km from shore in 2030 as it was already presented in chapter 5.5.
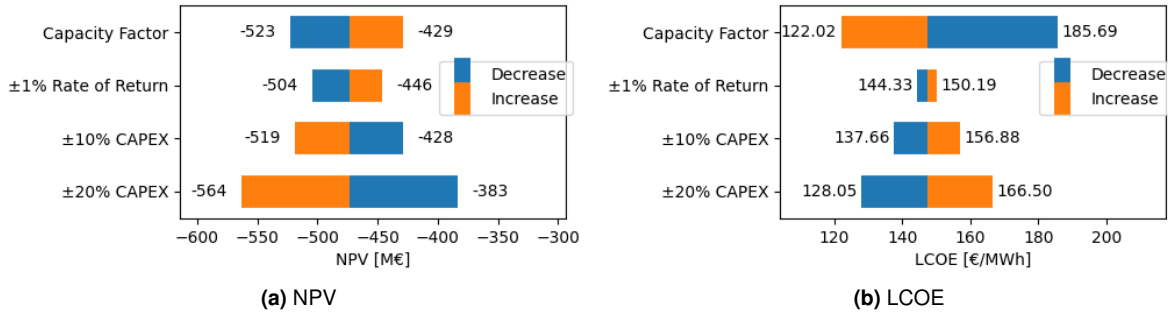
(a) NPV

(b) LCOE

Figure E.1: Sensitivity analysis for the conventional wind farm in 2020 for the location 25 km from shore

(a) NPV

(b) LCOH
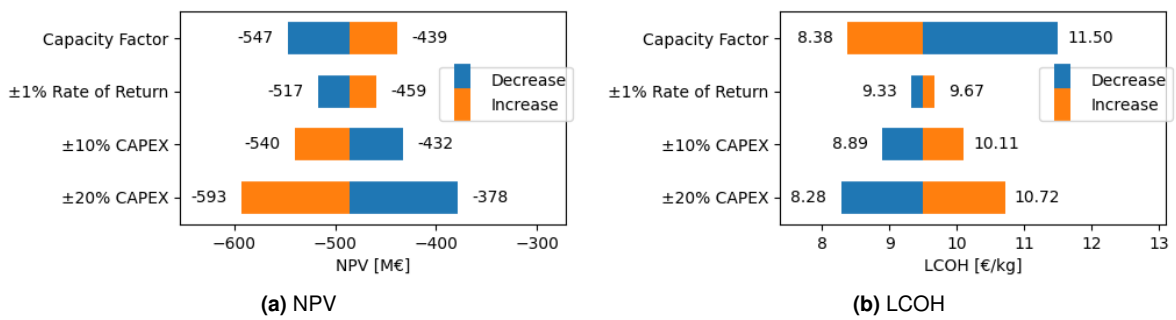
Figure E.2: Sensitivity analysis for the offshore electrolyzer system in 2020 the location 25 km from shore

(a) NPV

(b) LCOH
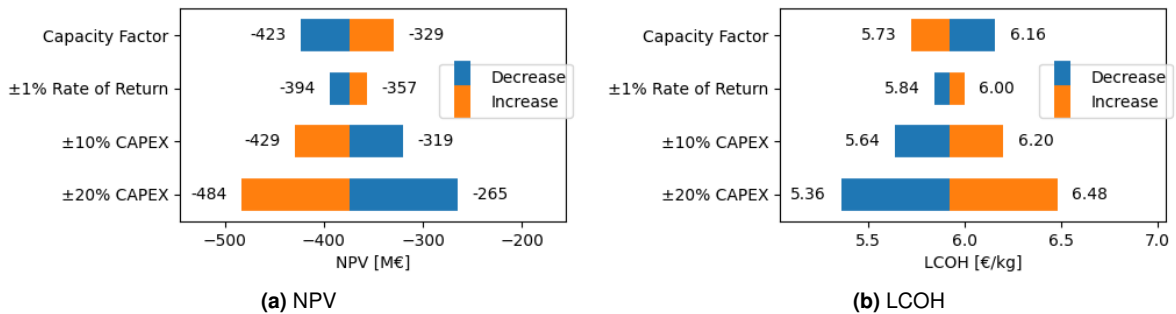
Figure E.3: Sensitivity analysis for the onshore electrolyzer system in 2020 the location 25 km from shore

(a) NPV

(b) LCOE
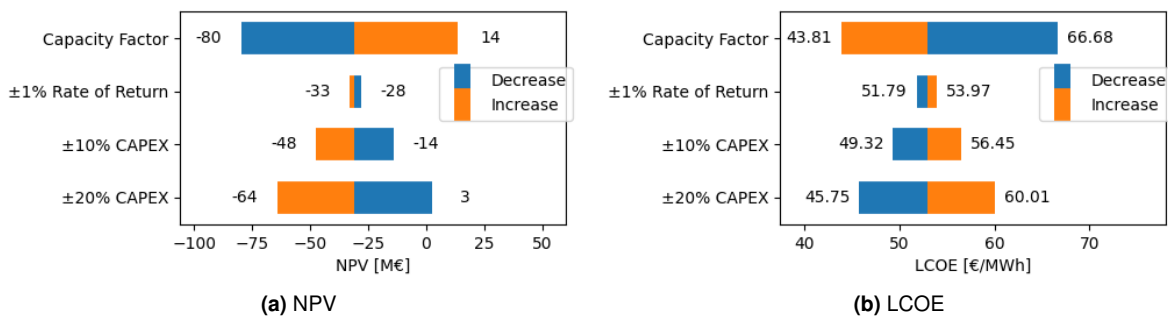
Figure E.4: Sensitivity analysis for the conventional wind farm in 2050 the location 25 km from shore

(a) NPV

(b) LCOH
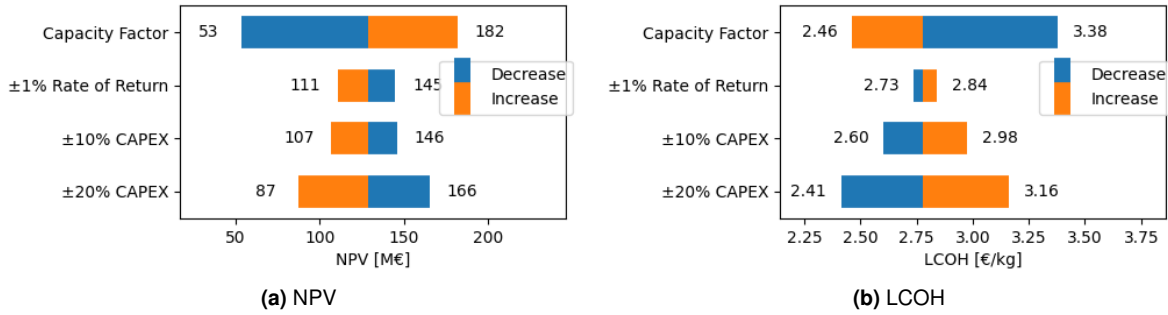
Figure E.5: Sensitivity analysis for the offshore electrolyzer system in 2050 the location 25 km from shore

(a) NPV

(b) LCOH
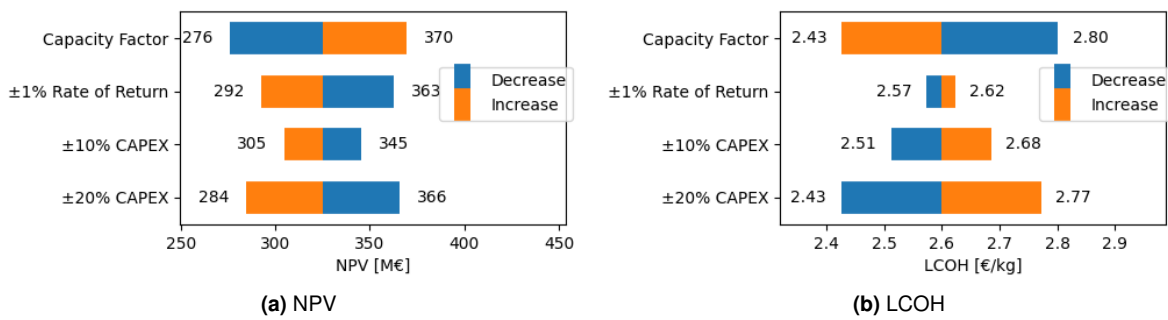
Figure E.6: Sensitivity analysis for the onshore electrolyzer system in 2050 the location 25 km from shore

(a) NPV

(b) LCOE
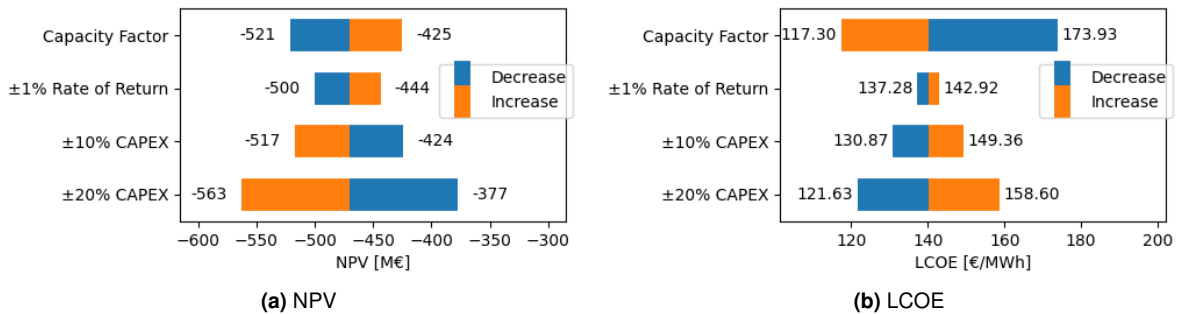
Figure E.7: Sensitivity analysis for the conventional wind farm in 2020 for the location 50 km from shore

(a) NPV

(b) LCOH
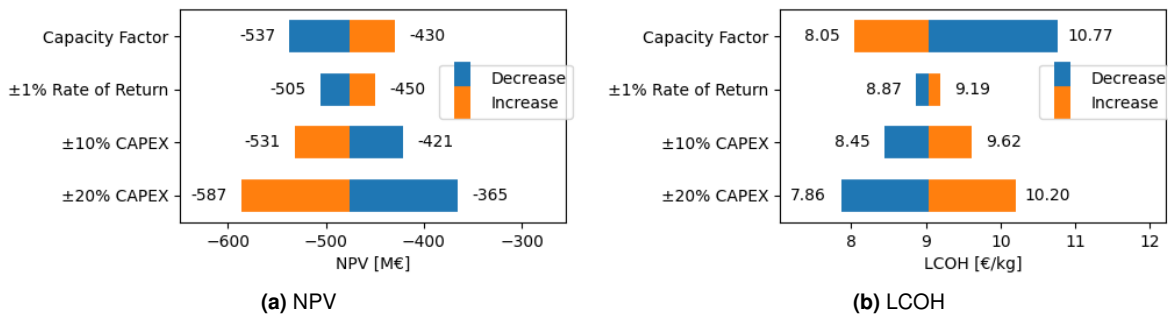
Figure E.8: Sensitivity analysis for the offshore electrolyzer system in 2020 the location 50 km from shore

(a) NPV

(b) LCOH
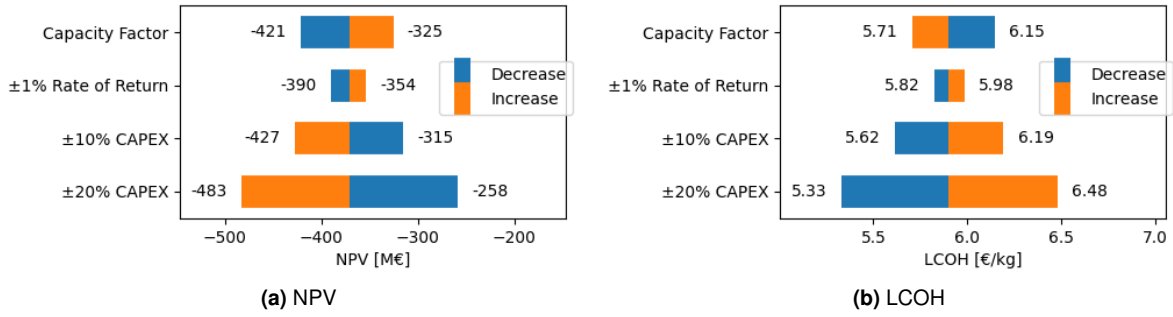
Figure E.9: Sensitivity analysis for the onshore electrolyzer system in 2020 the location 50 km from shore

(a) NPV

(b) LCOE
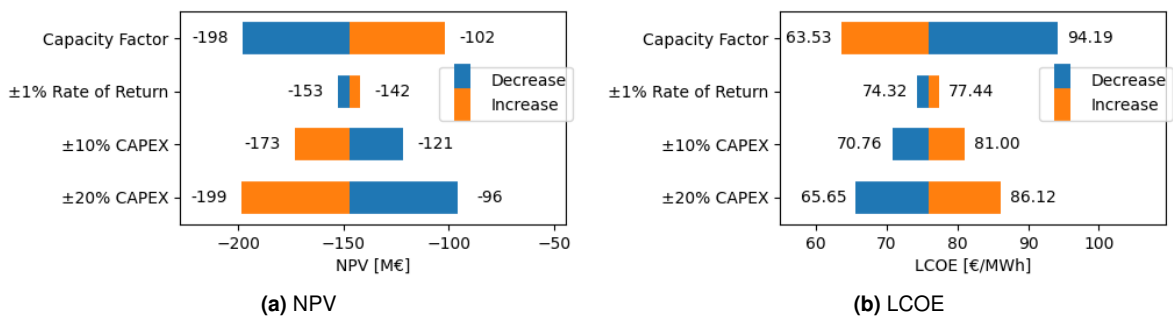
Figure E.10: Sensitivity analysis for the conventional wind farm in 2030 the location 50 km from shore

(a) NPV

(b) LCOH
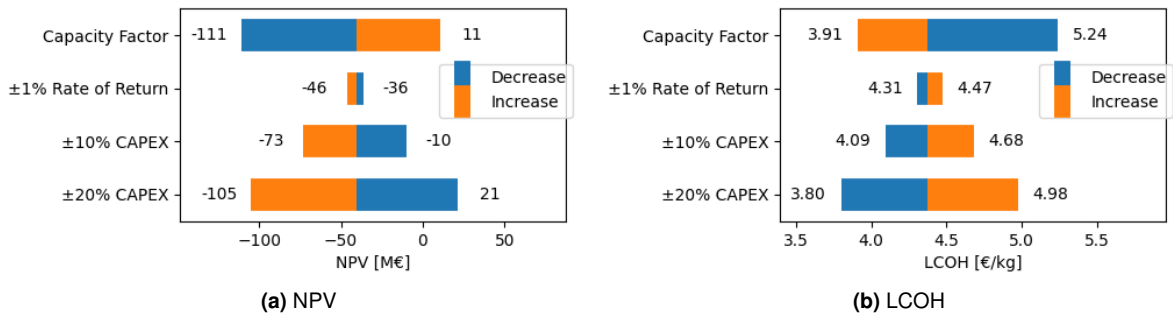
Figure E.11: Sensitivity analysis for the offshore electrolyzer system in 2030 the location 50 km from shore

(a) NPV

(b) LCOH
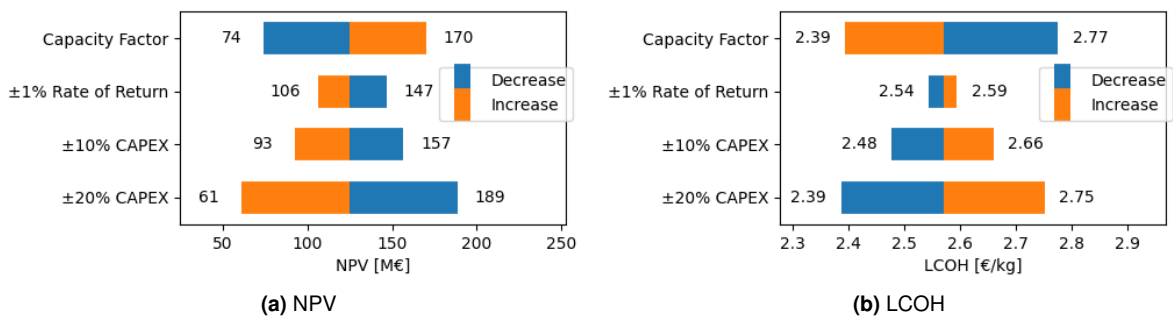
Figure E.12: Sensitivity analysis for the onshore electrolyzer system in 2030 the location 50 km from shore

(a) NPV

(b) LCOE
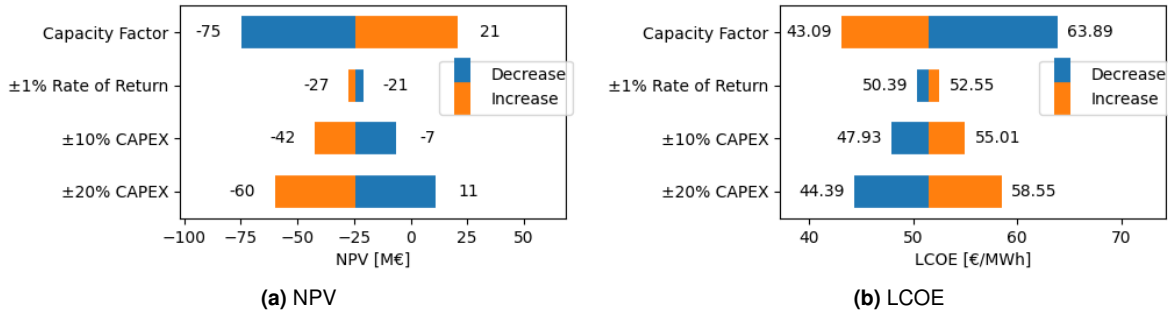
Figure E.13: Sensitivity analysis for the conventional wind farm in 2050 the location 50 km from shore

(a) NPV

(b) LCOH
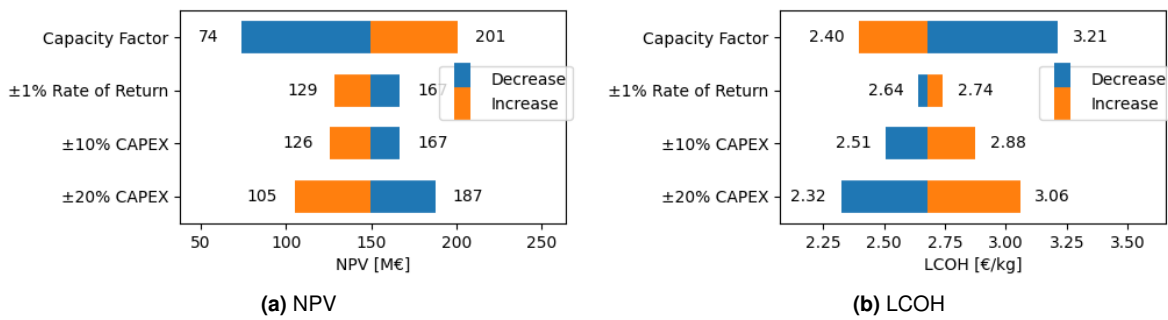
Figure E.14: Sensitivity analysis for the offshore electrolyzer system in 2050 the location 50 km from shore

(a) NPV

(b) LCOH

Figure E.15: Sensitivity analysis for the onshore electrolyzer system in 2050 the location 50 km from shore

F

Published Article

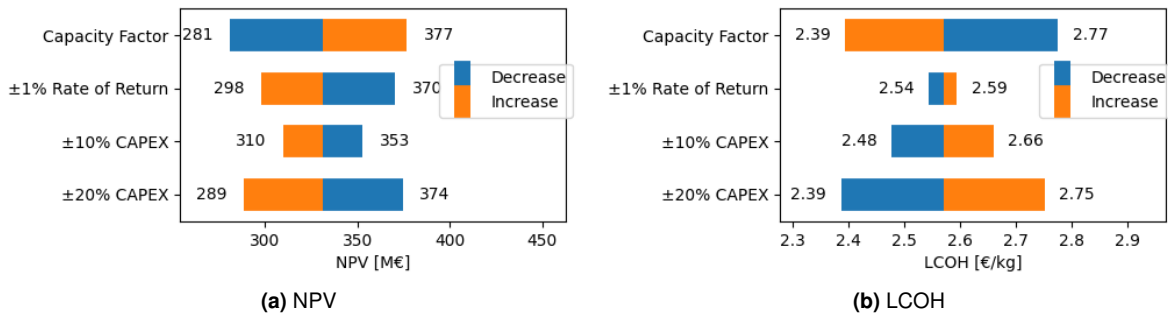*Review*

Hydrogen Production from Offshore Wind Parks: Current Situation and Future Perspectives

Gonçalo Calado [1] and Rui Castro [2,*]

1   Instituto Superior Técnico, University of Lisbon, 1049-001 Lisboa, Portugal; goncalo.calado@tecnico.ulisboa.pt
2   INESC-ID/IST, University of Lisbon, 1000-029 Lisboa, Portugal
*   Correspondence: rcastro@tecnico.ulisboa.pt

Abstract: With the increase in renewable energy connected to the grid, new challenges arise due to its variable supply of power. Therefore, it is crucial to develop new methods of storing energy. Hydrogen can fulfil the role of energy storage and even act as an energy carrier, since it has a much higher energetic density than batteries and can be easily stored. Considering that the offshore wind sector is facing significant growth and technical advances, hydrogen has the potential to be combined with offshore wind energy to aid in overcoming disadvantages such as the high installation cost of electrical transmission systems and transmission losses. This paper aims to outline and discuss the main features of the integration of hydrogen solutions in offshore wind power and to offer a literature review of the current state of hydrogen production from offshore wind. The paper provides a summary of the technologies involved in hydrogen production along with an analysis of two possible hydrogen producing systems from offshore wind energy. The analysis covers the system components, including hydrogen storage, the system configuration (i.e., offshore vs. onshore electrolyzer), and the potential uses of hydrogen, e.g., Power to Mobility, Power to Power, and Power to Gas.

1. Introduction

Hydrogen is a gas that can be easily produced using electrolysis and that has several potential applications, ranging from an energy source for transportation to being mixed into the natural gas grid, along with current applications in fuel refining and fertilizer production. Historically, hydrogen production is based on fossil fuels and emits a large amount of CO_2; however, in the last decades, significant advances have been made in electrolysis and renewable energy production, making possible the production of green hydrogen at a reasonable price point.

Furthermore, with governments pushing the reduction of carbon emissions and lowering the dependence on fossil fuels, the demand for green hydrogen has risen quickly and is expected to rise substantially in the coming years. With the help of incentives and policies, green hydrogen is undergoing significant investigation around the world, with the objective of producing hydrogen without carbon emissions that, with a small incentive, can compete with traditional hydrogen production methods.

Fuel cells are devices that use hydrogen to produce electricity, with the only by-products being water and heat. In recent years, fuel cells have also experienced significant advancements; they are starting to be used in commercial applications like passenger cars, trucks, buses, and grid-connected dispatchable power plants. One of the reasons electrical grids are still dependent on fossil fuels is due to their ability to regulate power production. Since typical renewable energy sources like wind and solar energy are intermittent, their power output can't be regulated (hydroelectric dams with reservoirs provide some flexibility but ultimately are dependent on rainfall upstream). Hydrogen can serve as an energy

storage solution, where dispatchable fuel cells that run on green hydrogen can produce power when needed without any carbon emissions.

Wind power produces roughly 5% of the world's electricity [1], with most installations onshore. However, higher wind speeds and more consistent wind can be found offshore, which leads to higher energy production per turbine installed; the disadvantages are higher cost and technical challenges due to the rough sea conditions to which the equipment is subjected. One of the challenges is transporting the electricity back to shore, since traditional AC power cables have higher capacitance and thus higher losses than overhead lines, and more recent High Voltage Direct Current (HVDC) systems are expensive due to the converter stations necessary at each end of the transmission line. Considering that the transportation of gas in a pipeline suffers much smaller losses (<0.1%) [2,3] than electricity passing through an offshore cable, a case can be made for the production of hydrogen offshore, with pipelines to transport it to shore. From an economic perspective, the cost per unit length of an offshore pipeline is higher than an offshore cable. However, the pipeline's energy transmission capacity is greater than the cable, resulting in lower normalized pipeline capital costs compared to an equivalent offshore electrical cable to transmit the same energy [3].

Two system configurations can be found: the first consists of an offshore wind farm, offshore electrolyzer, and onshore hydrogen storage, while in the second system the electrolyzer is located onshore. A fuel cell can be added in both systems to provide electricity in high-demand periods and act as frequency control for the grid. For the first system, the electricity generated by the wind turbines travels a short distance to the electrolyzer platform, where hydrogen is produced, compressed, and transported to shore in a pipeline. On the other hand, for the second system, the electricity is transmitted to shore by a traditional cable, where a choice can be made: sell the electricity directly to the grid or produce hydrogen. This is known as a hybrid system, where the operator can control the amount of power being sold to the grid or fed into the electrolyzer, even being able to buy electricity from the grid to produce hydrogen during periods of extremely low electricity prices, which provides load flexibility to the grid operator as well. Since the source of the electricity powering the electrolyzer is wind farms, no carbon is emitted during the production of hydrogen.

This paper is concerned with hydrogen production using electricity coming from offshore wind farms, i.e., green hydrogen production. The paper offers an overview of the current situation on the subject by highlighting the main features of the technologies used by the different components of the hydrogen production system as well as an outline of the system configuration options (offshore vs. onshore electrolyzer location) and potential uses of hydrogen. Moreover, the paper reviews the main recent research topics related to the subject through a thorough literature review, including state-of-the-art reports and journal papers. The aim is to point out directions of future developments in green hydrogen production from wind power and other renewables.

The remainder of the paper is organized as follows. In Section 2, a discussion of the system components used for hydrogen production from offshore wind power is offered. The system configurations, i.e., the option between the offshore and onshore location of the electrolyzer, are discussed in Section 3. A summary of the main hydrogen uses is presented in Section 4. Section 5 contains a literature review of the main subject areas being investigated, including a comparison regarding the Levelized Cost of Hydrogen (LCOH) produced from different renewable energy sources. Finally, in the last section, the main conclusions of the work performed are drawn.

2. System Components

The hydrogen production system is composed of the offshore wind farm, for electricity production, the electrolyzer, for hydrogen production, and the hydrogen storage system.

2.1. Offshore Wind

When analysing fixed bottom wind turbines or floating turbines the main differences are cost and the locations where each technology can be implemented. The fixed bottom is the most used technology by a significant margin, with 24,952 MW installed in Europe, compared to only 62 MW of floating wind installed in Europe at the end of 2020 [4]; thus, it is the most cost-effective solution in offshore wind farms. However, floating wind prices are expected to lower rapidly in the next few years and allow access to much deeper waters; this will be useful in countries that do not have shallow water far from shore. The water depth around Europe is assessed in [5]; only the North Sea, Irish Sea, and a few other areas have a somewhat shallow depth where fixed bottom foundations can be installed. On the other hand, the water around the Iberian Peninsula and southern Europe can get be much deeper not too distant from the shore.

The report in [6] shows a projection of the Levelized Cost Of Energy (LCOE) of both bottom fixed and floating wind until 2050. The report indicates a current LCOE of 175 €/MWh for floating and 90 €/MWh for fixed bottom technologies. In 2050, these two figures are estimated to converge to 35 €/MWh.

The installation of fixed bottom wind turbines involves the use of a specialized boat capable of burying the foundations deep in the seabed, along with a crane to assemble the tower, nacelle, and individual blades. Comparing with floating wind, this newer approach can be fully assembled on land or dry dock and afterward be towed by a regular tugboat to the project's location. This much simpler installation can be another factor in lowering the costs; when more floating substructures are built, economies of scale have their effect. Europe is the leader in offshore wind power, and most of the installed power is in the North Sea (79%, according to WindEurope [4]), a location with high wind speed [5] and relatively shallow water and thus a good candidate for fixed bottom installations.

Around 80% of offshore wind resources are located in waters deeper than 60 m (where fixed bottom installations are not feasible), and average wind speeds increase further from shore [7]. To access this potential, floating wind currently represents the best approach; with the number of installations planned in the coming years, the future of floating wind is looking bright.

The first floating wind farm ever built on a commercial level is Hywind Scotland [8,9], composed of 5 turbines of 6 MW each, supported by a spar buoy. It has been producing energy since 2017. The buoys are 78 m in length and are attached to the seabed by 3 mooring lines. Although this is a simple design, added installation problems can arise from the dimensions of the buoy, such as the inability to be assembled on a simple port. More specifically, for hydrogen production, the individual electrolyzer approach is not as straightforward due to the cylindrical shape of a spar buoy, which limits the amount of space available to install an electrolyzer and the remaining infrastructure. Consequently, this structure requires more substantial modifications when compared to a semi-submersible platform, making the latter the most cost-competitive floating platform for an individual electrolyzer project [10].

One of the first wind farms deployed on a commercial level using a semi-submersible platform is WindFloat Atlantic in Viana do Castelo, Portugal. It was commissioned in 2020 [4] and is composed of 3 turbines of 8.4 MW each, supported by a semi-submersible structure made of 3 cylindrical buoys 30 m high and 50 m apart. Some advantages of this design are the simple assembly of the wind turbine on the structure in port and, due to hydrogen production by individual electrolyzers, the unobstructed area of 1082 m^2, with some modifications. Several other projects using similar platform designs are planned in the coming years [4].

2.2. Electrolyzer Technologies

An electrolyzer is a device that receives DC electricity and demineralized water and separates the hydrogen and oxygen atoms from the water molecule through a chemical reaction, generating high purity oxygen and hydrogen. While different technologies for electrolyzers operate in slightly different ways, all have an anode and cathode that are separated by an electrolyte.

Currently, there are two technologies used in commercial applications for the production of hydrogen: Alkaline Electrolyzer (AEL) and Proton Exchange Membrane Electrolyzer (PEMEL) [11,12]. Another technology undergoing intense research and development is Solid Oxide Electrolyzer (SOE), which promises high efficiencies and flexibility, but at the cost of both high operating temperatures (700 to 900 °C) and durability [11,12].

2.2.1. Alkaline Electrolyzers

AELs are currently the cheapest technology and have the longest lifetime, due in part to being the oldest of the technologies mentioned above [11,12]. This type of electrolyzer has been used in the industry for roughly 100 years; thus, while further progress is expected, both PEMEL and SOE development will surely be faster [11]. However, they cannot react as fast to changes in production, require complex maintenance of the alkaline fluid, cannot operate below a certain threshold for safety reasons, take longer to start, and present a rather low current density when compared to PEMEL, around 5 times lower [13]. In addition, the output pressure of the hydrogen produced is lower, which requires higher compression for transport and storage, reducing the advantage the lower CAPEX provided initially.

Historically, this type of electrolyzer has been operated at almost constant power while connected to the grid and recently has seen improvements in the ability to change hydrogen production rate without relevant efficiency losses. One of the highest-powered electrolyzers is a 4 MW module [14], which is claimed to have a dynamic response fast enough to follow the production of a renewable power plant. Furthermore, it is also said that the current density is double compared to the previous generation, that the output pressure is 30 bar, and that it has increased longevity compared to newer technologies [15].

2.2.2. Proton Exchange Membrane Electrolyzers

PEMELs are more recent than AELs and come with several advantages, such as much faster start-up times, higher current densities which lead to smaller electrolyzer footprints, higher hydrogen purity (>99.8%), operation beyond nominal power, and higher output pressure [11–13].

The report in [11] offers a comparison between the main features of PEMEL and AEL in 2017 and projected to 2025. With regard to the AEL (PEMEL figures in brackets) efficiency, an increase from the current 65% (57%) to 68% (64%) in 2025 is expected. At the same time, a decrease in the AEL (PEMEL) CAPEX from the current 750 €/kW (1200 €/kW) to 480 €/kW (700 €/kW) is foreseen by 2025. As far as the electrical consumption is concerned, some improvements are also to be expected. Currently, an AEL (PEMEL) consumes about 51 kWh (58 kWh) of electricity to produce 1 kg of hydrogen. The figure is foreseen to drop to 49 kWh/kg (52 kWh/kg) by 2025.

When combined with a renewable power source, the ability to easily adjust the power to suit the conditions and a quick start-up time are two great features that allow this technology to extract the most out of intermittent power sources. During periods of shutdown, low amounts of energy are required to maintain system operation [11,12]; this is an important fact to consider if the electrolyzer is to be kept offshore or if it will not be grid-connected. Furthermore, a backup power source must be provided if coupled with a renewable power source, since the intermittent nature of this type of power does not guarantee the necessary energy during shutdown periods.

Despite PEMELs having made significant progress in recent years in efficiency, output pressure, ramp up and ramp down times, and CAPEX, they are still considerably more expensive than AEL and do not have the same longevity [12]. The main reason for the high

price is the significant amount of platinum needed to build the stack of the electrolyzer. The efficiency curve in Figure 1 is a typical efficiency curve of a generic electrolyzer. It is based on the average of efficiency curves of several commercial electrolyzers as taken from [11].
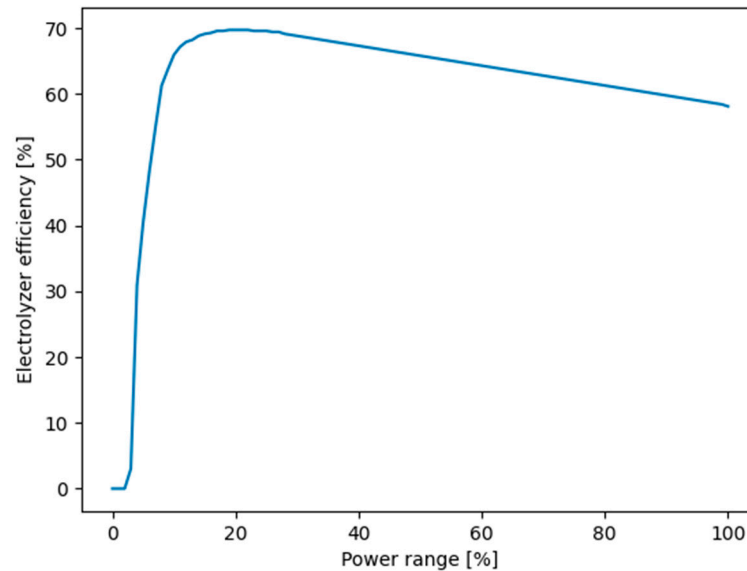

Figure 1. Efficiency curve of a PEMEL. Adapted from IRENA [11].

2.2.3. Solid Oxide Electrolyzer

The SOE is the newest of the three technologies and currently is rarely used in commercial applications due to the high operating temperatures (usually in the range of 700–900 °C) and lower longevity. This type of electrolyzer promises better efficiency than all other technologies and unlike PEMEL does not require any precious metals, which makes it possible to reach a lower CAPEX once the technology matures [12]. While the high operating temperature is a disadvantage, especially for intermittent power sources, it does not present as big an obstacle when coupled with nuclear or combined cycle power plants. In the case of renewable energy, Concentrated Solar Power (CSP) accompanied with an SOE is an option under study, since the waste heat from CSP can be used for heating the SOE [11].

2.3. Hydrogen Storage

Storage of hydrogen is similar to natural gas, with a few key differences: mainly, when some metals come in contact with hydrogen they can suffer hydrogen embrittlement, which leads to increased degradation and chance of material failure [15]. Another difference to consider is increased leakage, especially in underground natural structures such as aquifers, but also in links between pipeline sections or links in valves, due to the small size of the hydrogen molecule [15]. The bacterial reaction also constitutes a problem, since some bacteria decompose hydrogen, leading to what can be considered losses, as the purity of stored hydrogen decreases [2]. The main approaches in storing hydrogen are gaseous storage and liquid storage; other approaches like chemical storage exist, but only on a much smaller scale, so they won't be considered.

Gaseous storage can be divided into two methods: fabricated tanks (usually metal) and storage in natural underground structures like aquifers and salt caverns. Hydrogen density has a nearly linear relation with pressure [16], so a greater storage pressure leads to a smaller volume needed to store a certain amount of hydrogen gas. However, due to material properties and operational costs, hydrogen is not stored at pressures higher than 100 bar [15], which corresponds to a density of roughly 7.8 kg/m^3 [15].

A simple model can be developed to compute the rough dimensions of the storage facilities needed.

The flow rate of a typical 25 MW electrolyzer is $Q_n = 5000 \text{ Nm}^3/\text{h}$ [17]. To convert the hydrogen flow rate (Q_n) from Nm^3/h to mass (M) in ton/day, Equation (1) is used.

$$M = \frac{24Q_n}{11.1} \times 10^{-3} \tag{1}$$

In Equation (1), the factor 24 converts hours into days, the factor 11.1 comes from knowing that 1 kg of hydrogen equals 11.1 Nm^3 of hydrogen (Normal conditions are 0 °C temperature and 1 atm pressure), and the factor 10^{-3} is to convert kg to ton.

The corresponding hydrogen volume V in m^3/day is

$$V = \frac{M}{7.8 \times 10^{-3}} \tag{2}$$

where 7.8×10^{-3} ton/m^3 is the hydrogen density for a pressure of 100 bar at a temperature of 20 °C.

A linear variation of the hydrogen flow rate with the electrolyzer power was considered. This allowed us to obtain the flow rates for the electrolyzer power ranging from 25 MW to 1000 MW. Table 1 contains the electrolyzer power, flow rate, mass (Equation (1)) and volume (Equation (2)) of hydrogen produced per day if the electrolyzers are run at full power.

Table 1. Electrolyzer power, flow rate, and mass and volume of hydrogen produced.

Power (MW)	Flow Rate (Nm³/h)	Hydrogen Mass (ton/day)	Hydrogen Volume (m³/day)
25	5000	10.8	1386
100	20,000	43.2	5544
500	100,000	216	27,720
1000	200,000	432	55,440

The linear approximation used was based on a similar commercial 17.5 MW PEMEL that produces 340 kg/h [18]. When linearly scaled to 25 MW, a production rate of 11.6 tons/day is achieved, a similar value to the one presented in Table 1 (which is 10.8 tons/day).

To estimate the dimensions of the cylindrical storage tanks, the equation for a cylinder's volume (Equation (3)) was used, where V is the storage tank volume, h is the height, and r is the radius.

$$V = h \cdot \pi \cdot r^2 \tag{3}$$

Table 2 contains the possible approximate radius and height for cylindrical tanks to be able to store all the hydrogen produced during 24 h with the electrolyzers at full power.

Table 2. Possible approximate dimensions for gaseous storage facilities.

Power (MW)	Hydrogen Volume (m³/day)	Cylinder Radius (m)	Cylinder Height (m)
25	1386	9	6
100	5544	13	11
500	27,720	25	15
1000	55,440	30	20

Table 2 shows that even for large electrolyzer projects (1000 MW, for instance) the required storage facilities are feasible, and the corresponding dimensions are reasonable and therefore practicable.

The most cost-effective and practical way of storing large quantities of hydrogen as a gas is using underground natural structures. Aquifers are not as well sealed as salt caverns, which leads to increased leakage [15,19]. While some leakage might be reasonable when storing natural gas, due to the small size of the hydrogen molecule the leakage rate increases significantly; for this reason, aquifers are not adequate to store hydrogen. Salt caverns are the best underground storage structures for several reasons, including low construction costs, low leakage rates, fast withdrawal and injection rates, and a harsh environment for bacteria, which decreases unwanted bacterial activity [2,15,19]. Initial research shows no significant difference between storing hydrogen compared to natural gas in these structures, and pure hydrogen is already stored using this approach in Teeside, the UK, and Texas, USA [2,19].

The second approach consists of storing liquid hydrogen in metal tanks, a process similar to what is widely used for Liquified Natural Gas (LNG). The main advantage is the high density in the liquid state of 70 kg/m^3 [15], which is almost 10 times the density of hydrogen in a gas state at a pressure of 100 bar. However, the liquefaction of hydrogen is a very energy-intensive process, with anywhere from 6 to 10 kWh of electricity needed to liquefy 1 kg [15,20] of hydrogen. The current installed liquefaction capacity is around 355 tons per day [15], below the necessary capacity needed for a 1 GW plant. The main reasons for the low liquefaction capacity are the high initial investment associated with liquefaction plants and the high energy consumption to liquefy the hydrogen.

3. System Configurations

There are two possible options for the system configuration related to the location of the electrolyzer: it can be placed offshore, near the wind farm, or onshore, near the existing grid coupling point.

3.1. Offshore Electrolyzer Scenario

One of the significant costs in an offshore wind farm is the equipment to bring the electricity to shore, namely the cables, transformers, and power electronics. Considering a High Voltage Alternating Current (HVAC) transmission system, losses are around 1% to 5% for wind farms with nominal power from 500 to 1000 MW and located 50–100 km from shore [21,22]. For a HVDC system, losses range from 2% to 4%, depending on nominal power and distance [21,22]. However, hydrogen travelling through a pipeline has considerably lower losses, under 0.1% [2,3], along with reduced initial costs for an underwater pipeline compared to underwater electrical cables and the power electronics needed. Figure 2 contains an overview of the centralized offshore electrolyzer system.
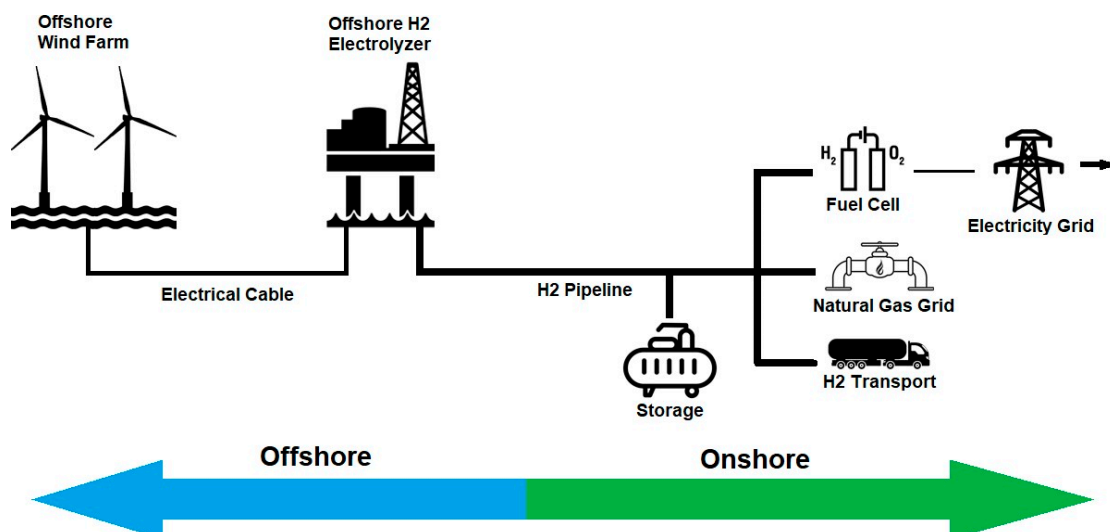

Figure 2. Offshore electrolyzer system.

PEMELs represent the best choice for this system due to the smaller footprint and easier maintenance [11], which in an offshore scenario means the platform can be smaller and the maintenance trips can be further apart.

Since the output pressure of a PEMEL is around 30 bar [11,17], additional compression is required to export the hydrogen to shore. The hydrogen compressor and export pipeline must be sized according to the distance to shore, operating pressure of the electrolyzer, flow of hydrogen, and pressure drop along the pipeline. A study done by North Sea Energy [23] estimated the required pipeline diameter and pressure, assuming an output pressure of 68 bar and 20 m/s maximum travel speed. The results show that for a 1 to 2 GW wind farm located 50 to 200 km from shore, the minimum diameter of the pipeline ranges from 0.25 to 0.41 m, while the minimum input pressure ranges from 83 to 100 bar.

To size the PEMEL, the nominal power does not need to be equal to the wind farm's nominal power, since the wind farm might not spend large periods of time at nominal power. From an economic point of view, the most interesting approach might be to slightly undersize the electrolyzer, since the revenue lost when the wind farm is at nominal power could be lower than the additional cost of a more powerful electrolyzer [6]. Furthermore, the energy used in purifying the water and compressing the hydrogen for transmission, along with the wake and array losses, lowers the actual available power for the electrolyzer [24].

A backup power source must be provided for the electrolyzer during periods of shutdown, when the electrolyzer must consume a small amount of power to remain in stand-by mode [11]. Periods of shutdown are not common and do not last long, due to the PEMEL capability of being able to start operating at 1% nominal power, although with low efficiency.

Two electrolyzer configurations are possible: a unique centralized electrolyzer fed by the whole wind park or individual electrolyzers, one per wind turbine. The details of each configuration are given below. The main components for the centralized electrolyzer system are the same as for the individual electrolyzer system, since the operating principle is similar. The components are

- PEMEL and the supporting electronics
- AC-DC rectifiers (possibly already included in electrolyzer)
- Desalination unit and reservoir for desalinated water
- Seawater pumps
- Export pipeline
- Backup power source
- Communication equipment

3.1.1. Centralized Electrolyzer

In a centralized electrolyzer system, the individual installation of the wind turbines is the same as a typical offshore wind farm, with turbines in strategic places to minimize losses by the wake effect. The power produced by each individual turbine is transmitted to a central platform through regular underwater cables; while voltages can differ, newer and higher power turbines, such as the Haliade-X 13 MW [25], operate at 66 kV.

Once the electrical power reaches the central platform, most of it can be rectified to DC; the other part is used to power the seawater pumps and hydrogen compressor in AC. The DC power is used mainly to produce hydrogen but also to power the backup power source and the supporting systems. The produced hydrogen exits the electrolyzer at high purity and with a pressure of 30 bar, so the next step is compressing it to the desired pipeline input pressure. After being compressed, the hydrogen is fed into the export pipeline, where it is transmitted to the shore.

3.1.2. Individual Electrolyzers

When sufficient wind is present, most of the electricity is fed into the rectifiers to power the electrolyzers and possibly refill the backup power source. The remaining power is used to power the seawater pumps, which need AC electricity. In the case of no offshore compression, the produced hydrogen exits the electrolyzer and is exported by a small dimension pipeline to a subsea collection manifold, which receives the hydrogen produced by each turbine-electrolyzer system and exports it to shore using a bigger diameter pipeline. However, if offshore compression is needed, the hydrogen exits the electrolyzer and is exported by a small dimension pipeline to a collection manifold in a platform, compressed to a desired pressure, and exported to shore by a pipeline.

This approach becomes more viable as the nominal power of a turbine keeps increasing, since more powerful electrolyzers can be installed individually, and economies of scale can play their part [23]. In [23], it is projected that the price per MW of a PEMEL will decrease from the current (2020) 0.75 M€/MW to 0.2 M€/MW by 2050. It is also projected that at around 10 MW, the cost per MW of hydrogen production power starts decreasing at a much slower rate, especially after the year 2030.

Since bottom fixed and some floating options, such as a spar buoy, require significant modifications to be able to support the extra infrastructure, the semi-submersible platform like the one used in WindFloat Atlantic is the best choice for the individual electrolyzer approach [10]. To make the platform suitable for all the equipment, modifications need to take place, such as creating a floor on which to put the equipment that is shielded from waves and possible water splashing, as well as modifying the buoys and ballast to accommodate the additional weight.

3.2. Onshore Electrolyzer Scenario

This approach is also known as a hybrid system, where the energy produced is transmitted to shore as electricity in conventional cables; once onshore, the energy can be sold directly to the grid or used to produce hydrogen. The main advantage of this system is flexibility: when the market price for electricity is high, the investor can sell electricity directly to the grid; when the market price is low or grid level curtailment must occur, the energy can be redirected to an electrolyzer to produce hydrogen. Curtailment occurs when the production of electricity is greater than the consumption, which leads to a need to reduce the production. Figure 3 contains an overview of the onshore electrolyzer system.
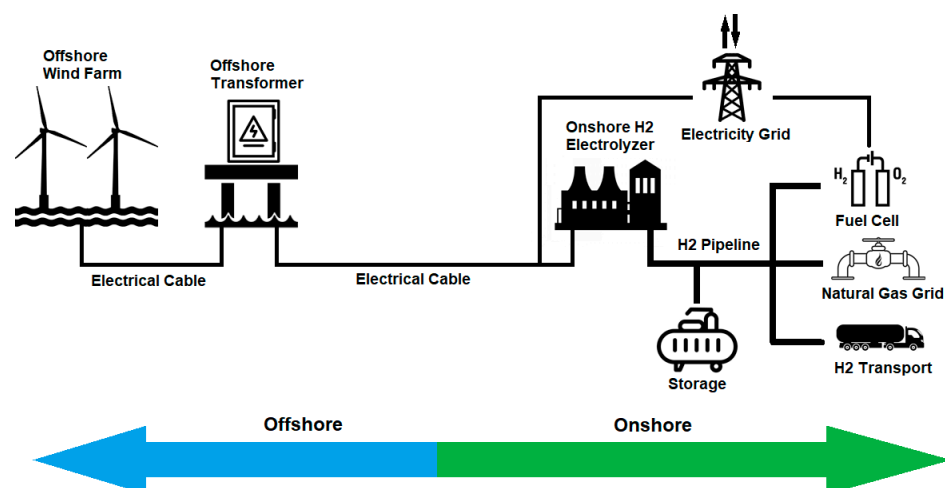

Figure 3. Onshore electrolyzer system.

Since in this approach the electrolyzer will be onshore, it is possible to place the electrolyzer and all other sensitive equipment inside a building, where they can be sheltered from the elements; this also provides a better work environment for the personnel responsible for the operation and maintenance. Furthermore, since access to the elec-

trolyzer is much simpler than if it was offshore, the increased maintenance requirements and decreased power density of an AEL do not present as big an obstacle, so the reduced CAPEX of this technology means both AEL and PEMEL are viable when the electrolyzer is installed on land.

HVDC is a more expensive technology that only becomes interesting when wind farms are located far from shore and/or have high nominal powers [26]. In the case of HVAC, longer lines imply more powerful line-reactive compensators to account for the capacitive losses, which in turn increases the cost. Since HVDC transmission does not show capacitive losses—only ohmic losses occur—the transmission losses and costs are significantly lower for HVDC. To summarize, transmission losses and costs are lower in the case of HVDC, and even though the initial investment for HVDC transmission (stations and equipment) is higher than HVAC, the difference in cost diminishes when the transmission distance increases. The break-even distance for which HVDC becomes preferable is around 50–100 km for underground and underwater cables [26].

Regarding the source of water, the two possible options are connecting the electrolyzer to the freshwater grid, an option that might not be viable due to environmental concerns in areas with recurring droughts, like southern Europe, or installation of a desalination unit next to the electrolyzer. Even though the water produced by a desalination unit is clean, and the water in freshwater grids has been previously treated, further treatment such as deionizing the water is still required for both options before being used in electrolysis [27].

4. Hydrogen Utilization

One of the properties of hydrogen that makes it so interesting is the wide array of utilization cases. Historically, hydrogen production was based on fossil fuels, so there wasn't an incentive to adopt hydrogen as an energy source since it had a carbon footprint. However, recent studies project significant cost reductions in electrolyzers in the coming years [11,20,27], with the possibility of green hydrogen becoming competitive with hydrogen produced from fossil fuels. Hydrogen electrolysis can also be a great way of reducing emissions, be it by working as energy storage to help when renewable resources are scarce or by reducing emissions caused by other polluting ways of producing hydrogen. The use cases for hydrogen can be divided into three main areas: generating electricity, Power to Gas (P2G), and hydrogen as the end product.

4.1. Generating Electricity

Hydrogen currently represents the best non-fossil fuel for some heavy vehicles that require large energy storage and fast recharge rates, such as long-haul trucks, buses, hybrid trains designed to operate on both electrified and non-electrified train tracks, and even for a common car, since refilling the hydrogen tank takes a few minutes and gives around 600 km of range [28]. This application is denominated as Power to Mobility (P2M).

For grid applications, the fast response time of some fuel cells makes them adequate as dispatchable power plants for peak demand or for frequency control. This application is denominated as Power to Power (P2P). Furthermore, some solid oxide systems can operate with high efficiencies in both electrolyzer and fuel cell modes; however, it should be noted this technology has not reached the commercial level yet [12,29].

The main fuel cell technologies are Polymer Electrolyte Membrane, also known as Proton Exchange Membrane (PEMFC), Alkaline (AFC), Phosphoric Acid (PAFC), Molten Carbonate (MCFC), and Solid Oxide (SOFC) [30]. The first two are considered low-temperature fuel cells, and the remaining are high-temperature fuel cells. As far as the efficiencies are concerned, they range from 40% (PAFC) to 60% (PEM, AFC, SOFC), with MCFC in between (50%).

Both AFC and PEMFC have quick start-up times; however, PEMFC presents greater power density, so it is the primary choice to equip hydrogen-based vehicles. Due to this emerging market, intensive research and development of PEMFC is being performed by

car and bus manufacturers; consequently, cost reductions and increased durability are expected in the coming years.

Most stationary installations of fuel cells are at high operating temperature [31], with one example being the 50 MW Daesan Hydrogen-Fuel-Cell Power Generation that started operating in South Korea in 2020. The plant is composed of 114 PAFC fuel cells and will produce around 400,000 MWh of energy annually [32,33].

In the past few years, PAFC and MCFC have presented the highest growth rate, though this is expected to change due to several companies offering PEMFC in the order of >1 MW [31], some of them stackable modules.

4.2. Power to Gas

Hydrogen is a highly flammable gas, so it is possible to inject some hydrogen into the natural gas grid without significant modifications to the grid or the systems that use natural gas. This application is denominated as P2G. Some pilot projects already in operation blend up to 20% hydrogen in localized natural gas grids such as small communities or universities [34]. Several studies support the idea that a low concentration of hydrogen (up to 15–20%) in the natural gas grid does not significantly increase the risk associated with utilization of the gas [35,36].

Another approach is being studied at several locations, including Central do Ribatejo in Portugal by EDP [37], where a 1 MW electrolyzer produces hydrogen during ramp down periods and stores it at 300 bar (storage capacity of 400 kg, which is around 13 MWh). The project plans to study the injection of hydrogen in the natural gas grid and the co-combustion of hydrogen and natural gas in a regular gas turbine. This installation is part of an international project named FLEXnCONFU, which aims to integrate hydrogen and ammonia in the electrical grid [38].

4.3. Hydrogen as the End Product

Arguably the best industry to sell green hydrogen is the already existing industry for hydrogen, predominantly used in refineries and for ammonia production. The estimated demand in 2018 was above 80 million tons [27]. Since this industry is already in place, the source of hydrogen can simply be gradually replaced by green hydrogen, especially as the LCOH of green hydrogen continues to decrease.

While ammonia can be the end product, it can also act as a carrier of hydrogen in order to facilitate transport with an equivalent hydrogen density of 122.4 kg/m^3 at a temperature of around 25 °C and a pressure of 10 to 20 bar. When compared to liquid hydrogen, the density is roughly 75% higher, and it can be transported at ambient temperatures and low pressures. The main disadvantage is the increased cost and complexity of producing the ammonia and afterwards decomposing it to recoup the hydrogen [20].

5. State-of-the-Art Review

The annual production of hydrogen in the EU is roughly 9.75Mt; this is currently being produced using carbon-intensive methods, which would require 290 TWh of electricity if the hydrogen was produced solely from electrolysis, around 10% of current production in the EU. In 2020, G. Kakoulaki et al. [39] concluded that the EU has enough renewable energy resources spread throughout member countries to satisfy the hydrogen demand solely using green hydrogen, thus allowing for decarbonization of the sector.

Electrolyzers can play a role in adding flexibility to an electricity grid. A technical analysis was conducted by D. Gusain et al. [40] to study the use of electrolyzers as flexibility service providers. A model for large-scale PEMEL was developed, along with the simulation of different use cases, to assess frequency regulation, flexibility provision, and long-term impact analysis of a PEMEL connected to the CIGRE MV grid [41]. For the first use case, the electrolyzer's response was adequate, and even though the test had a 40 min duration, no cell degradation took place. For the second case, the electrolyzer was used to correct the difference between the expected power injection and the real power injected at

a certain bus. The bus had a wind farm attached, so a forecast was made of the expected power produced throughout the day. The results showed the electrolyzer ensured that the real power was equal to the forecast power, which means an electrolyzer can be used to provide flexibility to the grid operator. In the final case, the electrolyzer was run at a constant current for a year; a drop in efficiency of 0.8% was calculated. Over a duration of five years, the efficiency drop increased to 3.5%. The impact derived from these efficiency drops must be taken into account in long-term strategies, so that the flexibility provided by the electrolyzer is always correctly assessed.

The sizing of electrolyzers must weigh numerous factors, namely the power produced by the wind farm and if there is a grid connection to provide power to the electrolyzer during low wind periods. The main advantage of the grid connection is a more consistent hydrogen production rate, and the main disadvantage is not being able to guarantee 100% carbon-free hydrogen due to consuming power from the grid. José G. García Clúa et al. [42] state that the ratio between the wind turbine's nominal wind speed (v_N) and the mean wind speed (v_m) of the installation site and the shape coefficient of a Weibull probability function k are the main influences in sizing the nominal powers of the electrolyzer and the wind turbine. The paper concludes that for v_N/v_m lower than 1.67, the electrolyzer makes good use of the available turbine power; however, the wind potential of the site is not fully exploited. On the other hand, for v_N/v_m greater than 1.77, the opposite happens. The recommended operation point is v_N/v_m in the range of 1.67 to 1.77, since in this range a balance between making good use of the available turbine power and exploiting the wind potential of the location is struck.

A techno-economic analysis of grid-connected hydrogen production was performed by T. Nguyen et al. [43], in which several electricity pricing schemes and hydrogen storage solutions were analyzed. The pricing schemes considered were flat rates in five Canadian provinces and real-time pricing in Germany, California, and Ontario. The study concludes that a real-time pricing scheme yields lower LCOH, since the electrolyzer can reduce consumption during periods of high energy prices, and that including storage is a good alternative to increase flexibility, especially when underground storage can be implemented. A capacity factor ranging between 0.9 and 1 was found to be optimal, since this minimizes consumption during peak hours but ensures a high utilization of the CAPEX. The lowest LCOH obtained was 2.49–2.74 €/kg for AEL (2.26–3.01 €/kg for PEMEL) with underground storage in a real-time pricing scheme in Ontario; this is competitive with hydrogen produced using Steam Methane Reform (SMR) with carbon capture, which is around 2.51–3.45 €/kg.

A similar study on offshore hydrogen production with underground storage was developed by Van Nguyen Dinh et al. [24], where the CAPEX and OPEX used were consistent with the forecast for offshore wind power and electrolyzers in the year 2030. The results show that for a 101.3 MW wind farm 15 km off the coast of Arklow, Ireland, at a selling price of 5 €/kg, the Discounted Payback Period (DPB), considering storage for 2, 7, 21, and 45 days of average hydrogen production, is 7.8, 8.6, 11.1, and 16.2 years, respectively.

The wind potential in Patagonia is enormous, being anywhere from 4100 to 5200 full-load hours on average, which leads to an LCOE of electricity as low as 25.6 €/MWh. In 2018, Philipp-Matthias Heuser et al. [44] analyzed a link between Japan and Patagonia, where hydrogen is produced and liquefied in Patagonia and shipped to Japan. The analysis estimated that the LCOH is 2.16 €/kg at the output of the electrolyzer, with an increase of 0.57 €/kg after transport to the shipping port and a further 0.58 €/kg to liquefy the hydrogen and store it in liquid form, which brings the final LCOH to 3.31 €/kg. The cost of transport to Japan is 1.13 €/kg, so the cost of hydrogen upon arrival in Japan is 4.44 €/kg.

With the increasing presence of renewable energy in the grid, higher levels of curtailment in renewable power plants will take place. Considering this reasoning, a study was conducted to compare three scenarios using an offshore wind farm [45]: sell all electricity to the grid (scenario 1), convert all electricity to hydrogen (scenario 2), or a hybrid system

where electricity is sold to the grid when prices are high and converted to hydrogen when curtailment occurs or electricity prices are low (scenario 3). A model was developed for a 504 MW wind farm located 14.5 km off the coast of Arklow, Ireland, and all three scenarios were simulated. The results obtained were an LCOE in scenario 1 of 38.1 €/MWh for 0% curtailment and 47.6 €/MWh for 20% curtailment, while the LCOH for scenario 2 was 3.77 €/kg. For scenario 3, if the hydrogen price was 4 €/kg, only at curtailment levels higher than 17% could adding hydrogen generation provide an equal or higher Net Present Value (NPV). If the hydrogen price was 4.25 €/kg, then the level of curtailment for which hydrogen generation becomes profitable is 10%.

Another article comparing the three scenarios described above was written by Pengfei Xiao et al. [46] in 2020, where the model was developed for a wind farm in Denmark. Here, the electricity price for the first and third scenarios varied from 80 €/MWh to 160 €/MWh, depending on the time of day, with the hydrogen price fixed at 6.27 €/kg in the scenarios where hydrogen was produced. The article concluded that the hybrid approach yields greater economic interest compared to the other scenarios, with most of the hydrogen being produced at night when the electricity price is lower.

A slightly different approach was taken by Peng Hou et al. [47], where a 72 MW offshore wind farm was considered for the production of hydrogen, with two possible operating scenarios. In the first scenario, all of the energy was converted to hydrogen in an electrolyzer, stored, and then converted back to electricity in a fuel cell to sell to the grid during peak hours. In the second scenario, the electricity generated by the wind turbines could be sold to the grid or fed into an electrolyzer, with the possibility of buying energy from the grid when prices are extremely low. The electricity prices considered were the electricity prices for Denmark in 2015. The study concluded that the first scenario was not economically viable due to the low round-trip efficiency of the electrolyzer and fuel cell. However, for the second scenario, considering a 50% capacity factor for the electrolyzer, the DPB was 24.4, 5.5, and 2.6 years and the nominal power of the electrolyzer was 5.5, 13.5, and 23.4 MW for a hydrogen price of 2, 5, and 9 €/kg, respectively.

A model to determine the most suitable electrolyzer technology and to compare solar and wind as the energy sources of a green hydrogen production system was developed by Christian Schnuelle et al. [48]. Several scenarios were included in the article, such as onshore and offshore wind as well as nominal powers of the electrolyzer of 40%, 60%, or 80% of the respective power plant's nominal power. All the renewable energy generation profiles considered were measured in northwest Germany in 2017. Considering a fixed electricity price, dependent on the installation chosen and typical annual load duration curves, the authors state that AEL proved the most economically viable option, mainly due to higher efficiencies and improved stack life, which reduces the investment in replacing stacks and the lower initial investment. The lowest LCOH achieved was 4.33 €/kg. Despite being more expensive, PEMEL offers an advantage regarding energy utilization, since it can operate at lower power and better harness the renewable resources available.

To compare the subject of this paper to other green hydrogen applications, two articles regarding hydrogen production using solar energy were analyzed. The first considers various locations in Morocco [49], with different types of Photovoltaic (PV) panel installations, from fixed to two-axis tracking, and a CSP installation. Even though fixed PV panels produced the lowest LCOH of 4.74 €/kg, a better balance was achieved using one-axis tracking, which produced 30% more hydrogen and a small LCOH increase to 4.88 €/kg.

The second article analyzed not only green hydrogen production using PV or CSP to harness the solar energy in the Atacama Desert, Chile, but also the existing technologies to transport hydrogen in a higher energy density—liquefied hydrogen and ammonia carrier [20]. The lowest LCOH in 2018, 1.82 €/kg, was obtained using PV, a power purchase agreement, and converting the electricity to hydrogen in an AEL. In 2025, LCOH reductions are expected to be around 20% to 34%, higher in PEMEL than AEL, to a minimum value of 1.39 €/kg. The cost of liquefying hydrogen (1.28 €/kg) is lower than the cost to convert

to and from ammonia (total 2.04 €/kg), but due to the higher energy density and ease of transport, a case can be made for ammonia as a means of transporting hydrogen.

Both of the articles agree that despite CSP with thermal storage allowing for a much higher capacity factor, which reduces the nominal power of the electrolyzer, the reduction in CAPEX in the electrolyzer is smaller than the increase in CAPEX by using CSP instead of PV.

Regarding the applications of hydrogen, Rodica Loisel et al. [50] developed a model with an offshore wind farm off the coast of Saint Nazaire, France. The paper simulated the economic viability of each application individually, then combined the two applications (for example, P2P and P2G), and presented a final scenario where all applications considered were implemented. In all scenarios, the electrolyzer's nominal power was considerably lower than the wind farm nominal power; consequently, most of the energy produced was sold directly to the electricity grid at wholesale prices, with the remaining energy being reserved for secondary and tertiary reserves. The study concluded that the most economically viable approach was P2G, with a hydrogen price of 4.2 €/kg. However, even the most profitable approach presents a negative NPV. It should be noted that combining many applications led to a higher investment cost and ultimately reduced the project's profit.

Focusing on P2P, where fuel cells can play a role as long-term energy storage and fast-acting dispatchable power plants, a review of the main fuel cell technologies was conducted in 2018 [51]. After analyzing each technology, the authors concluded that since fuel cells do not have great electrical efficiencies (40% to 55%), the best way to harvest their potential is to utilize the heat generated, either for heating in the case of low-temperature fuel cells (PEMFC and AFC) or Combined Heat and Power (CHP) in the case of high-temperature fuel cells (AFC, MCFC, and SOFC). Integrating CHP yields an increase of 10% to 30% in efficiency. In addition, micro gas turbines can be used to provide further heat to the combined cycle, which might also lead to an increase in efficiency.

A challenge associated with a high percentage of renewable power in electricity grids is frequency containment, usually ensured by big synchronous generators in traditional power plants due to their high inertia. PEMFC presents high current density and fast response times; consequently, it might be an option to help maintain the grid frequency. To assess the role this technology can play in frequency containment, F.A. Alshehri et al. [52] developed a dynamic model to simulate PEMFC, validated that the model's response resembled the response shown in the existing literature, and compared the Frequency Containment Reserve (FCR) of PEMFC and synchronous generators. The scenarios consisted of a 50 MW disturbance for different system inertia with values 100%, 50%, and 25%, for both synchronous generators and PEMFC as FCR. For all scenarios, PEMFC provided the best nadir (lowest frequency recorded) and a faster rate of frequency stabilization, while the values representing Rate-of-Change-of-Frequency remained the same for both scenarios.

Continuing with the analysis for the viability of grid-connected fuel cells, an assessment was conducted in 2013 [53]. The authors of the assessment concluded that the start-up time of the fuel cell must be taken into account (around 10 min). Furthermore, the dynamic loading on the system severely influences the longevity of the fuel cells; a load ranging from 0–100% presented a much lower power output after 100 operating hours than a load ranging from 40–100% after 400 operating hours. As long as some requirements and the operating conditions mentioned above are respected, grid-connected fuel cells are viable.

In the past, green hydrogen production has not been able to compete with other methods of producing hydrogen due to the increased cost. However, costs are rapidly decreasing, and affordable green hydrogen can become a reality by the year 2030, as is pointed out in several articles analyzed in this section. Both solar and wind have the potential to be the renewable energy source used in the production of hydrogen, with researchers on all continents studying different approaches. With the prospect of clean hydrogen, innovative uses are also being studied, from P2G to grid-connected fuel cells and electrolyzers to aid in grid stability and energy storage. In order to transport large quantities of hydrogen, liquified hydrogen and ammonia carrier are technologies that are currently

being developed and that show potential to further lower the cost of implementing green hydrogen solutions.

Table 3 contains a summary of the LCOH observed throughout the literature review. LCOH is calculated by adding all the expenses of the project (CAPEX and OPEX correctly adjusted according to the rate of return) and dividing by the amount of hydrogen produced by the electrolyzer in kg. The cost of hydrogen is influenced mainly by the electricity cost and the cost of the required infrastructure, which means AEL typically has a lower LCOH than PEMEL due to the lower cost. The same applies to the electricity source: the lower LCOH values are observed in locations with low electricity prices, such as the electricity grid in Ontario [43], solar PV in Chile [20], or onshore wind in Patagonia [44].

Table 3. Summary of LCOH.

Electricity Source	AEL (€/kg)	PEMEL (€/kg)
Grid	2.49–2.74 [43]	2.26–3.01 [43]
Solar PV	2.04–5.00 [20,48]	2.71–7.98 [20,48,49]
Solar CSP	3.03 [20]	3.79–8.5 [20,49]
Onshore Wind	4.33 [48]	2.73–6.61 [44,48]
Offshore Wind	9.17 [48]	3.77–11.75 [24,45,48,50]

The more economically viable electricity sources for producing green hydrogen are solar PV and onshore wind, mainly because the LCOE of these two energy sources is considerably lower than solar CSP and offshore wind. The LCOE is the factor that influences the LCOH the most [20,45]; therefore, technologies with the lowest LCOE are the best suited to being the electricity source in green hydrogen projects. More specifically, the lowest LCOH for solar PV was found in the Atacama Desert in Chile [20], and the lowest LCOH for onshore wind was found in Patagonia [44], two locations with abundant availability of their respective renewable resources.

6. Conclusions

Hydrogen has several applications, including being mixed with natural gas in P2G, powering vehicles in P2M, and providing energy storage and grid balancing services in P2P. In the last decades, hydrogen has had carbon emissions associated with its production, and for this reason its potential has not been fully explored. However, due to recent advancements in electrolyzers and renewable energy, the cost competitiveness of green hydrogen is quickly rising and is expected to match fossil-fuel-based hydrogen in the coming years.

Compared to wind energy on land, offshore wind has higher wind speeds and is more consistent, making it a more attractive resource to generate electricity. The main drawbacks have been the higher cost and technical challenges associated with transmitting the electricity to shore, though this has improved in the past years. Offshore wind farms are increasing in size and are built further and further away from shore; nonetheless, they have been experiencing LCOE reductions, almost reaching competitive values. Furthermore, with the development of floating wind platforms, wind farms can be placed in deeper waters, allowing more locations to be accessible for electricity generation.

Two hydrogen production systems based on offshore wind energy are currently proposed, in which not only are electricity and hydrogen produced but grid balancing services are provided, such as frequency control. The first system utilizes an offshore electrolyzer; hydrogen is produced, compressed, and transported in a pipeline to shore. The main advantages are the reduced cost of a submarine pipeline compared to a submarine electrical cable and supporting power electronics, along with the reduction in transmission losses of gas in a pipeline (0.1%) in comparison to conventional wind farms (up to 5%). In the second system, the electrolyzer is located on land, so the electricity generated offshore is transmitted through an electrical cable to land. Once the electricity reaches the shore, it can be sold directly as electricity when the price is high during peak periods or can be fed

into an electrolyzer to produce hydrogen when the electricity prices are low or curtailment must occur. The advantage is the increased flexibility provided to the operator, with the option of selling electricity or producing hydrogen, depending on the most economically viable choice.

The literature shows the decreasing costs for green hydrogen production, both for wind and solar energy, along with the forecast of how the technology is expected to evolve: less expensive, longer lasting, and more efficient electrolyzers. Furthermore, the integration of fuel cells and electrolyzers at a grid level can aid in overcoming some of the challenges of generating electricity from renewable energy sources, like frequency control and energy storage.

Nomenclature

AEL	Alkaline Electrolyzer
AFC	Alkaline Fuel Cell
CHP	Combined Heat and Power
CSP	Concentrated Solar Power
DPB	Discounted Payback Period
FCR	Frequency Containment Reserve
HVAC	High Voltage Alternating Current
HVDC	High Voltage Direct Current
LCOE	Levelized Cost Of Energy
LCOH	Levelized Cost Of Hydrogen
LNG	Liquified Natural Gas
MCFC	Molten Carbonate Fuel Cell
NPV	Net Present Value
P2G	Power to Gas
P2M	Power to Mobility
P2P	Power to Power
PAFC	Phosphoric Acid Fuel Cell
PEMEL	Proton Exchange Membrane Electrolyzer
PEMFC	Proton Exchange Membrane Fuel Cell
PV	Photovoltaic
SDGs	United Nations Sustainable Development Goals
SMR	Steam Methane Reform
SOE	Solid Oxide Electrolyzer
SOFC	Solid Oxide Fuel Cell

References

1. IEA. *Key World Energy Statistics*; IEA: Paris, France, 2020. Available online: https://www.iea.org/reports/key-world-energy-statistics-2020 (accessed on 7 April 2021).
2. Panfilov, M. 4—Underground and pipeline hydrogen storage. In *Compendium of Hydrogen Energy, Woodhead Publishing Series in Energy*; Gupta, R.B., Basile, A., Veziroglu, T.N., Eds.; Woodhead Publishing: Sawston, UK, 2016; pp. 91–115. [CrossRef]
3. Miao, B.; Giordano, L.; Chan, S.H. Long-distance renewable hydrogen transmission via cables and pipelines. *Int. J. Hydrogen Energy* **2021**, in press. [CrossRef]
4. WindEurope. Offshore Wind in Europe: Key Trends and Statistics 2020. 2021. Available online: https://windeurope.org/intelligence-platform/product/offshore-wind-in-europe-key-trends-and-statistics-2020/ (accessed on 7 April 2021).
5. The European Marine Observation and Data Network (EMODnet). Available online: https://portal.emodnet-bathymetry.eu/ (accessed on 7 April 2021).
6. Offshore Renewable Energy (ORE) Catapult. Offshore Wind and Hydrogen: Solving the Integration Challenge. 2020. Available online: https://ore.catapult.org.uk/?orecatapultreports=offshore-wind-and-hydrogen-solving-the-integration-challenge (accessed on 7 April 2021).
7. Airborne WindEurope. High-altitude Wind Energy Map Published. Available online: https://airbornewindeurope.org/resources/high-altitude-wind-energy-map-published-2/ (accessed on 7 April 2021).
8. Equinor. Hywind Scotland. Available online: https://www.equinor.com/en/what-we-do/floating-wind/hywind-scotland.html (accessed on 7 April 2021).
9. WindEurope. Offshore Wind in Europe: Key Trends and Statistics 2017. 2018. Available online: https://windeurope.org/intelligence-platform/product/the-european-offshore-wind-industry-key-trends-and-statistics-2017/ (accessed on 7 April 2021).
10. ERM. Dolphyn Hydrogen Phase 1—Final Report. October 2019. Available online: https://assets.publishing.service.gov.uk/government/uploads/system/uploads/attachment_data/file/866375/Phase_1_-_ERM_-_Dolphyn.pdf (accessed on 26 April 2021).
11. IRENA. Hydrogen from Renewable Power: Technology Outlook for the Energy Transition. 2018. Available online: https://irena.org/publications/2018/Sep/Hydrogen-from-renewable-power (accessed on 7 April 2021).
12. Buttler, A.; Spliethoff, H. Current status of water electrolysis for energy storage, grid balancing and sector coupling via power-to-gas and power-to-liquids: A review. *Renew. Sustain. Energy Rev.* **2018**, *82*, 2440–2454. [CrossRef]
13. Guo, Y.; Li, G.; Zhou, J.; Liu, Y. Comparison between hydrogen production by alkaline water electrolysis and hydrogen production by PEM electrolysis. *IOP Conf. Ser. Earth Environ. Sci.* **2019**, *371*, 042022. [CrossRef]
14. McPhy. Augmented McLyzer. Available online: https://mcphy.com/en/equipment-services/electrolyzers/augmented/ (accessed on 7 April 2021).
15. Andersson, J.; Grönkvist, S. Large-scale storage of hydrogen. *Int. J. Hydrogen Energy* **2019**, *44*, 11901–11919. [CrossRef]
16. Dagdougui, H.; Sacile, R.; Bersani, C.; Ouammi, A. Chapter 4—hydrogen storage and distribution: Implementation scenarios. In *Hydrogen Infrastructure for Energy Applications*; Dagdougui, H., Sacile, R., Bersani, C., Ouammi, A., Eds.; Academic Press: Cambridge, MA, USA, 2018; pp. 37–52. [CrossRef]
17. Hydrogenics. Large Scale PEM Electrolysis: Technology Status and Upscaling Strategies. Available online: https://www.google.com/url?sa=t&rct=j&q=&esrc=s&source=web&cd=&ved=2ahUKEwjz7KHVme3vAhVECxoKHSUdCCkQFjACegQIAxAD&url=http%3A%2F%2Fhybalance.eu%2Fwp-content%2Fuploads%2F2019%2F10%2FLarge-scale-PEM-electrolysis.pdf&usg=AOvVaw1YjdSYyby88zmNHVsqeAsz (accessed on 7 April 2021).
18. Siemens. Decarbonizing Energy with Green Hydrogen: Technology Available and Proven in Production Today. Available online: https://assets.new.siemens.com/siemens/assets/api/uuid:390d0f48-499e-4451-a3c2-faa30c5bafe7/version:1598442587/power-to-x-technical-paper-siemens-short.pdf (accessed on 29 May 2021).
19. Kruck, O.; Crotogino, F.; Prelicz, R.; Rudolph, T. Overview on all known underground storage technologies for hydrogen. In Project HyUnder–Assessment of the Potential, the Actors and Relevant Business Cases for Large Scale and Seasonal Storage of Renewable Electricity by Hydrogen Underground Storage in Europe. Report D. 2013, Volume 3. Available online: http://hyunder.eu/wp-content/uploads/2016/01/D3.1_Overview-of-all-known-underground-storage-technologies.pdf (accessed on 26 April 2021).
20. Gallardo, F.I.; Ferrario, A.M.; Lamagna, M.; Bocci, E.; Garcia, D.A.; Baeza-Jeria, T.E. A techno-economic analysis of solar hydrogen production by electrolysis in the north of Chile and the case of exportation from Atacama desert to Japan. *Int. J. Hydrogen Energy* **2021**, *46*, 13709–13728. [CrossRef]
21. Negra, N.B.; Todorovic, J.; Ackermann, T. Loss evaluation of HVAC and HVDC transmission solutions for large offshore wind farms. *Electr. Power Syst. Res.* **2006**, *76*, 916–927. [CrossRef]
22. Papadopoulos, A.; Rodrigues, S.; Kontos, E.; Todorcevic, T.; Bauer, P.; Pinto, R.T. Collection and transmission losses of offshore wind farms for optimization purposes. In Proceedings of the 2015 IEEE Energy Conversion Congress and Exposition (ECCE), Montreal, QC, Canada, 20–24 September 2015; pp. 6724–6732. [CrossRef]
23. North Sea Energy. A Vision on Hydrogen Potential from the North Sea. 2019. Available online: https://north-sea-energy.eu/static/29bef9235ee0548a2425dea4356a2f1e/NSE3-D1.6-D1.7-D1.8-Offshore-Hydrogen-Roadmap-linked-to-national-hydrogen-grid.pdf (accessed on 7 April 2021).

24. Dinh, V.N.; Leahy, P.; McKeogh, E.; Murphy, J.; Cummins, V. Development of a viability assessment model for hydrogen production from dedicated offshore wind farms. *Int. J. Hydrogen Energy* **2020**, in press. [CrossRef]

25. General Electric. Switch It Up: This Tech Helps Take the World's Largest Offshore Wind Turbine to a New Level. 2018. Available online: https://www.ge.com/news/reports/switch-tech-helps-take-worlds-largest-offshore-wind-turbine-new-level (accessed on 7 April 2021).

26. Alassi, A.; Bañales, S.; Ellabban, O.; Adam, G.; MacIver, C. HVDC transmission: Technology review, market trends and future outlook. *Renew. Sustain. Energy Rev.* **2019**, *112*, 530–554. [CrossRef]

27. IRENA. Green Hydrogen Cost Reduction: Scaling Up Electrolyzers to Meet the 1.5 °C Climate Goal. 2020. Available online: https://www.irena.org/publications/2020/Dec/Green-hydrogen-cost-reduction (accessed on 7 April 2021).

28. Toyota. 2021 Toyota Mirai. Available online: https://www.toyota.com/mirai/ (accessed on 29 May 2021).

29. Wood, A.; He, H.; Joia, T.; Brown, C.C. Reversible solid oxide fuel cell development at versa power systems. *ECS Trans.* **2015**, *66*, 23. [CrossRef]

30. US. Department of Energy. Comparison of Fuel Cell Technologies. 2016. Available online: https://www.energy.gov/eere/fuelcells/comparison-fuel-cell-technologies (accessed on 7 April 2021).

31. Weidner, E.; Ortiz Cebolla, R.; Davies, J. *Global Deployment of Large Capacity Stationary Fuel Cells–Drivers of, and Barriers to, Stationary Fuel Cell Deployment*; JRC115923; EUR 29693 EN; Publications Office of the European Union: Luxembourg, 2019; ISBN 978-92-76-00841-5. [CrossRef]

32. Doosan starts installation of hydrogen-fueled 50 MW fuel cell power plant in South Korea. *Fuel Cells Bull.* **2018**, *2018*, 1. [CrossRef]

33. Fuel Cells Works. Daesan Hydrogen Fuel Cell Power Plant Completed with Help of Doosan Fuel Cells. Available online: https://fuelcellsworks.com/news/daesan-hydrogen-fuel-cell-power-plant-completed-with-help-of-doosan-fuel-cells/ (accessed on 26 April 2021).

34. HyDeploy. Available online: https://hydeploy.co.uk/ (accessed on 7 April 2021).

35. Melaina, M.W.; Antonia, O.; Penev, M. Blending hydrogen into natural gas pipeline networks: A review of key issues. *Tech. Rep.* **2013**. [CrossRef]

36. Quarton, C.J.; Samsatli, S. Power-to-gas for injection into the gas grid: What can we learn from real-life projects, economic assessments and systems modelling? *Renew. Sustain. Energy Rev.* **2018**, *98*, 302–316. [CrossRef]

37. EDP. FLEXnCONFU: Power-to-X to Increase the Flexibility of Thermal Plants. Available online: https://www.edp.com/en/innovation/flexnconfu-power-to-increase-the-flexibility-of-thermal-plants (accessed on 26 April 2021).

38. FLEXnCONFU. Available online: https://flexnconfu.eu/demonstration/ (accessed on 29 May 2021).

39. Kakoulaki, G.; Kougias, I.; Taylor, N.; Dolci, F.; Moya, J.; Jager-Waldau, A. Green hydrogen in Europe—a regional assessment: Substituting existing production with electrolysis powered by renewables. *Energy Convers. Manag.* **2021**, *228*, 113649. [CrossRef]

40. Gusain, D.; Cvetković, M.; Bentvelsen, R.; Palensky, P. Technical assessment of large-scale PEM electrolyzers as flexibility service providers. In Proceedings of the 2020 IEEE 29th International Symposium on Industrial Electronics (ISIE), Delft, The Netherlands, 24 September 2020; pp. 1074–1078. [CrossRef]

41. CIGRE. Available online: https://www.cigre.org/ (accessed on 26 April 2021).

42. Clúa, J.G.G.; Mantz, R.J.; de Battista, H. Optimal sizing of a grid-assisted wind-hydrogen system. *Energy Convers. Manag.* **2018**, *166*, 402–408. [CrossRef]

43. Nguyen, T.; Abdin, Z.; Holm, T.; Me´rida, W. Grid-connected hydrogen production via large-scale water electrolysis. *Energy Convers. Manag.* **2019**, *200*, 112108. [CrossRef]

44. Heuser, P.-M.; Ryberg, D.S.; Grube, T.; Robinius, M.; Stolten, D. Techno-economic analysis of a potential energy trading link between Patagonia and Japan based on CO_2 free hydrogen. *Int. J. Hydrogen Energy* **2019**, *44*, 12733–12747. [CrossRef]

45. McDonagh, S.; Ahmed, S.; Desmond, C.; Murphy, J.D. Hydrogen from offshore wind: Investor perspective on the profitability of a hybrid system including for curtailment. *Appl. Energy* **2020**, *265*, 114732. [CrossRef]

46. Xiao, P.; Hu, W.; Xu, X.; Liu, W.; Huang, Q.; Chen, Z. Optimal operation of a wind-electrolytic hydrogen storage system in the electricity/hydrogen markets. *Int. J. Hydrogen Energy* **2020**, *45*, 24412–24423. [CrossRef]

47. Hou, P.; Enevoldsen, P.; Eichman, J.; Hu, W.; Jacobson, M.Z.; Chen, Z. Optimizing investments in coupled offshore wind -electrolytic hydrogen storage systems in Denmark. *J. Power Sources* **2017**, *359*, 186–197. Available online: http://dx.doi.org/10.1016/j.jpowsour.2017.05.048 (accessed on 26 April 2021). [CrossRef]

48. Schnuelle, C.; Wassermann, T.; Fuhrlaender, D.; Zondervan, E. Dynamic hydrogen production from PV & wind direct electricity supply—modeling and techno-economic assessment. *Int. J. Hydrogen Energy* **2020**, *45*, 29938–29952. [CrossRef]

49. Touili, S.; Merrouni, A.A.; El Hassouani, Y.; Amrani, A.i.; Rachidi, S. Analysis of the yield and production cost of large-scale electrolytic hydrogen from different solar technologies and under several Moroccan climate zones. *Int. J. Hydrogen Energy* **2020**, *45*, 26785–26799. [CrossRef]

50. Loisel, R.; Baranger, L.; Chemouri, N.; Spinu, S.; Pardo, S. Economic evaluation of hybrid off-shore wind power and hydrogen storage system. *Int. J. Hydrogen Energy* **2015**, *40*, 6727–6739. [CrossRef]

51. Guaitolini, S.V.M.; Yahyaoui, I.; Fardin, J.F.; Encarnac¸ao, L.F.; Tadeo, F. A review of fuel cell and energy cogeneration technologies. In Proceedings of the 2018 9th International Renewable Energy Congress (IREC), Hammamet, Tunisia, 20–22 March 2018; pp. 1–6. [CrossRef]

52. Alshehri, F.; Torres, J.R.; Perilla, A.; Tuinema, B.; van der Meijden, M.; Palensky, P.; Gonzalez-Longatt, F. Generic model of PEM fuel cells and performance analysis in frequency containment period in systems with decreased inertia. In Proceedings of the 2019 IEEE 28th International Symposium on Industrial Electronics (ISIE), Vancouver, BC, Canada, 12–14 June 2019; pp. 1810–1815. [CrossRef]

53. Bernstein, P.A.; Heuer, M.; Wenske, M. Fuel cell system as a part of the smart grid. In Proceedings of the 2013 IEEE Grenoble Conference, Grenoble, France, 16–20 June 2013; pp. 1–4. [CrossRef]